Superfluidity in Fermi systems within the framework of Density Functional Theory

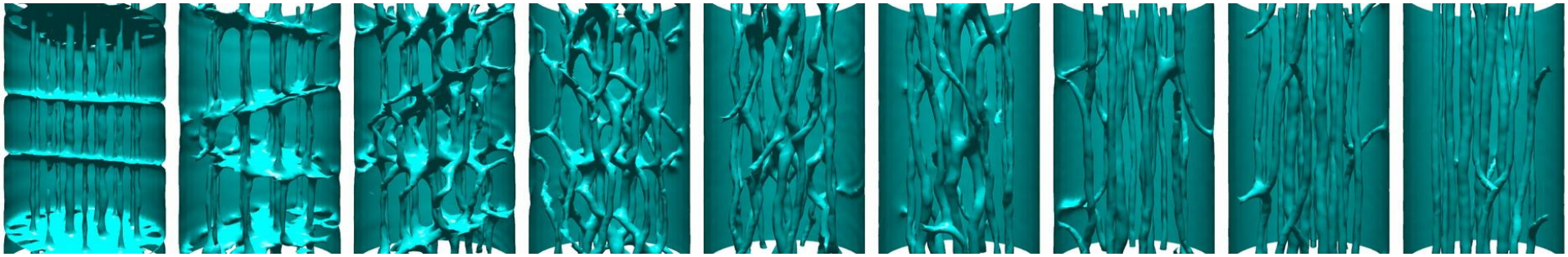

Piotr Magierski

Warsaw University of Technology (WUT)

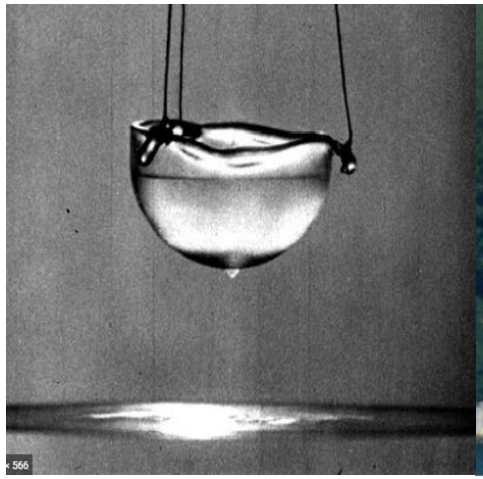

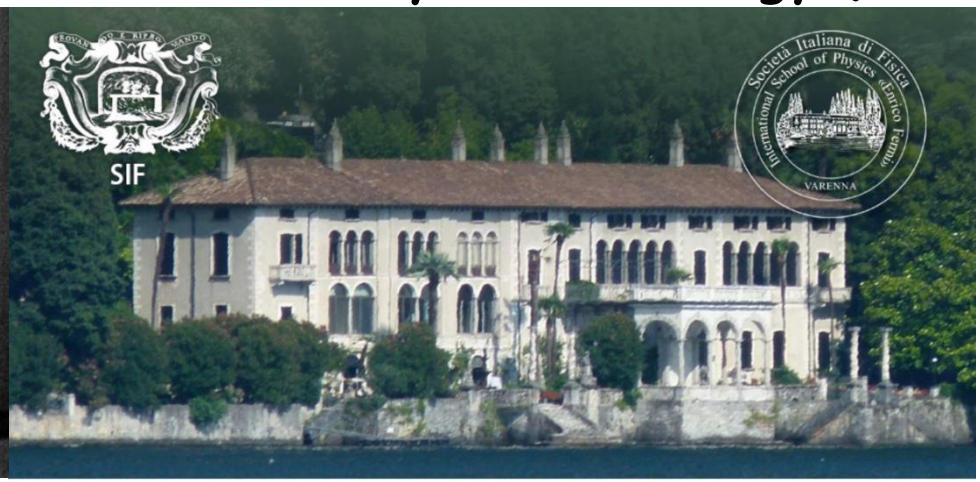

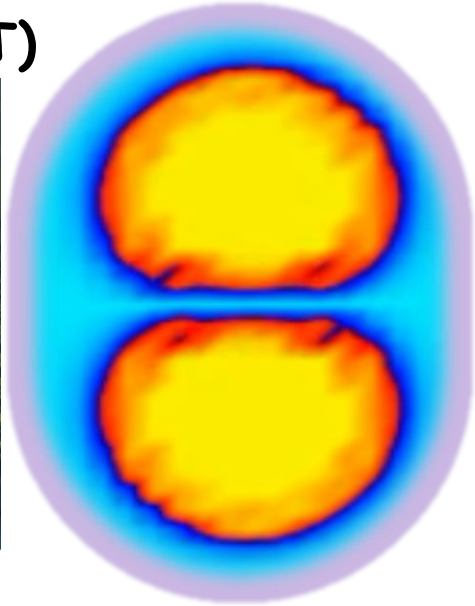

International School of Physics "Enrico Fermi" 2024

NUCLEAR STRUCTURE AND REACTIONS FROM A BROAD PERSPECTIVE

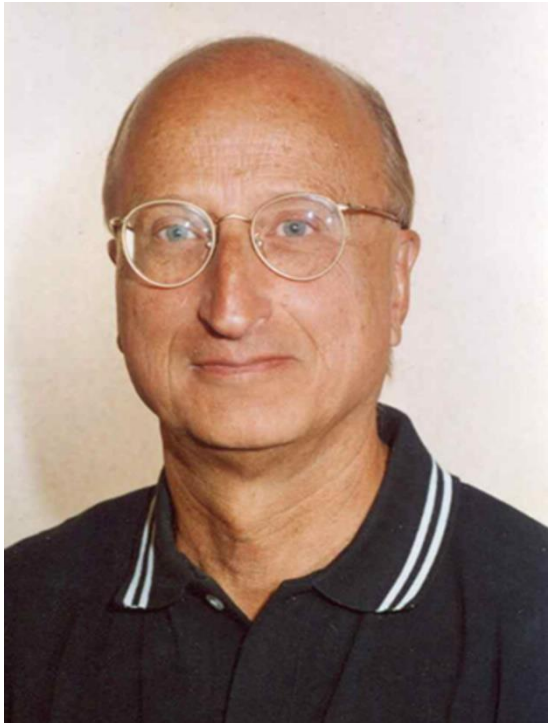

Ricardo Americo Broglia (1939-2022)

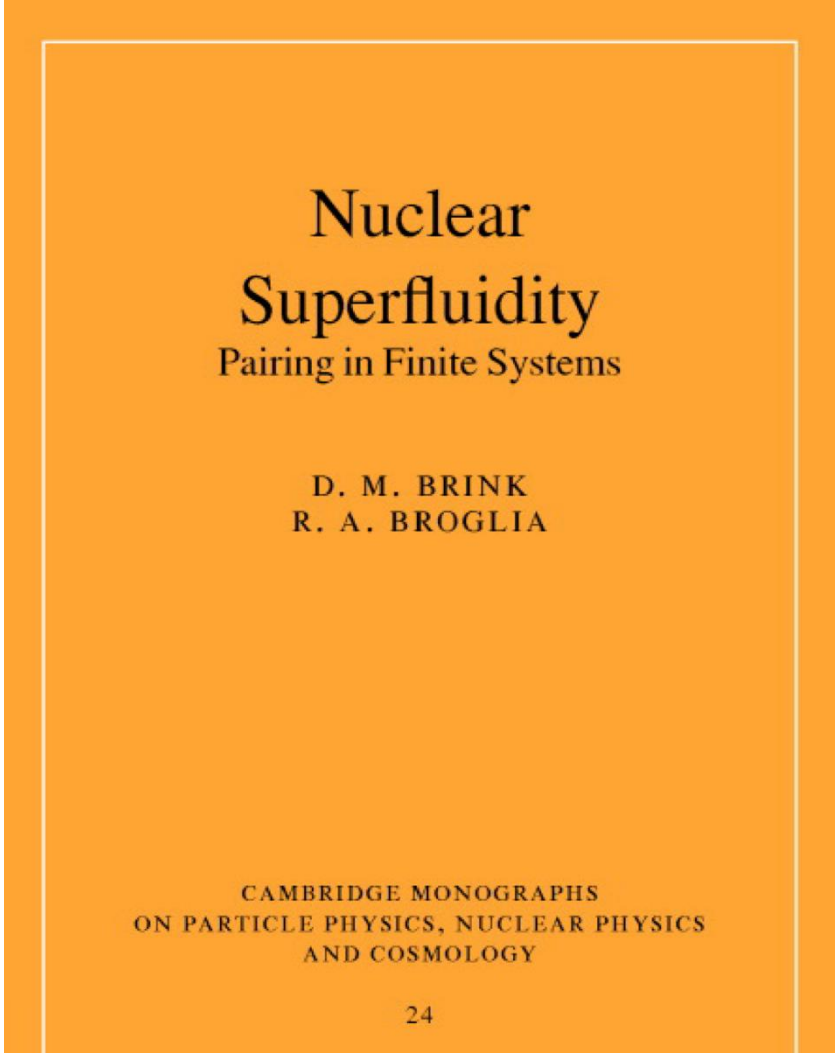

From a review:

This book is an important addition to the fundamental physics literature. A good background in basic concepts of nuclear theory, including the shell and collective models is a prerequisite, and, for some sections, knowledge of certain techniques in the theory of direct nuclear reactions is required. Thus, fore-armed, the dedicated reader will come away from this work richly rewarded.

OUTLINE

1. **Basics of Density Functional Theory**

2. **Basics of Density Functional Theory for Superfluids**

3. **Applications:**

- **Nuclear fission and collisions**
- **Modelling neutron star interior: vortex dynamics**
- **Ultracold Fermi gases**

Cooper pairs

2Δ - Energy gap

k_F

$\varepsilon_F = \frac{\hbar^2 k_F^2}{2m}$

Attractive interaction

Fermi sphere

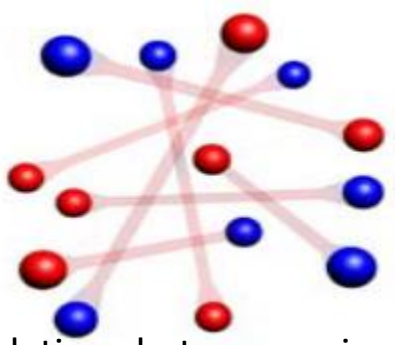

Correlations between pairs (Cooper) of particles of opposite spins.

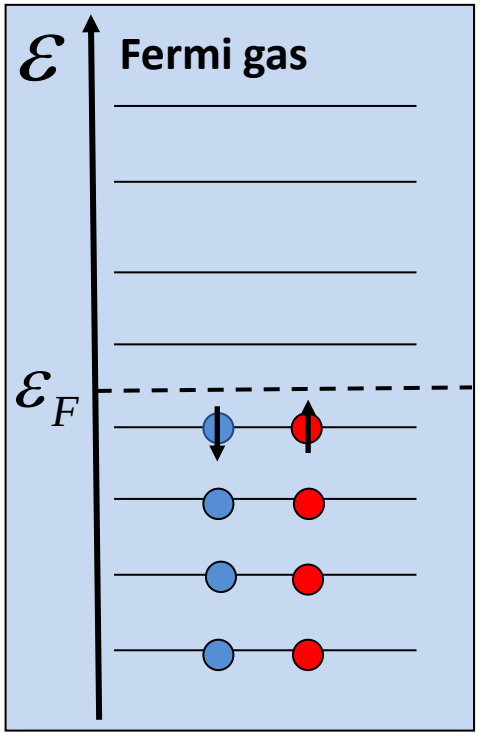

Energy of elementary excitation (quasiparticle):

$$E_{qp} = \sqrt{(\varepsilon - \varepsilon_F)^2 + |\Delta|^2} > |\Delta|$$

BCS theory:

$$|BCS\rangle = \prod_k \left(u_k + v_k a^\dagger_{k\uparrow} a^\dagger_{-k\downarrow}\right)|vacuum\rangle$$

$$\Delta = f(u_k, v_k)$$

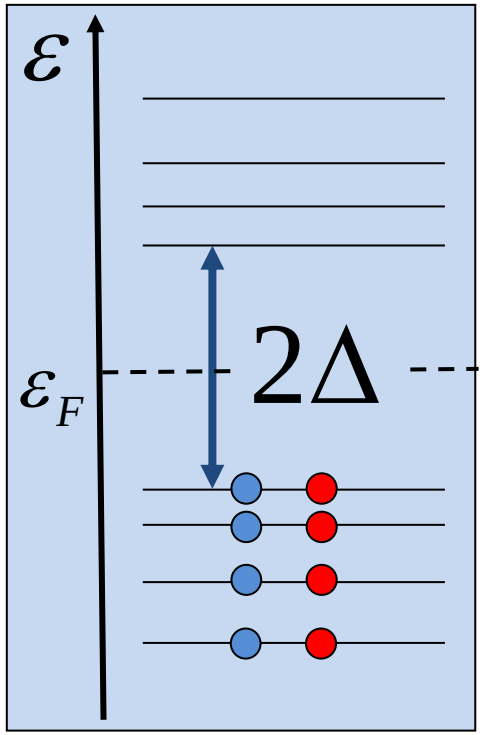

Robert B. Laughlin, Nobel Lecture, December 8, 1998:

One of my favorite times in the academic year occurs [..] when I give my class of extremely bright graduate students [..] a take home exam in which they are asked TO DEDUCE SUPERFLUIDITY FROM FIRST PRINCIPLES.

There is no doubt a special place in hell being reserved for me at this very moment for this mean trick, for the task is IMPOSSIBLE. Superfluidity [..] is an EMERGENT phenomenon – a low energy collective effect of huge number of particles that CANNOT be deduced from the microscopic equations of motion in a RIGOROUS WAY and that DISAPPEARS completely when the system is taken apart.

[..]students who stay in physics long enough [..] eventually come to understand that the REDUCTIONIST IDEA IS WRONG a great deal of the time and perhaps ALWAYS.

Critical temperatures for superconductivity and superfluidity

- ✓ **Ultracold atomic gases:** $T_c \approx 10^{-12} - 10^{-9}$ eV
- ✓ **Liquid ^{3}He:** $T_c \approx 10^{-7}$ eV
- ✓ **Metals and alloys:** $T_c \approx 10^{-3} - 10^{-2}$ eV
- ✓ **Atomic nuclei and neutron stars:** $T_c \approx 10^{5} - 10^{6}$ eV
- • **Color superconductivity (quarks) :** $T_c \approx 10^{7} - 10^{8}$ eV

(1 eV $\approx 10^4$ K)

Superfluidity and superconductivity

- **Requirement**: Bose-Einstein (BEC) condensation of interacting *bosons*.
- **Result**: linear dispersion relation
- **Consequence**: no viscosity (below certain flow velocity)
- **Theoretical description**: „Condensate wave function"

$$\Psi(\vec{r}) = \left|\Psi\left(\vec{r}\right)\right| e^{i\phi(\vec{r})}$$

- **Requirement**: arbitrary weak attraction between *fermions.*
- **Result**: formation of Cooper pairs
- **Consequence**: no resistance
- **Theoretical description**: Field of Cooper pairs

$$\Delta(\vec{r}) = \left|\Delta\left(\vec{r}\right)\right| e^{i\phi(\vec{r})}$$

Both phenomena are actually like two sides of the same coin!

GOAL:
Unified description of superfluid dynamics of fermionic systems far from equilibrium based on microscopic theoretical framework.

Microscopic framework = explicit treatment of fermionic degrees of freedom.

The fundamental equation describing dynamics is known:

$$i\hbar \frac{\partial}{\partial t}\psi = \hat{H}\psi$$

However, if we would like to apply this equation to e.g.nuclear fission, even if we knew nuclear Hamiltonian precisely, the problem of motion of more than 200 strongly interacting nucleons, described in terms of true many-body wave function is computationally intractable.

„In general the many-electron wave function for a system of N electrons is not a legitimate scientific concept when $N>N_0$, where $N_0 \approx 10^3$."

J.H. Van Vleck, Phys. Rev. 49, 232 (1936)

The wave function of ^{240}Pu depends on 720 coordinates!
In a lattice of size: 10fm x 10fm x 10fm with lattice constant 1fm, one needs to store approximately 2^{7176} numbers (without spin).

On the other hand, in most cases we need to extract one-body observables, only.

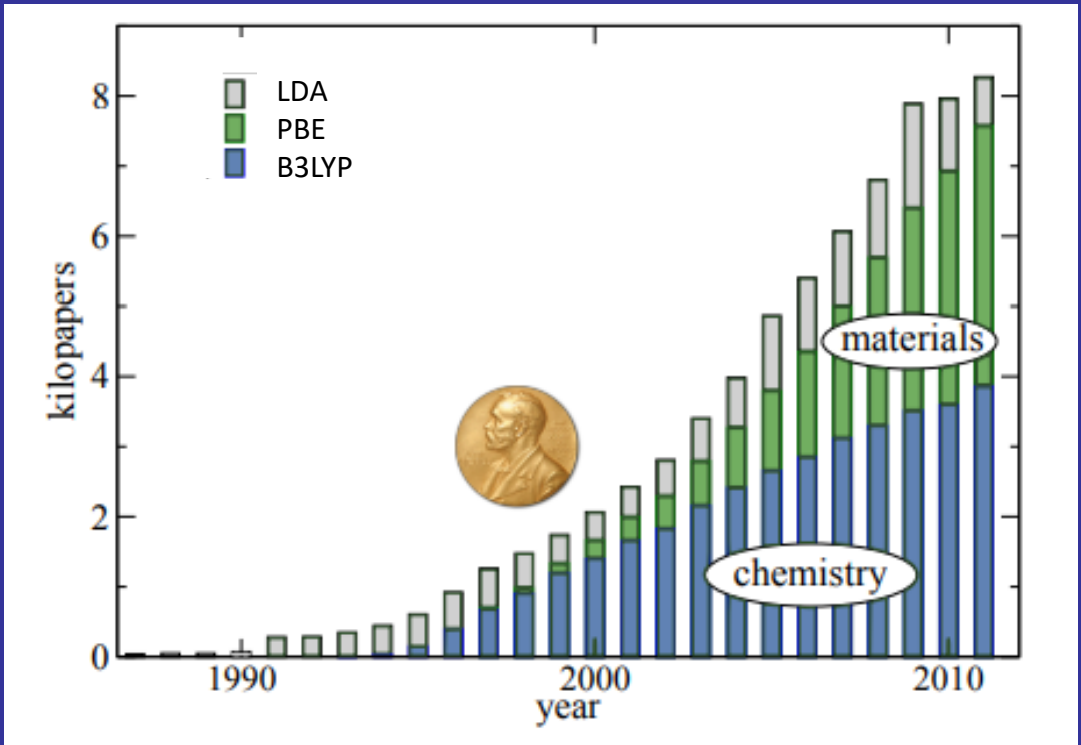

Number of papers using variants of DFT from K.Burke,J.Chem.Phys.136,150901(2012)

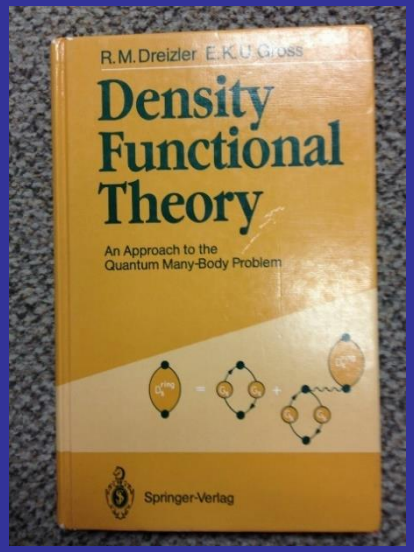

1990

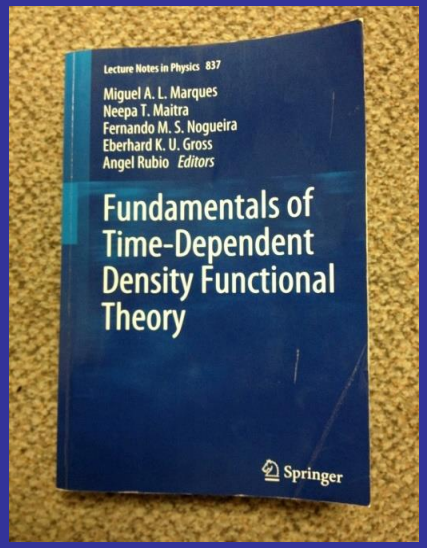

2012

Hohenberg-Kohn Theorem

HOHENBERG P. and KOHN W., *Phys. Rev.*, **136** (1964) B864.

Hamiltonian describing the system of N interacting fermions:

$$\hat{H} = \hat{T} + \hat{V}^{ext} + \hat{V}^{int} = \sum_{\sigma=\uparrow,\downarrow} \int d^3\boldsymbol{r}\, \hat{\psi}^{\dagger}_{\sigma}(\boldsymbol{r}) \left[-\frac{\hbar^2}{2m}\nabla^2 + V^{ext}_{\sigma}(\boldsymbol{r}) \right] \hat{\psi}_{\sigma}(\boldsymbol{r})$$

$$+ \frac{1}{2} \sum_{\sigma,\sigma'=\uparrow,\downarrow} \int d^3\boldsymbol{r} \int d^3\boldsymbol{r'} \hat{\psi}^{\dagger}_{\sigma}(\boldsymbol{r})\, \hat{\psi}^{\dagger}_{-\sigma'}(\boldsymbol{r'})\, V^{int}_{\sigma,\sigma'}(\boldsymbol{r},\boldsymbol{r'}) \quad \hat{\psi}_{-\sigma'}(\boldsymbol{r'})\, \hat{\psi}_{\sigma}(\boldsymbol{r}),$$

The goal:

$$\hat{H}\Psi(\sigma_1\boldsymbol{r}_1, \sigma_2\boldsymbol{r}_2, ..., \sigma_N\boldsymbol{r}_N) = E_{gs}(N)\Psi(\sigma_1\boldsymbol{r}_1, \sigma_2\boldsymbol{r}_2, ..., \sigma_N\boldsymbol{r}_N)$$

Ground state wave function generates the one-body density:

$$\rho_{\sigma}(\boldsymbol{r}) = N_{\sigma} \sum_{\sigma_2,...,\sigma_N=\downarrow,\uparrow} \int d^3\boldsymbol{r_2}...d^3\boldsymbol{r_N} |\Psi(\sigma\boldsymbol{r}, \sigma_2\boldsymbol{r}_2, ..., \sigma_N\boldsymbol{r}_N)|^2,$$

$$\int d^3\boldsymbol{r}\rho_{\sigma}(\boldsymbol{r}) = N_{\sigma}.$$

$$\rho(\boldsymbol{r}) = \rho_{\uparrow}(\boldsymbol{r}) + \rho_{\downarrow}(\boldsymbol{r})$$

Hence we have two mappings: *A* and *B*

$$\hat{V}^{ext} \xrightarrow{\text{A}} |\Psi[\hat{V}^{ext}]\rangle \xrightarrow{\text{B}} \rho[\Psi]$$

Hohenberg-Kohn theorem: mappings *A* and *B* are invertible!

Proof:

1) Mapping *A*

Let us consider: $\hat{V}_1^{ext} \neq \hat{V}_2^{ext} + \text{const}$

Then

$$\hat{H}_1\Psi_1(\sigma_1\boldsymbol{r}_1, \sigma_2\boldsymbol{r}_2, ..., \sigma_N\boldsymbol{r}_N) = (\hat{T} + \hat{V}_1^{ext} + \hat{V}^{int})\Psi_1(\sigma_1\boldsymbol{r}_1, \sigma_2\boldsymbol{r}_2, ..., \sigma_N\boldsymbol{r}_N) =$$
$$= E_{1gs}\Psi_1(\sigma_1\boldsymbol{r}_1, \sigma_2\boldsymbol{r}_2, ..., \sigma_N\boldsymbol{r}_N)$$
$$\hat{H}_2\Psi_2(\sigma_1\boldsymbol{r}_1, \sigma_2\boldsymbol{r}_2, ..., \sigma_N\boldsymbol{r}_N) = (\hat{T} + \hat{V}_2^{ext} + \hat{V}^{int})\Psi_2(\sigma_1\boldsymbol{r}_1, \sigma_2\boldsymbol{r}_2, ..., \sigma_N\boldsymbol{r}_N) =$$
$$= E_{2gs}\Psi_2(\sigma_1\boldsymbol{r}_1, \sigma_2\boldsymbol{r}_2, ..., \sigma_N\boldsymbol{r}_N)$$

Now, suppose that: $|\Psi_1\rangle = |\Psi_2\rangle$

Then, substracting these equations we get:

$$(\hat{V}_1^{ext} - \hat{V}_2^{ext})\Psi_1(\sigma_1\boldsymbol{r}_1, \sigma_2\boldsymbol{r}_2, ..., \sigma_N\boldsymbol{r}_N) = (E_{1gs} - E_{2gs})\Psi_1(\sigma_1\boldsymbol{r}_1, \sigma_2\boldsymbol{r}_2, ..., \sigma_N\boldsymbol{r}_N)$$

But:

$$(\hat{V}_1^{ext} - \hat{V}_2^{ext})\Psi_1(\sigma_1\boldsymbol{r}_1, \sigma_2\boldsymbol{r}_2, ..., \sigma_N\boldsymbol{r}_N) = \sum_{i=1}^{N}(V_{1\sigma_i}^{ext}(\boldsymbol{r}_i) - V_{2\sigma_i}^{ext}(\boldsymbol{r}_i))\Psi_1(\sigma_1\boldsymbol{r}_1, \sigma_2\boldsymbol{r}_2, ..., \sigma_N\boldsymbol{r}_N),$$

Therefore:

$$\sum_{i=1}^{N}\left(\hat{V}_{1\sigma_i}^{ext}(\boldsymbol{r}_i)-\hat{V}_{2\sigma_i}^{ext}(\boldsymbol{r}_i)\right)=E_{1gs}-E_{2gs},$$

However, it contradicts the initial assumption: $\hat{V}_1^{ext}\neq\hat{V}_2^{ext}+\text{const}$

Therefore mapping *A* is invertible.

$$\hat{V}^{ext}\xrightarrow{\text{A}}|\Psi[\hat{V}^{ext}]\rangle\xrightarrow{\text{B}}\rho[\Psi]$$

2) Mapping *B*

Note that:

$$E_{1gs}=\langle\Psi_1|\hat{H}_1|\Psi_1\rangle<\langle\Psi_2|\hat{H}_1|\Psi_2\rangle, \quad \textbf{(I)}$$

$$E_{2gs}=\langle\Psi_2|\hat{H}_2|\Psi_2\rangle<\langle\Psi_1|\hat{H}_2|\Psi_1\rangle, \quad \textbf{(II)}$$

And evaluating:

$$\begin{aligned}\langle\Psi_2|\hat{H}_1|\Psi_2\rangle &= \langle\Psi_2|(\hat{T}+\hat{V}_1^{ext}+\hat{V}^{int})|\Psi_2\rangle=\langle\Psi_2|(\hat{T}+\hat{V}_2^{ext}+\hat{V}^{int}-\hat{V}_2^{ext}+\hat{V}_1^{ext})|\Psi_2\rangle= \\ &= \langle\Psi_2|(\hat{H}_2-\hat{V}_2^{ext}+\hat{V}_1^{ext})|\Psi_2\rangle=\langle\Psi_2|\hat{H}_2|\Psi_2\rangle+\langle\Psi_2|(\hat{V}_1^{ext}-\hat{V}_2^{ext})|\Psi_2\rangle= \\ &= E_{2gs}+\sum_{\sigma_1,\ldots,\sigma_N=\downarrow,\uparrow}\int d^3\boldsymbol{r_1}\ldots d^3\boldsymbol{r_N}\sum_{i=1}^{N}\left(V_{1\sigma_i}^{ext}(\boldsymbol{r}_i)-V_{2\sigma_i}^{ext}(\boldsymbol{r}_i)\right)|\Psi_2(\sigma_1\boldsymbol{r}_1,\sigma_2\boldsymbol{r}_2,\ldots,\sigma_N\boldsymbol{r}_N)|^2= \\ &= E_{2gs}+\int d^3\boldsymbol{r}\sum_{\sigma=\uparrow\downarrow}(V_{1\sigma}^{ext}(\boldsymbol{r})-V_{2\sigma}^{ext}(\boldsymbol{r})\rho_{2\sigma}(\boldsymbol{r}),\end{aligned}$$

which implies that from the eq.(I) we get:

$$E_{1gs}<E_{2gs}+\int d^3\boldsymbol{r}(V_1^{ext}(\boldsymbol{r})-V_2^{ext}(\boldsymbol{r})\rho_2(\boldsymbol{r})$$

But analogously from eq. (II) one gets: $$E_{2gs} < E_{1gs} + \int d^3\boldsymbol{r}(V_2^{ext}(\boldsymbol{r}) - V_1^{ext}(\boldsymbol{r})\rho_1(\boldsymbol{r})$$

Now, suppose that: $\rho_1(\boldsymbol{r}) = \rho_2(\boldsymbol{r})$

Then substracting these two eqs. leads to contradiction:

$$E_{1gs} - E_{2gs} < E_{2gs} - E_{1gs},$$

Therefore mapping ***B*** is invertible.

Concluding: two mappings ***A*** and ***B*** are invertible!

$$\hat{V}^{ext} \overset{\text{A}}{\Longleftrightarrow} |\Psi[\hat{V}^{ext}]\rangle \overset{\text{B}}{\Longleftrightarrow} \rho[\Psi]$$

As a consequence we may treat the following expression as a functional of the density:

$$\langle \Psi[\rho]|\hat{H}|\Psi[\rho]\rangle = E[\rho]$$

Hence, there are three conclusions one can draw from the above considerations:

- The ground state and the expectation value of any operator can be expressed through the density ρ: $\langle \Psi[\rho]|\hat{A}|\Psi[\rho]\rangle = A[\rho]$
- Since both mappings A and B are invertible therefore $\rho_{gs} \Longleftrightarrow \hat{V}^{ext}$ and for a fixed $\hat{V}^{ext}$ the energy is a functional $E_{V^{ext}}[\rho]$, which reaches minimum for $\rho = \rho_{gs}$:

$$\frac{\delta E_{V^{ext}}}{\delta \rho(\boldsymbol{r})} = 0 \Longrightarrow \rho = \rho_{gs}.$$

  Clearly $E_{V^{ext}}[\rho] > E_{V^{ext}}[\rho_{gs}]$ if $\rho \neq \rho_{gs}$.

- The invertibility of the mapping $B : \Psi \longrightarrow \rho$ does not depend on $\hat{V}^{ext}$, which means that there exist a universal functional $F[\rho]$:

$$F[\rho] = E_{V^{ext}}[\rho] - \int d^3\boldsymbol{r} V^{ext}(\boldsymbol{r})\rho(\boldsymbol{r}) =$$
$$= \langle \Psi[\rho]|(\hat{T} + \hat{V}^{int})|\Psi[\rho]\rangle$$

  The universality means, that the functional F is characteristic for the particular system (depending on the mutual interaction between fermions, their mass, and the kinetic term).

1. Can we construct explicitly the form of functional $F[\rho]$?

2. Can we solve equations originating from the condition:

$$\frac{\delta E_{V^{ext}}}{\delta \rho(\boldsymbol{r})} \Rightarrow \frac{\delta F}{\delta \rho(\boldsymbol{r})} = V^{ext}(\boldsymbol{r}) \ ?$$

Kohn-Sham procedure: construct fictitious system of noninteracting fermions producing the same density:

KOHN W. and SHAM L. J., *Phys. Rev.*, **140** (1965) A1133.

$$\rho_0(\boldsymbol{r}) = \sum_{i=1}^{N} |\phi_i(\boldsymbol{r})|^2,$$

$$E^0_{V_0^{ext}}[\rho_0] = \langle \Psi[\rho_0] | (\hat{T} + \hat{V}_0 \quad) | \Psi[\rho_0] \rangle.$$

The minimization of the functional describing a noninteracting system leads to:

$$\frac{\delta E^0_{V_0} \quad [\rho]}{\delta \rho} = \frac{\delta T[\rho]}{\delta \rho} + V_0 \quad (\boldsymbol{r}) = \mu$$

And should lead to the same density as the minimization of the original functional:

$$\frac{\delta E_{V^{ext}}[\rho]}{\delta \rho} = \frac{\delta T[\rho]}{\delta \rho} + V^{ext}(\boldsymbol{r}) + \frac{\delta V^{int}[\rho]}{\delta \rho} = \mu,$$

Comparing these two conditions one gets the expression for the external potential V_0 for noninteracting system, generating the same density:

$$V_0 \quad (\boldsymbol{r}) = V^{ext}(\boldsymbol{r}) + \frac{\delta V^{int}[\rho]}{\delta \rho(\boldsymbol{r})} = V^{ext}(\boldsymbol{r}) + \sum_{\sigma'=\uparrow\downarrow} \int d^3\boldsymbol{r'} V^{int}_{\sigma,\sigma'}(\boldsymbol{r},\boldsymbol{r'})\rho(\boldsymbol{r'}) + \frac{\delta V^{corr}[\rho]}{\delta \rho(\boldsymbol{r})},$$

Kohn-Sham scheme:

$$\left(-\frac{\hbar^2}{2m}\nabla^2 + V_0 \quad (\boldsymbol{r})\right) \phi_i \boldsymbol{r}) = \epsilon_i \phi_i \boldsymbol{r}),$$

$$\rho(\boldsymbol{r}) = \sum_i \theta(\mu - \epsilon_i)|\phi_i(\boldsymbol{r})|^2,$$

$$V_0 \quad (\boldsymbol{r}) = V^{ext}(\boldsymbol{r}) + V^H(\boldsymbol{r}) + \frac{\delta V^{corr}[\rho]}{\delta \rho(\boldsymbol{r})}.$$

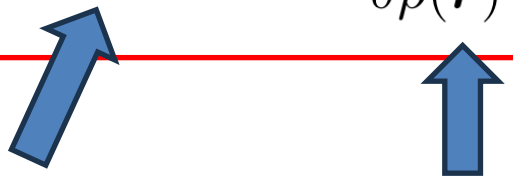

Hartree term

Exchange-correlation term

How to construct energy density functionals?

1. Postulate simple functional forms capturing the relevant physics with a number of parameters (the smaller is the better).
2. Use the ab-initio results to fix these parameters.
3. Validate the functional with different ab initio and experimental results.
4. Make interesting and verifiable physical predictions.

Superfluidity in Fermi systems

Presence of off-diagonal long range order (ODLRO):

$$\lim_{|\boldsymbol{r}_1-\boldsymbol{r}_2|\to\infty} \langle \hat{\psi}^\dagger_\uparrow(\boldsymbol{r}_1)\,\hat{\psi}^\dagger_\downarrow(\boldsymbol{r}_1)\,\hat{\psi}_\downarrow(\boldsymbol{r}_2)\,\hat{\psi}_\uparrow(\boldsymbol{r}_2)\rangle \neq 0$$

YANG C. N., *Rev. Mod. Phys.*, **34** (1962) 694.

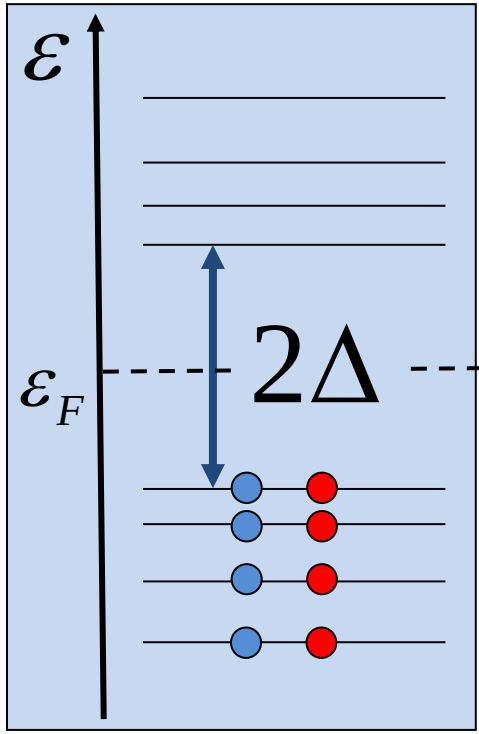

Cannot be reproduced in noninteracting Fermi system.

For example in the uniform Fermi gas:

$$g_2(\boldsymbol{r}) = \langle \hat{\psi}^\dagger_\uparrow(\boldsymbol{r}_1+\boldsymbol{r})\,\hat{\psi}^\dagger_\downarrow(\boldsymbol{r}_1+\boldsymbol{r})\,\hat{\psi}_\downarrow(\boldsymbol{r}_1)\,\hat{\psi}_\uparrow(\boldsymbol{r}_1)\rangle = \langle \hat{\psi}^\dagger_\uparrow(\boldsymbol{r}_1+\boldsymbol{r}))\,\hat{\psi}_\uparrow(\boldsymbol{r}_1)\rangle\langle \hat{\psi}^\dagger_\downarrow(\boldsymbol{r}_1+\boldsymbol{r}))\,\hat{\psi}_\downarrow(\boldsymbol{r}_1)\rangle$$

$$g_2(\boldsymbol{r}) = \left(\int_{k<k_F} \frac{d^3\boldsymbol{k}}{(2\pi)^3} e^{-i\boldsymbol{k}\cdot\boldsymbol{r}}\right)^2 = \left(\frac{1}{(2\pi)^3}\right)^2 \left(2\pi\int_0^{k_F} k^2dk \int_{-1}^{1} d\cos\theta e^{-ikr\cos\theta}\right)^2 =$$

$$= \left(\frac{1}{(2\pi)^3}\right)^2 \left(2\pi\int_0^{k_F} k^2dk \frac{-1}{ikr}\left(e^{-ikr}-e^{ikr}\right)\right)^2 = \left(\frac{1}{(2\pi)^3}\right)^2 \left(\frac{\pi}{r}\int_0^{k_F} dkk\sin(kr)\right)^2 =$$

$$= \left(\frac{1}{8\pi^2}\right)^2 \frac{1}{r^2}\left(\frac{-k_F\cos(k_Fr)}{r}+\frac{\sin(k_Fr)}{r^2}\right)^2 = \left(\frac{k_F^3}{8\pi^2}\frac{j_1(k_Fr)}{k_Fr}\right)^2.$$

$$\lim_{r\to\infty} g_2(r) = \lim_{r\to\infty}\left(\frac{k_F^3}{8\pi^2}\frac{j_1(k_Fr)}{k_Fr}\right)^2 = 0 \quad !$$

One needs to introduce another density!

Let us introduce anomalous density:

$$\chi_{\uparrow\downarrow}(\boldsymbol{r},\boldsymbol{r}') = \langle \hat{\psi}_{\downarrow}(\boldsymbol{r}')\,\hat{\psi}_{\uparrow}(\boldsymbol{r})\rangle$$

And therefore:

$$\lim_{|\boldsymbol{r}_1-\boldsymbol{r}_2|\to\infty} \langle \hat{\psi}^{\dagger}_{\uparrow}(\boldsymbol{r}_1)\,\hat{\psi}^{\dagger}_{\downarrow}(\boldsymbol{r}_1)\,\hat{\psi}_{\downarrow}(\boldsymbol{r}_2)\,\hat{\psi}_{\uparrow}(\boldsymbol{r}_2)\rangle = \chi^{*}_{\uparrow\downarrow}(\boldsymbol{r}_1)\chi_{\uparrow\downarrow}(\boldsymbol{r}_2)$$

Therefore now, besides the potential, which couples to the normal density:

$$E^{ext}[\rho] = -\sum_{\sigma=\uparrow\downarrow}\int d^3\boldsymbol{r} V^{ext}_{\sigma}(\boldsymbol{r})\rho_{\sigma}(\boldsymbol{r})$$

we introduce the external potential which couples to the anomalous density:

$$E^{ext}[\chi] = -\frac{1}{2}\sum_{\sigma,\sigma'=\uparrow\downarrow}\int d^3\boldsymbol{r}\int d^3\boldsymbol{r}'\left(\Delta^{ext}_{\sigma,\sigma'}{}^{*}(\boldsymbol{r},\boldsymbol{r}')\chi_{\sigma,\sigma'}(\boldsymbol{r},\boldsymbol{r}') + \Delta^{ext}_{\sigma,\sigma'}(\boldsymbol{r},\boldsymbol{r}')\chi^{*}_{\sigma,\sigma'}(\boldsymbol{r},\boldsymbol{r}')\right)$$

Similarly, like in the original HK theorem, one can show the existence of one-to-one correspondence between densities ρ and χ and the potentials $V_\sigma^{ext}(\boldsymbol{r}) - \mu_\sigma$ and $\Delta^{ext}_{\sigma,\sigma'}(\boldsymbol{r},\boldsymbol{r}')$. Thus the ground state densities can be obtained through the minimizations of the functional $E_{V^{ext},\Delta^{ext}}$

$$\frac{\delta E_{(V^{ext}-\mu),\Delta^{ext}}}{\delta\rho} = 0,$$
$$\frac{\delta E_{(V^{ext}-\mu),\Delta^{ext}}}{\delta\chi} = 0,$$

which determine ρ_{gs} and χ_{gs}.

Consequently, there exist a universal density functional depending on normal and anomalous Densities:

$$F[\rho,\chi] = E_{(V^{ext}-\mu),\Delta^{ext}} - E^{ext}[\rho] - E^{ext}[\chi] =$$
$$= \langle\Psi[\rho,\chi]|(\hat{T}+\hat{V}^{int})|\Psi[\rho,\chi]\rangle$$

Oliveira L. N., Gross E. K. U. and Kohn W., *Phys. Rev. Lett.*, **60** (1988) 2430.

Kohn-Sham scheme for Fermi superfluids

Fictitious noninteracting system:

$$\hat{H}_0 = \sum_{\sigma=\uparrow,\downarrow} \int d^3\boldsymbol{r} \hat{\psi}^\dagger_\sigma(\boldsymbol{r}) \left[-\frac{\hbar^2}{2m}\nabla^2 + V_{0\sigma}\ (\boldsymbol{r}) - \mu_\sigma \right] \hat{\psi}_\sigma(\boldsymbol{r}) +$$

$$+ \sum_{\sigma,\sigma'=\uparrow\downarrow} \int d^3\boldsymbol{r} \int d^3\boldsymbol{r}' \left(\Delta_{0\sigma\sigma'}(\boldsymbol{r},\boldsymbol{r}') \hat{\psi}^\dagger_\sigma\,(\boldsymbol{r})\, \hat{\psi}^\dagger_{-\sigma'}\,(\boldsymbol{r}') + \Delta^*_{0\sigma\sigma'}(\boldsymbol{r},\boldsymbol{r}') \hat{\psi}^\dagger_\sigma\,(\boldsymbol{r})\, \hat{\psi}^\dagger_{-\sigma'}\,(\boldsymbol{r}') \right)$$

Original interacting system in external potentials:

$$\hat{H} = \hat{T} + \hat{V}^{ext} + \hat{\Delta}^{ext} + \hat{V}^{int} = \sum_{\sigma=\uparrow,\downarrow} \int d^3\boldsymbol{r}\ \hat{\psi}^\dagger_\sigma(\boldsymbol{r}) \left[-\frac{\hbar^2}{2m}\nabla^2 + V^{ext}_\sigma(\boldsymbol{r}) - \mu_\sigma \right] \hat{\psi}_\sigma(\boldsymbol{r}) +$$

$$+ \sum_{\sigma,\sigma'=\uparrow\downarrow} \int d^3\boldsymbol{r} \int d^3\boldsymbol{r}' \left(\Delta^{ext}_{\sigma\sigma'}(\boldsymbol{r},\boldsymbol{r}') \hat{\psi}^\dagger_\sigma\,(\boldsymbol{r})\, \hat{\psi}^\dagger_{-\sigma'}\,(\boldsymbol{r}') + \Delta^{ext*}_{\sigma\sigma'}(\boldsymbol{r},\boldsymbol{r}') \hat{\psi}^\dagger_\sigma\,(\boldsymbol{r})\, \hat{\psi}^\dagger_{-\sigma'}\,(\boldsymbol{r}') \right)$$

$$+ \frac{1}{2} \sum_{\sigma,\sigma'=\uparrow,\downarrow} \int d^3\boldsymbol{r} \int d^3\boldsymbol{r}' \hat{\psi}^\dagger_\sigma\,(\boldsymbol{r})\, \hat{\psi}^\dagger_{-\sigma'}\,(\boldsymbol{r}')\, V^{int}_{\sigma,\sigma'}(\boldsymbol{r},\boldsymbol{r}') \hat{\psi}_{-\sigma'}\,(\boldsymbol{r}')\, \hat{\psi}_\sigma\,(\boldsymbol{r})\,,$$

Minimization of the energy of noninteracting system, leads to:

$$\sum_{\sigma'=\uparrow\downarrow}\int d^3\boldsymbol{r}'\mathcal{H}_{\sigma\sigma'}(\boldsymbol{r},\boldsymbol{r}')\begin{pmatrix}u_{n,\sigma'}(\boldsymbol{r}')\\ v_{n,\sigma'}(\boldsymbol{r}')\end{pmatrix}=E_n\begin{pmatrix}u_{n,\sigma}(\boldsymbol{r})\\ v_{n,\sigma}(\boldsymbol{r})\end{pmatrix},$$

$$\mathcal{H}=\begin{pmatrix}h_{\sigma\sigma'}(\boldsymbol{r},\boldsymbol{r}') & \Delta_{0\sigma,\sigma'}(\boldsymbol{r},\boldsymbol{r}')\\ \Delta^*_{0\sigma,\sigma'}(\boldsymbol{r},\boldsymbol{r}') & -h^*_{\sigma\sigma'}(\boldsymbol{r},\boldsymbol{r}')\end{pmatrix},$$

where:

$$h_{\sigma\sigma'}(\boldsymbol{r},\boldsymbol{r}')=\delta(\boldsymbol{r}-\boldsymbol{r}')\delta_{\sigma\sigma'}\left(-\frac{\hbar^2}{2m}\nabla^2+V_{0\sigma}\ \ (\boldsymbol{r})-\mu_\sigma\right)$$

And the requirement to generate the same densities as for interacting system implies:

$$V_0\quad(\boldsymbol{r})=V^{ext}(\boldsymbol{r})+\sum_{\sigma'}\int d^3\boldsymbol{r}'V^{int}_{\sigma,\sigma'}(\boldsymbol{r},\boldsymbol{r}')\rho(\boldsymbol{r}')+\frac{\delta V^{corr}[\rho,\chi]}{\delta\rho},$$

$$\Delta_{0\sigma\sigma'}(\boldsymbol{r},\boldsymbol{r}')=\Delta^{ext}_{\sigma\sigma'}(\boldsymbol{r},\boldsymbol{r}')+V^{int}_{\sigma,\sigma'}(\boldsymbol{r},\boldsymbol{r}')\chi_{\sigma,\sigma'}(\boldsymbol{r},\boldsymbol{r}')+\frac{\delta\Delta^{corr}[\rho,\chi]}{\delta\chi}$$

With densities defined as:

$$\rho_\sigma(\boldsymbol{r})=\sum_n|v_{n,\sigma}(\boldsymbol{r})|^2,$$

$$\chi_{\sigma,\sigma'}(\boldsymbol{r},\boldsymbol{r}')=\sum_n v^*_{n,\sigma}(\boldsymbol{r})u_{n,\sigma}(\boldsymbol{r}'),$$

$$\mathcal{B} = \begin{pmatrix} U & V^* \\ V & U^* \end{pmatrix}$$ Bogoliubov transformation (unitary)

$$\hat{\alpha}_n = \sum_{\sigma=\uparrow\downarrow} \int d^3\boldsymbol{r} \left(u^*_{n\sigma}(\boldsymbol{r})\hat{\psi}_\sigma(\boldsymbol{r}) + v^*_{n\sigma}(\boldsymbol{r})\hat{\psi}^\dagger_\sigma(\boldsymbol{r}) \right).$$

$$\hat{H}_0 = \sum_n E_n \hat{\alpha}^\dagger_n \hat{\alpha}_n + const.,$$

Note that the particle number is now not conserved: $[\hat{N}, \hat{H}_0] \neq 0$

$$\hat{N} = \sum_{\sigma=\uparrow,\downarrow} \int d^3\boldsymbol{r} \hat{\psi}^\dagger_\sigma(\boldsymbol{r})\hat{\psi}_\sigma(\boldsymbol{r}).$$

Local superfluid density approximation

$$\Delta_{\sigma,\sigma'}(\boldsymbol{r},\boldsymbol{r}') = \Delta_{\sigma,-\sigma}(\boldsymbol{r},\boldsymbol{r}')\delta(\boldsymbol{r}-\boldsymbol{r}').$$

Kohn, W., Gross, E.K.U., Oliveira, L.N. (1989): J. de Physique (Paris) **50**, 2601
S. Kurth, M. Marques, M. Lüders, E.K.U. Gross, Phys. Rev. Lett. 83 2628 (1999).

Integro-differential equations become differential equations!

$$\mathcal{H}\begin{pmatrix} u_{n,\uparrow}(\boldsymbol{r}) \\ u_{n,\downarrow}(\boldsymbol{r}) \\ v_{n,\uparrow}(\boldsymbol{r}) \\ v_{n,\downarrow}(\boldsymbol{r}) \end{pmatrix} = E_n \begin{pmatrix} u_{n,\uparrow}(\boldsymbol{r}) \\ u_{n,\downarrow}(\boldsymbol{r}) \\ v_{n,\uparrow}(\boldsymbol{r}) \\ v_{n,\downarrow}(\boldsymbol{r}) \end{pmatrix},$$

$$\mathcal{H} = \begin{pmatrix} h_{\uparrow\uparrow}(\boldsymbol{r}) - \mu_\uparrow & h_{\uparrow\downarrow}(\boldsymbol{r}) & 0 & \Delta(\boldsymbol{r}) \\ h_{\downarrow\uparrow}(\boldsymbol{r}) & h_{\downarrow\downarrow}(\boldsymbol{r}) - \mu_\downarrow & -\Delta(\boldsymbol{r}) & 0 \\ 0 & -\Delta^*(\boldsymbol{r}) & -h^*_{\uparrow\uparrow}(\boldsymbol{r}) + \mu_\uparrow & h_{\uparrow\downarrow}(\boldsymbol{r}) \\ \Delta^*(\boldsymbol{r}) & 0 & h_{\downarrow\uparrow}(\boldsymbol{r}) & -h^*_{\downarrow\downarrow}(\boldsymbol{r}) + \mu_\downarrow \end{pmatrix},$$

Problem: **anomalous density diverges**.

E.g. for the uniform system:

$$u_{\boldsymbol{k}\sigma}(\boldsymbol{r}) = \sqrt{\frac{1}{2}\left(1 + \frac{\frac{\hbar^2 k^2}{2m} - \mu}{\sqrt{\left(\frac{\hbar^2 k^2}{2m} - \mu\right)^2 + |\Delta|^2}}\right)} e^{i\boldsymbol{k}\cdot\boldsymbol{r}}$$

$$v_{\boldsymbol{k}\sigma}(\boldsymbol{r}) = \sqrt{\frac{1}{2}\left(1 - \frac{\frac{\hbar^2 k^2}{2m} - \mu}{\sqrt{\left(\frac{\hbar^2 k^2}{2m} - \mu\right)^2 + |\Delta|^2}}\right)} e^{i\boldsymbol{k}\cdot\boldsymbol{r}}$$

$$\begin{aligned} \chi_{\uparrow\downarrow}(\boldsymbol{r},\boldsymbol{r}') &= \frac{1}{(2\pi)^3}\int d^3\boldsymbol{k} v_{\boldsymbol{k}\uparrow}(\boldsymbol{r})^* u_{\boldsymbol{k}\downarrow}(\boldsymbol{r}') = \\ &= \frac{1}{2(2\pi)^3}\int d^3\boldsymbol{k} \frac{|\Delta| e^{-i\boldsymbol{k}\cdot(\boldsymbol{r}-\boldsymbol{r}')}}{\sqrt{\left(\frac{\hbar^2 k^2}{2m} - \mu\right)^2 + |\Delta|^2}} = \\ &= \frac{1}{(2\pi)^2}\frac{1}{|\boldsymbol{r}-\boldsymbol{r}'|}\int_0^\infty k dk \frac{\sin(k|\boldsymbol{r}-\boldsymbol{r}'|)}{\sqrt{\left(\frac{\hbar^2 k^2}{2m} - \mu\right)^2 + |\Delta|^2}}. \end{aligned}$$

$$\lim_{|\boldsymbol{r}-\boldsymbol{r}'|\to 0} \chi_{\uparrow\downarrow}(\boldsymbol{r},\boldsymbol{r}') \propto \frac{1}{|\boldsymbol{r}-\boldsymbol{r}'|}$$

Needs to be regularized!

Time dependent Density Functional Theory

The theorem relating density to many-body wave functions in the nonstationary situation has been proven by Runge and Gross . It says that that the densities $\rho(\boldsymbol{r})$ and $\rho'(\boldsymbol{r})$ evolving from some initial state $|\Psi(t=0)\rangle$ under the influence of two external potentials $V^{ext}(\boldsymbol{r},t)$ and $V^{'ext}(\boldsymbol{r},t)$ (sufficiently regular, i.e. expandable in Taylor series around $t=0$) will be different, unless $V^{ext}(\boldsymbol{r},t)-V^{'ext}(\boldsymbol{r},t)=f(t)$, where f is a function of time, only. Therefore, under this assumption there is one-to-one mapping between the density $\rho(\boldsymbol{r},t)$ and the potential $V^{ext}(\boldsymbol{r},t)$. The important component of the proof is the continuity relation $\frac{\partial\rho(\boldsymbol{r},t)}{\partial t}+\nabla\cdot\boldsymbol{j}(\boldsymbol{r},t)=0$ which has to be fulfilled.

RUNGE E. and GROSS E. K. U., *Phys. Rev. Lett.*, **52** (1984) 997.

Time dependent Kohn-Sham scheme:

$$\left(-\frac{\hbar^2}{2m}\nabla^2+V_0\quad(\boldsymbol{r},t)\right)\phi_i\boldsymbol{r},t)=i\hbar\frac{\partial}{\partial t}\phi_i\boldsymbol{r},t),$$

$$\rho(\boldsymbol{r},t)=\sum_{i=1}^{N}|\phi_i(\boldsymbol{r},t)|^2,$$

$$V_0\quad(\boldsymbol{r},t)=V^{ext}(\boldsymbol{r},t)+V^H\quad(\boldsymbol{r},t)+\frac{\delta V^{corr}[\rho]}{\delta\rho}(\boldsymbol{r},t).$$

Time dependent Kohn-Sham scheme for superfluids:

O.-J. Wacker, R. Kümmel, E.K.U. Gross, Phys. Rev. Lett. 73, 2915 (1994).

$$\sum_{\sigma'=\uparrow\downarrow}\left(\hat{h}_{\sigma\sigma'}(\boldsymbol{r},t)u_{\sigma'}(\boldsymbol{r},t)+\int d^3\boldsymbol{r}'\Delta_{0\sigma\sigma'}(\boldsymbol{r},\boldsymbol{r}',t)v_{n\sigma'}(\boldsymbol{r},t)\right)=i\hbar\frac{\partial}{\partial t}u_\sigma(\boldsymbol{r},t),$$

$$\sum_{\sigma'=\uparrow\downarrow}\left(-\hat{h}^*_{\sigma\sigma'}(\boldsymbol{r},t)v_{\sigma'}(\boldsymbol{r},t)+\int d^3\boldsymbol{r}'\Delta^*_{0\sigma\sigma'}(\boldsymbol{r},\boldsymbol{r}',t)u_{n\sigma'}(\boldsymbol{r},t)\right)=i\hbar\frac{\partial}{\partial t}v_\sigma(\boldsymbol{r},\boldsymbol{t})$$

Densities:

$$\rho_\sigma(\boldsymbol{r},t)=\sum_n|v_{n,\sigma}(\boldsymbol{r},t)|^2,$$

$$\chi_{\sigma,\sigma',t}(\boldsymbol{r},\boldsymbol{r}',t)=\sum_n v^*_{n,\sigma}(\boldsymbol{r},t)u_{n,\sigma}(\boldsymbol{r}',t),$$

Potentials:

$$V_{0\sigma}(\boldsymbol{r},t)=V^{ext}_\sigma(\boldsymbol{r},t)+\sum_{\sigma'}\int d^3\boldsymbol{r}'V^{int}_{\sigma,\sigma'}(\boldsymbol{r},\boldsymbol{r}')\rho_{\sigma'}(\boldsymbol{r}',t)+\frac{\delta V^{corr}[\rho,\chi,t]}{\delta\rho},$$

$$\Delta_{0\sigma\sigma'}(\boldsymbol{r},\boldsymbol{r}',t)=\Delta^{ext}_{\sigma\sigma'}(\boldsymbol{r},\boldsymbol{r}',t)+V^{int}_{\sigma,\sigma'}(\boldsymbol{r},\boldsymbol{r}')\chi_{\sigma,\sigma'}(\boldsymbol{r},\boldsymbol{r}',t)+\frac{\delta\Delta^{corr}[\rho,\chi,t]}{\delta\chi}$$

The main difference between static and time-dependent functionals is that the latter contains memory term *i.e.* dependence on the past densities.

J.F. Dobson, M.J. Brunner, E.K.U. Gross, Phys. Rev. Lett. 79 1905 (1997).

G. Vignale, C. A. Ullrich, S. Conti, Phys. Rev. Lett. 79 4878 (1997).

Adiabatic approximation (no memory effects)

$$\mathcal{H}(t)\begin{pmatrix}\tilde{u}_{n,\uparrow}(\boldsymbol{r},t)\\ \tilde{u}_{n,\downarrow}(\boldsymbol{r},\boldsymbol{t})\\ \tilde{v}_{n,\uparrow}(\boldsymbol{r},t)\\ \tilde{v}_{n,\downarrow}(\boldsymbol{r},\boldsymbol{t})\end{pmatrix}=i\hbar\frac{\partial}{\partial t}\begin{pmatrix}\tilde{u}_{n,\uparrow}(\boldsymbol{r},t)\\ \tilde{u}_{n,\downarrow}(\boldsymbol{r},t)\\ \tilde{v}_{n,\uparrow}(\boldsymbol{r},t)\\ \tilde{v}_{n,\downarrow}(\boldsymbol{r},t)\end{pmatrix},$$

$$\mathcal{H}(t)=\begin{pmatrix}h_{\uparrow\uparrow}(\boldsymbol{r},t) & h_{\uparrow\downarrow}(\boldsymbol{r},t) & 0 & \tilde{\Delta}_0(\boldsymbol{r},t)\\ h_{\downarrow\uparrow}(\boldsymbol{r},t) & h_{\downarrow\downarrow}(\boldsymbol{r},t) & -\tilde{\Delta}_0(\boldsymbol{r},t) & 0\\ 0 & -\tilde{\Delta}_0^*(\boldsymbol{r}) & -h^*_{\uparrow\uparrow}(\boldsymbol{r},t) & -h^*_{\uparrow\downarrow}(\boldsymbol{r},t)\\ \tilde{\Delta}_0^*(\boldsymbol{r}) & 0 & -h^*_{\downarrow\uparrow}(\boldsymbol{r},t) & -h^*_{\downarrow\downarrow}(\boldsymbol{r},t)\end{pmatrix},$$

Adiabatic approximation, although simplifies the equations, affects dissipative effects.

C. A. Ullrich, *Time-dependent density-functional theory: concepts and applications*, Oxford University Press, (2012).

Note that the expectation value of the particle number is conserved, if there is no external pairing potential:

$$\frac{dN}{dt}=\frac{\partial}{\partial t}\sum_n\sum_{\sigma=\uparrow\downarrow}\int d^3\boldsymbol{r}|v_{n\sigma}(\boldsymbol{r},t)|^2=\frac{d}{dt}Tr(\rho).$$

$$\frac{dN}{dt}=2Im\left(Tr(\Delta^{ext*}\chi)\right)/\hbar$$

Summarizing: Time Dependent DFT Basics

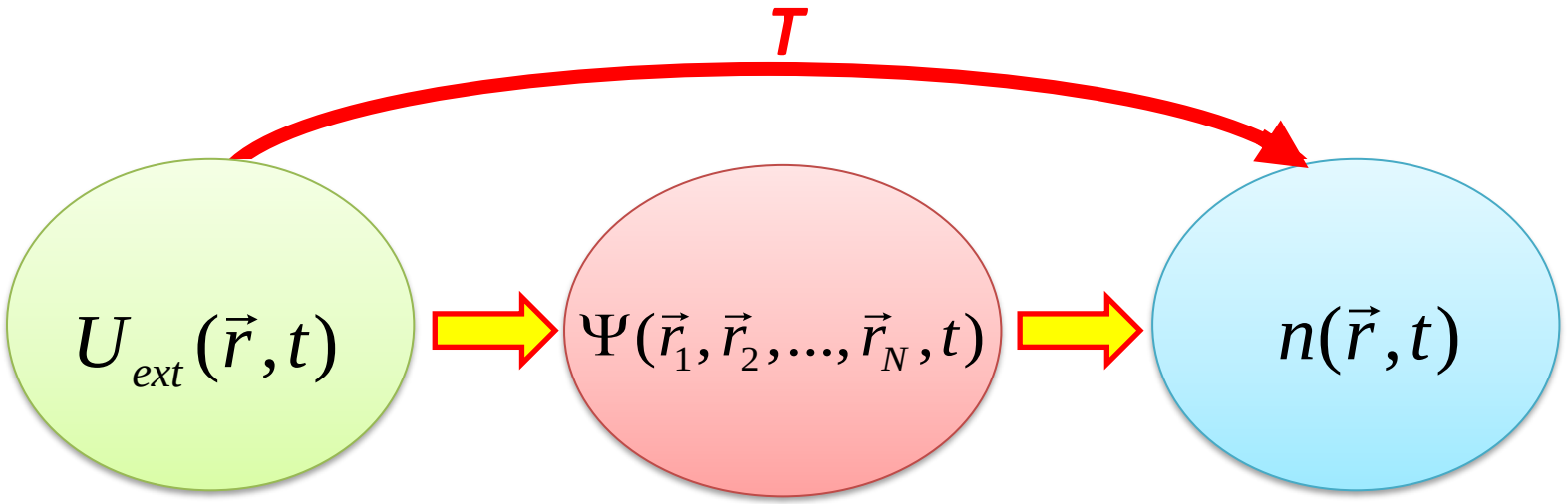

Runge-Gross mapping(1984):

$$i\hbar\frac{\partial}{\partial t}|\psi(t)\rangle = \hat{H}|\psi(t)\rangle, \quad |\psi_0\rangle = |\psi(t_0)\rangle$$

$$\frac{\partial n}{\partial t} + \nabla\cdot\vec{j} = 0$$

$$n(\vec{r}) \leftrightarrow e^{i\alpha(t)}\Psi[n](\vec{r}_1,\vec{r}_2,...,\vec{r}_N)$$

TDDFT variational principle also exists but it is more tricky:

$$F[\psi_0,n] = \int_{t_0}^{t_1}\langle\psi[n]|\left(i\hbar\frac{\partial}{\partial t} - \hat{H}\right)|\psi[n]\rangle\, dt$$

E. Runge, E.K.U Gross, PRL 52, 997 (1984)
B.-X. Xu, A.K. Rajagopal, PRA 31, 2682 (1985)
G. Vignale, PRA77, 062511 (2008)

Pairing correlations in DFT

One may extend DFT to superfluid systems by defining the pairing field:

$$\Delta(\mathbf{r}\sigma,\mathbf{r}'\sigma') = -\frac{\delta E(\rho,\chi)}{\delta\chi^*(\mathbf{r}\sigma,\mathbf{r}'\sigma')}.$$

L. N. Oliveira, E. K. U. Gross, and W. Kohn, Phys. Rev. Lett. 60 2430 (1988).

O.-J. Wacker, R. Kümmel, E.K.U. Gross, Phys. Rev. Lett. 73, 2915 (1994).

Triggered by discovery of high-Tc superconductors

and introducing anomalous density $\chi(\mathbf{r}\sigma,\mathbf{r}'\sigma') = \langle\hat{\psi}_{\sigma'}(\mathbf{r}')\hat{\psi}_{\sigma}(\mathbf{r})\rangle$

However in the limit of the local field these quantities diverge unless one renormalizes the coupling constant:

$$\begin{aligned}\Delta(\mathbf{r}) &= g_{eff}(\mathbf{r})\chi_c(\mathbf{r})\\ \frac{1}{g_{eff}(\mathbf{r})} &= \frac{1}{g(\mathbf{r})} - \frac{mk_c(\mathbf{r})}{2\pi^2\hbar^2}\left(1 - \frac{k_F(\mathbf{r})}{2k_c(\mathbf{r})}\ln\frac{k_c(\mathbf{r})+k_F(\mathbf{r})}{k_c(\mathbf{r})-k_F(\mathbf{r})}\right)\end{aligned}$$

which ensures that the term involving the kinetic and the pairing energy density is finite:

$$\frac{\tau_c(r)}{2m} - \Delta(r)\chi_c(r), \qquad \tau_c(r) = \nabla\cdot\nabla'\rho_c(r,r')\big|_{r=r'}$$

A. Bulgac, Y. Yu, Phys. Rev. Lett. 88 (2002) 042504

A. Bulgac, Phys. Rev. C65 (2002) 051305

It allows to reduce the size of the problem for static calculations by introducing the energy cutoff

Pairing correlations in time-dependent superfluid local density approximation (TDSLDA)

$$S = \int_{t_0}^{t_1} \left(\left\langle 0(t) \left| i \frac{d}{dt} \right| 0(t) \right\rangle - E[\rho(t), \chi(t)] \right) dt$$

Stationarity requirement produces the set of equations:

$$i\hbar \frac{\partial}{\partial t} \begin{pmatrix} U_\mu(\mathbf{r},t) \\ V_\mu(\mathbf{r},t) \end{pmatrix} = \begin{pmatrix} h(\mathbf{r},t) & \Delta(\mathbf{r},t) \\ \Delta^*(\mathbf{r},t) & -h^*(\mathbf{r},t) \end{pmatrix} \begin{pmatrix} U_\mu(\mathbf{r},t) \\ V_\mu(\mathbf{r},t) \end{pmatrix},$$

$$B(t) = \begin{pmatrix} U(t) & V^*(t) \\ V(t) & U^*(t) \end{pmatrix} = \exp[iG(t)] \qquad G(t) = \begin{pmatrix} h(t) & \Delta(t) \\ \Delta^\dagger(t) & -h^*(t) \end{pmatrix}$$

Orthogonality and completeness has to be fulfilled: $B^\dagger(t)B(t) = B(t)B^\dagger(t) = I,$

In order to fulfill the completeness relation of Bogoliubov transform all states need to be evolved!
Otherwise Pauli principle is violated, i.e. the evolved densities do not describe a fermionic system (spurious bosonic effects are introduced).

Consequence: the computational cost increases considerably.

P. Magierski, *Nuclear Reactions and Superfluid Time Dependent Density Functional Theory*, Frontiers in Nuclear and Particle Physics vol. 2, 57 (2019)
A. Bulgac, *Time-Dependent Density Functional Theory and Real-Time Dynamics of Fermi Superfluids*, Ann. Rev. Nucl. Part. Sci. 63, 97 (2013)

Solving time-dependent problem for superfluids...

The real-time dynamics is given by equations, which are formally equivalent to the Time-Dependent HFB (TDHFB) or Time-Dependent Bogolubov-de Gennes (TDBdG) equations

$$h \sim f_1(n,\nu,\ldots)\boldsymbol{\nabla}^2 + \boldsymbol{f}_2(n,\nu,\ldots)\cdot\boldsymbol{\nabla} + f_3(n,\nu,\ldots)$$

$$i\hbar\frac{\partial}{\partial t}\begin{pmatrix} u_{n,a}(\boldsymbol{r},t) \\ u_{n,b}(\boldsymbol{r},t) \\ v_{n,a}(\boldsymbol{r},t) \\ v_{n,b}(\boldsymbol{r},t) \end{pmatrix} = \begin{pmatrix} h_a(\boldsymbol{r},t) & 0 & 0 & \Delta(\boldsymbol{r},t) \\ 0 & h_b(\boldsymbol{r},t) & -\Delta(\boldsymbol{r},t) & 0 \\ 0 & -\Delta^*(\boldsymbol{r},t) & -h_a^*(\boldsymbol{r},t) & 0 \\ \Delta^*(\boldsymbol{r},t) & 0 & 0 & -h_b^*(\boldsymbol{r},t) \end{pmatrix} \begin{pmatrix} u_{n,a}(\boldsymbol{r},t) \\ u_{n,b}(\boldsymbol{r},t) \\ v_{n,a}(\boldsymbol{r},t) \\ v_{n,b}(\boldsymbol{r},t) \end{pmatrix}$$

We explicitly track fermionic degrees of freedom!

where *h* and Δ depends on "densities":

$$n_\sigma(\boldsymbol{r},t) = \sum_{E_n<E_c} |v_{n,\sigma}(\boldsymbol{r},t)|^2, \qquad \tau_\sigma(\boldsymbol{r},t) = \sum_{E_n<E_c} |\nabla v_{n,\sigma}(\boldsymbol{r},t)|^2,$$

$$\chi_c(r,t) = \sum_{E_n<E_c} u_{n,\uparrow}(\boldsymbol{r},t)v^*_{n,\downarrow}(\boldsymbol{r},t), \qquad \boldsymbol{j}_\sigma(\boldsymbol{r},t) = \sum_{E_n<E_c} \mathrm{Im}[v^*_{n,\sigma}(\boldsymbol{r},t)\nabla v_{n,\sigma}(\boldsymbol{r},t)],$$

$$\begin{aligned} \Delta(\mathbf{r}) &= g_{eff}(\mathbf{r})\chi_c(\mathbf{r}) \\ \frac{1}{g_{eff}(\mathbf{r})} &= \frac{1}{g(\mathbf{r})} - \frac{mk_c(\mathbf{r})}{2\pi^2\hbar^2}\left(1 - \frac{k_F(\mathbf{r})}{2k_c(\mathbf{r})}\ln\frac{k_c(\mathbf{r})+k_F(\mathbf{r})}{k_c(\mathbf{r})-k_F(\mathbf{r})}\right) \end{aligned}$$

A. Bulgac, Y. Yu, Phys. Rev. Lett. 88 (2002) 042504
A. Bulgac, Phys. Rev. C65 (2002) 051305

huge number of nonlinear coupled 3D Partial Differential Equations
(in practice n=1,2,…, 10^5 - 10^6)

- P. Magierski, *Nuclear Reactions and Superfluid Time Dependent Density Functional Theory*, Frontiers in Nuclear and Particle Physics, vol. 2, 57 (2019)
- A. Bulgac, *Time-Dependent Density Functional Theory and Real-Time Dynamics of Fermi Superfluids*, Ann. Rev. Nucl. Part. Sci. 63, 97 (2013)
- A. Bulgac, M.M. Forbes, P. Magierski, Lecture Notes in Physics, Vol. 836, Chap. 9, p.305-373 (2012)

Present computing capabilities:

- full 3D (unconstrained) superfluid dynamics
- spatial mesh up to 100^3
- max. number of particles of the order of 10^4
- up to 10^6 time steps

(for cold atomic systems – time scale: a few ms
for nuclei – time scale: 100 zs)

Superconducting systems of interest

$\frac{\Delta}{\varepsilon_F} \le 0.5$

Ultracold atomic (fermionic) gases. Unitary regime.

Dynamics of quantum vortices, solitonic excitations, quantum turbulence

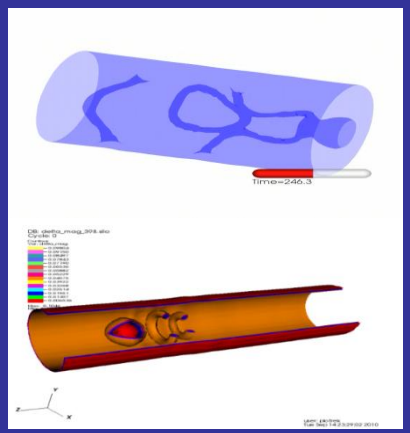

$\frac{\Delta}{\varepsilon_F} \le 0.1-0.2$

Astrophysical applications.

Modelling of neutron star interior (glitches): vortex dynamics, dynamics of inhomogeneous nuclear matter.

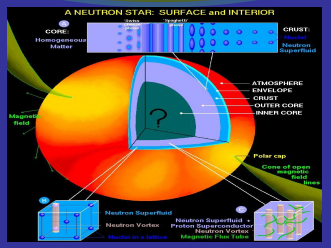

$\frac{\Delta}{\varepsilon_F} \le 0.03$

Nuclear physics.

Induced nuclear fission, fusion, collisions.

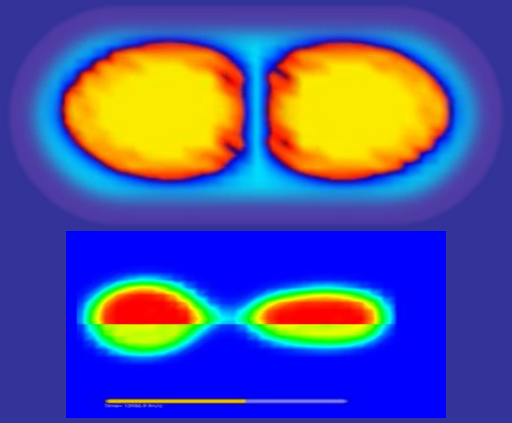

$\frac{\Delta}{\varepsilon_F}$ - Pairing gap to Fermi energy ratio

Nuclear Skyrme functional

$$E = \int d^3r \mathcal{H}(\mathbf{r})$$

where

$$\begin{aligned}\mathcal{H}(\mathbf{r}) &= C^{\rho}\rho^2 + C^{s}\vec{s}\cdot\vec{s} + C^{\Delta\rho}\rho\nabla^2\rho + C^{\Delta s}\vec{s}\cdot\nabla^2\vec{s} + C^{\tau}(\rho\tau - \vec{j}\cdot\vec{j}) + \\ &+ C^{sT}(\vec{s}\cdot\vec{T} - \mathbf{J}^2) + C^{\nabla J}(\rho\vec{\nabla}\cdot\vec{J} + \vec{s}\cdot(\vec{\nabla}\times\vec{j})) + C^{\nabla s}(\vec{\nabla}\cdot\vec{s})^2 + C^{\gamma}\rho^{\gamma} - \Delta\chi^*\end{aligned}$$

where

$$\begin{aligned}J_i &= \sum_{k,l}\epsilon_{ikl}\mathbf{J}_{kl} \\ \mathbf{J}^2 &= \sum_{k,l}\mathbf{J}_{kl}^2\end{aligned}$$

- density: $\rho(\mathbf{r}) = \rho(\mathbf{r},\mathbf{r}')|_{r=r'}$
- spin density: $\vec{s}(\mathbf{r}) = \vec{s}(\mathbf{r},\mathbf{r}')|_{r=r'}$
- current: $\vec{j}(\mathbf{r}) = \frac{1}{2i}(\vec{\nabla} - \vec{\nabla}')\rho(\mathbf{r},\mathbf{r}')|_{r=r'}$
- spin current (2nd rank tensor): $\mathbf{J}(\mathbf{r}) = \frac{1}{2i}(\vec{\nabla} - \vec{\nabla}')\otimes\vec{s}(\mathbf{r},\mathbf{r}')|_{r=r'}$
- kinetic energy density: $\tau(\mathbf{r}) = \vec{\nabla}\cdot\vec{\nabla}'\rho(\mathbf{r},\mathbf{r}')|_{r=r'}$
- spin kinetic energy density: $\vec{T}(\mathbf{r}) = \vec{\nabla}\cdot\vec{\nabla}'\vec{s}(\mathbf{r},\mathbf{r}')|_{r=r'}$
- anomalous (pairing) density: $\chi(\mathbf{r}) = \chi(\mathbf{r},\mathbf{r}')|_{r=r'}$

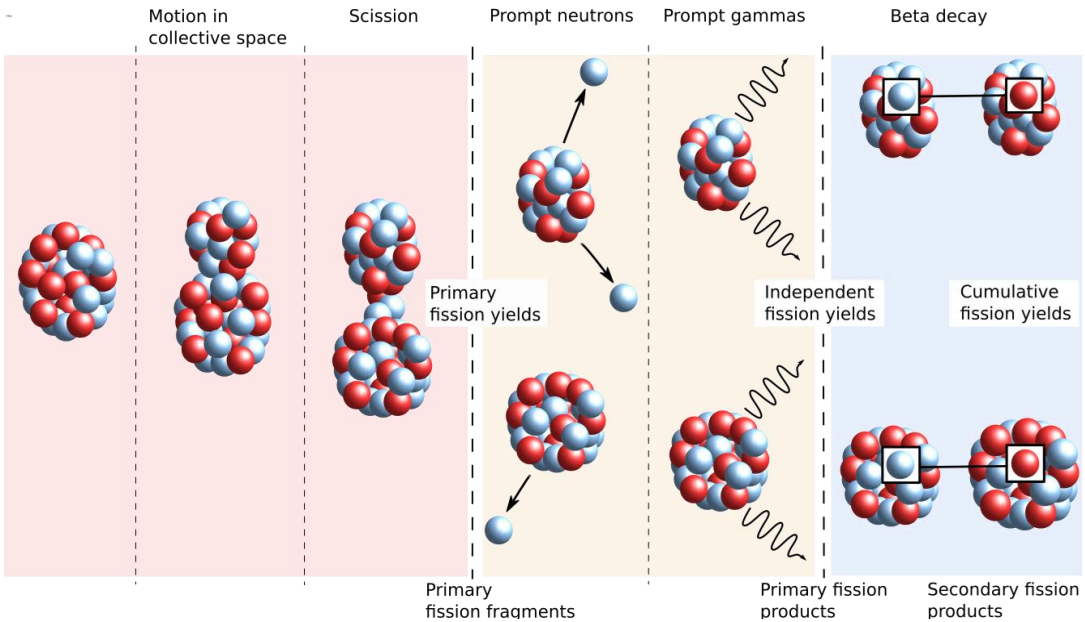

From LLNL-PRES-758023

Nuclear dynamics of interest

Potential energy versus deformation

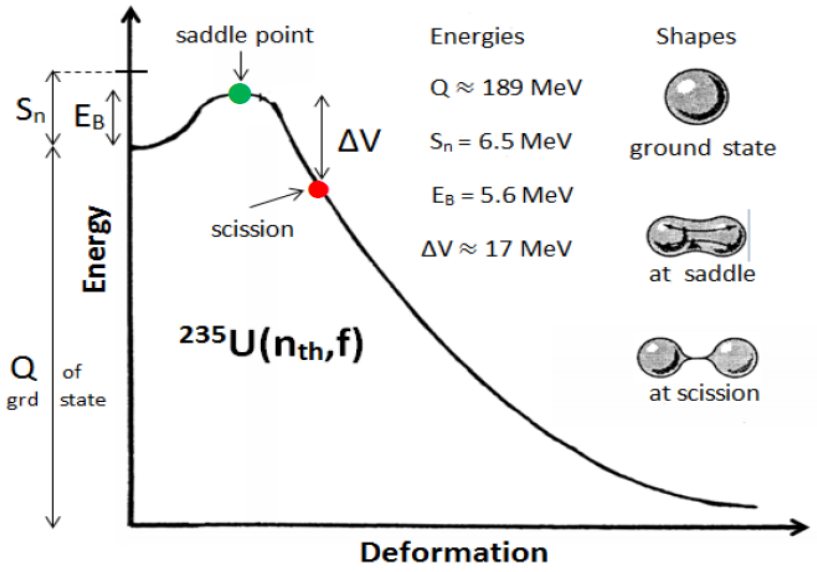

From F. Gonnenwein FIESTA2014

Estimation of characteristic time scales for low energy fission (<10MeV):

Ground state to saddle	**-**	**1 000 000 zs**
Saddle to scission	**-**	**10-100 zs**
Acceleration of fission fragments to 90% of their final velocity	**-**	**10 zs**
Neutron evaporation	**-**	**1 000 zs**

Typical framework for the theoretical description of nuclear dynamics (of medium or heavy nuclei) at low energies

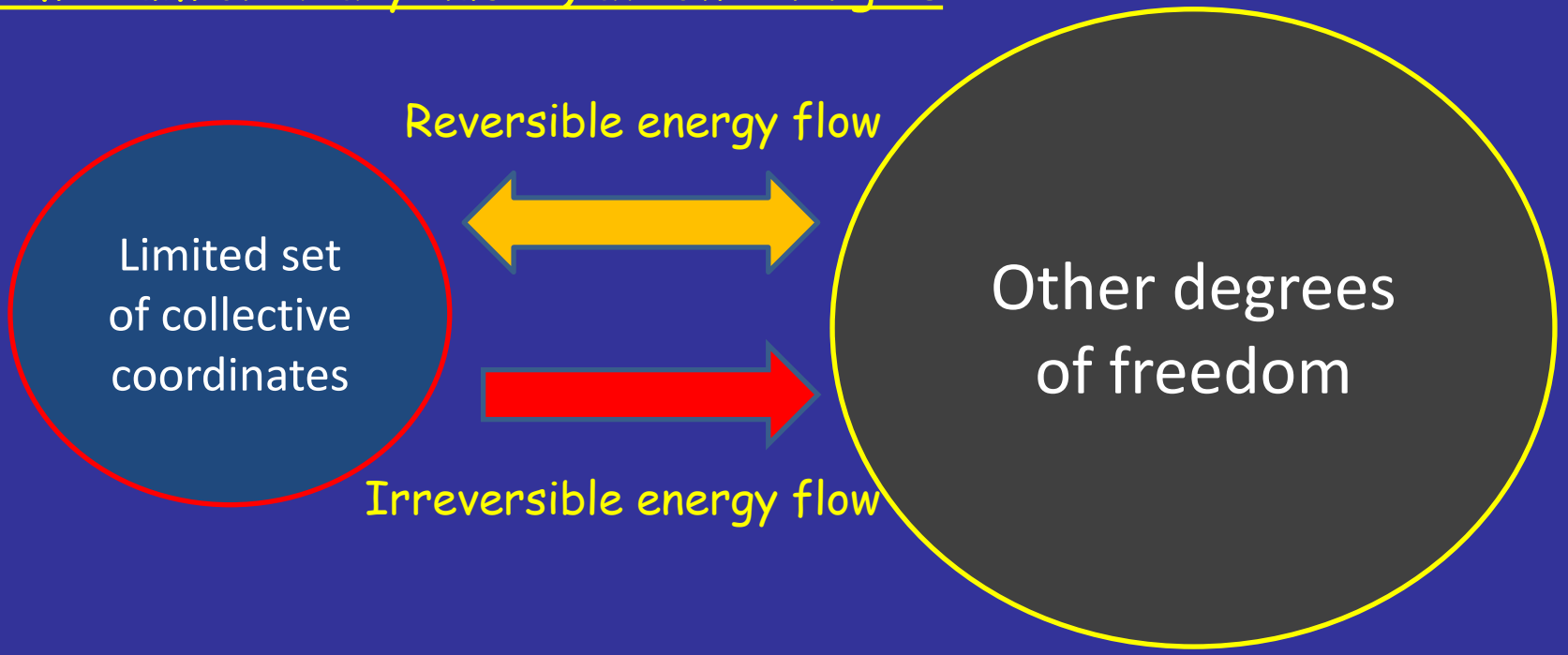

Reversible energy flow is determined by: mass parameters, potential energy surface.

Irreversible energy flow is determined by friction coefficients and leads to collective energy dissipation.

Consequently, questions associated with nuclear dynamics are directly related to the treatment of various components of this framework:

- Determination of the set of collective variables and their eq. of motion
- Treatment of other degrees of freedom
- Assumptions concerning energy flows

Physics of nuclear superfluid dynamics

Single-particle levels

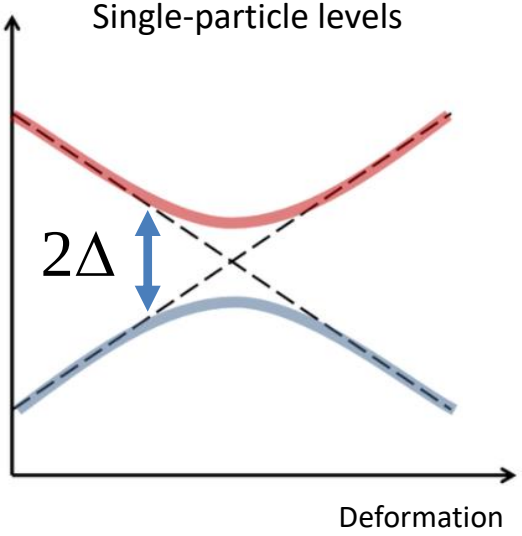

Quasiparticle energy:

$$E_{qp} = \sqrt{(\varepsilon - \mu)^2 + |\Delta|^2}$$

Potential energy surface

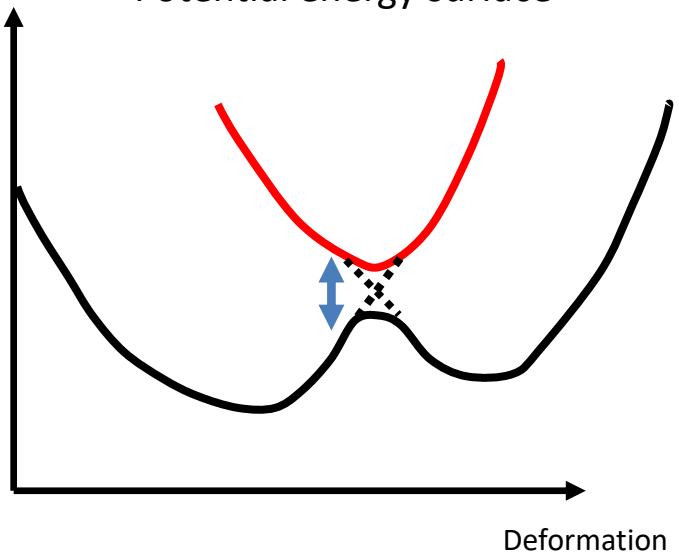

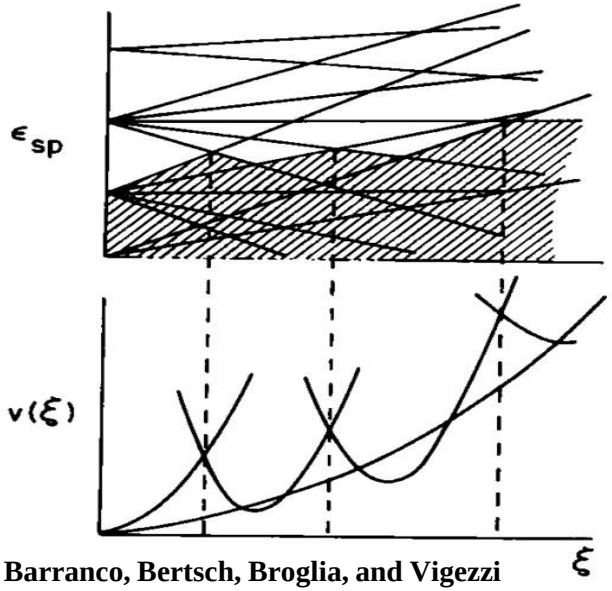

From Barranco, Bertsch, Broglia, and Vigezzi
Nucl. Phys. A512, 253 (1990)

As a consequence of pairing correlations large amplitude nuclear motion becomes more adiabatic.

While a nucleus elongates its Fermi surface becomes oblate and its sphericity must be restored
Hill and Wheeler, PRC, 89, 1102 (1953)
Bertsch, PLB, 95, 157 (1980)

Advantages of TDDFT for nuclear reactions

- The same framework describes various limits: eg. linear and highly nonlinear regimes, adiabatic and nonadiabatic (dynamics far from equilibrium).
- Interaction with basically any external probe (weak or strong) easy to implement.
- TDDFT does not require introduction of hard-to-define collective degrees of freedom and there are no ambiguities arising from defining potential energy surfaces and inertias.
- One-body dissipation, the window and wall dissipation mechanisms are automatically incorporated into the theoretical framework.
- All shapes are allowed and the nucleus chooses dynamically the path in the shape space, the forces acting on nucleons are determined by the nucleon distributions and velocities, and the nuclear system naturally and smoothly evolves into separated fission fragments.
- There is no need to introduce such unnatural quantum mechanical concepts as "rupture" and there is no worry about how to define the scission configuration.

Nuclear fission dynamics within TDDFT

Potential energy versus deformation

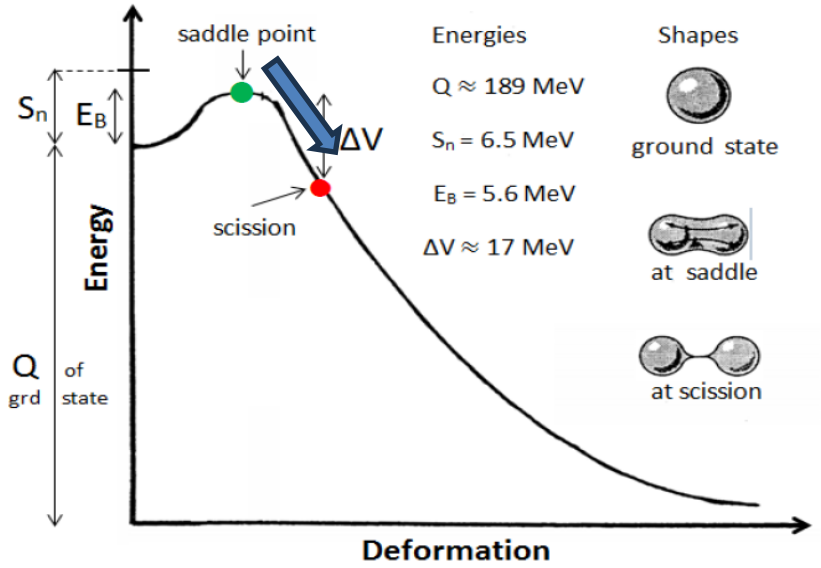

From F. Gonnenwein FIESTA2014

Estimation of characteristic time scales for low energy fission (<10MeV):

Ground state to saddle - 1 000 000 zs
Saddle to scission - 10-100 zs
Acceleration of fission fragments to 90% of their final velocity - 10 zs
Neutron evaporation - 1 000 zs
1 zs = 10^{-21} s

Total kinetic energy of the fragments

Induced fission of ^{240}*Pu within TDSLDA*

E^* (MeV)	E_n (MeV)	TKE_{TDSLDA} (MeV)	TKE_{syst} (MeV)	err (%)	Z_L	N_L
8.08	1.542	173	177.26	1.95	40.825	62.246
9.60	3.063	174	176.73	1.13	40.500	61.536
10.10	3.560	179	176.56	1.43	41.625	62.783
10.57	4.032	173	176.39	1.55	40.092	61.256
10.58	4.043	173	176.39	1.70	40.146	61.388
10.58	4.047	175	176.39	0.72	40.313	61.475
10.60	4.065	174	176.38	0.92	40.904	62.611
11.07	4.534	176	176.22	0.14	41.495	63.134
11.56	5.024	175	176.05	0.51	40.565	61.894
12.05	5.515	176	175.88	0.49	40.412	61.809
12.15	5.610	176	175.84	0.29	40.355	61.695
12.16	5.626	176	175.84	0.15	41.386	62.764

Calculated TKEs reproduce experimental data with accuracy < 2%

A. Bulgac, P.Magierski, K.J. Roche, and I. Stetcu, Phys. Rev. Lett. 116, 122504 (2016)

Fission dynamics of ^{240}Pu

Initial configuration of ^{240}Pu is prepared beyond the barrier at quadrupole deformation *Q=165b* and excitation energy *E=8.08 MeV*:

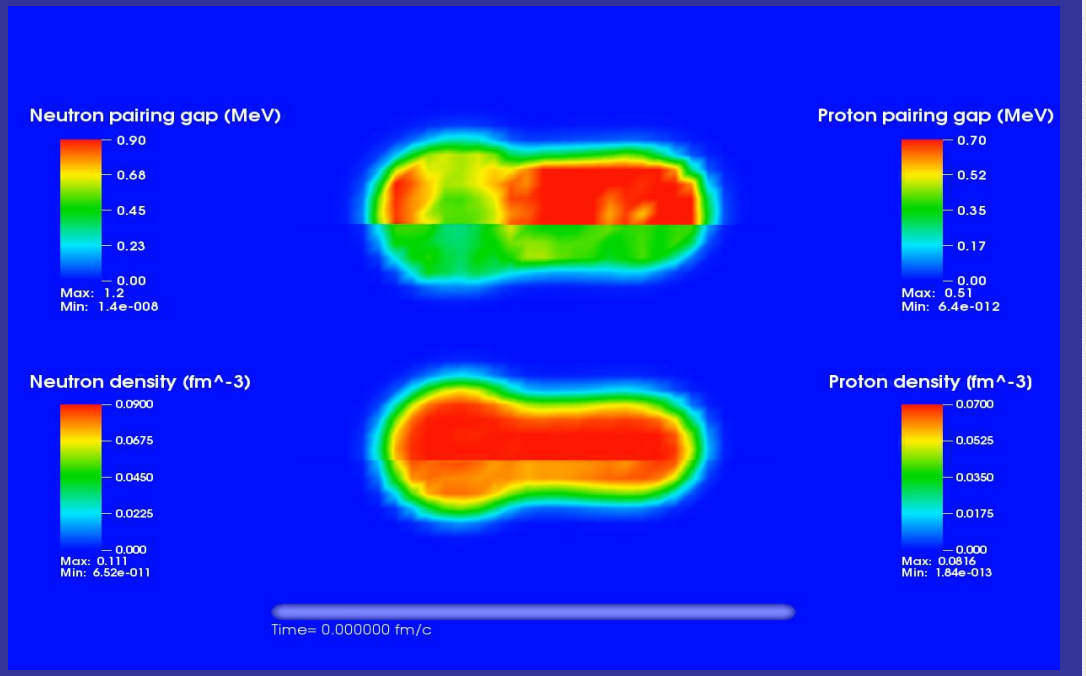

Accelerations in quadrupole and octupole moments along the fission path

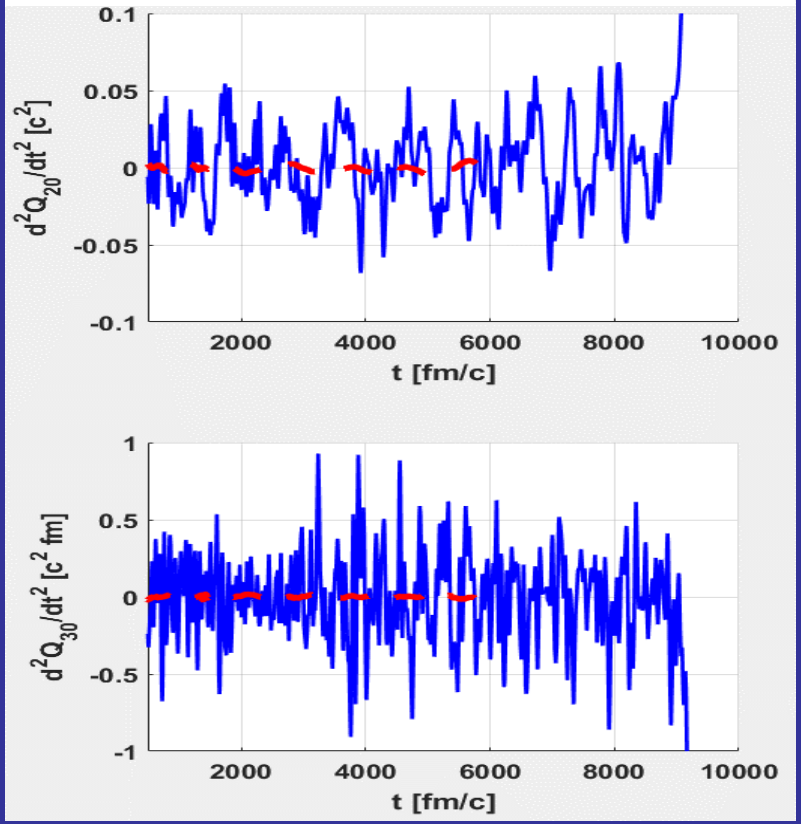

Note that despite the fact that nucleus is already beyond the saddle point the collective motion on the time scale of 1000 fm/c and larger is characterized by the constant velocity (*see red dashed line for an average acceleration*) till the very last moment before splitting. On times scales, of the order of 300 fm/c and shorter, the collective motion is a subject to random-like kicks indicating strong coupling to internal d.o.f

A. Bulgac, P. Magierski, K.J. Roche, and I. Stetcu, Phys. Rev. Lett. 116, 122504 (2016)

Nuclear induced fission dynamics:

It is important to realize that these results indicate that the motion is not adiabatic, although it is slow.

Although the average collective velocity is constant till the very last moment before scission, the system heats up as the energy flows irreversibly from collective to intrinsic degrees of freedom.

This may create problems for approaches based on ATDHF(B) or TDGCM as no irreversible energy transfer between collective and Intrinsic is possible there.

TDSLDA trajectories on the collective potential surface originating from various initial configurations

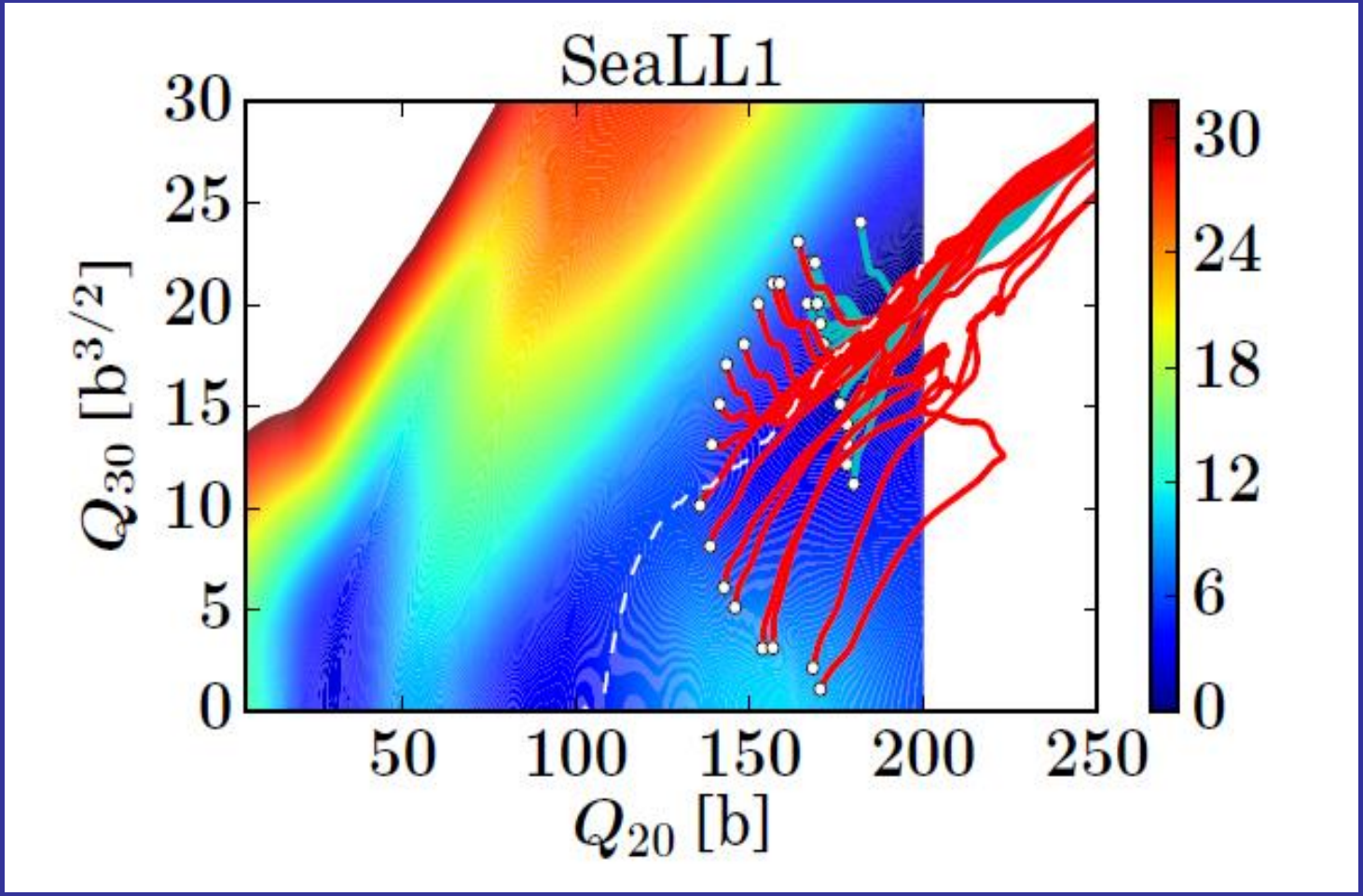

A. Bulgac, et al. Phys. Rev. *C* 100, 034615 (2019)

The final scission configuration is relatively independent on the initial condition (providing it starts at or beyond the saddle point).

One needs a kind of stochastic extension to account for fluctuations to be able to reproduce fragment mass distribution.

Remarks on the fragment kinetic and excitation energy sharing within the TDDFT

In the to-date approaches it is usually assumed that the excitation energy has 3 components (Schmidt&Jurado:Phys.Rev.C83:061601,2011 Phys.Rev.C83:014607,2011):

- deformation energy
- collective energy (energy stored in collective modes)
- intrinsic energy (specified by the temperature)

It is also assumed that the intrinsic part of the energy is sorted according to the total entropy maximization of two nascent fragments (i.e. according to temperatures, level densities) and the fission dynamics does not matter.

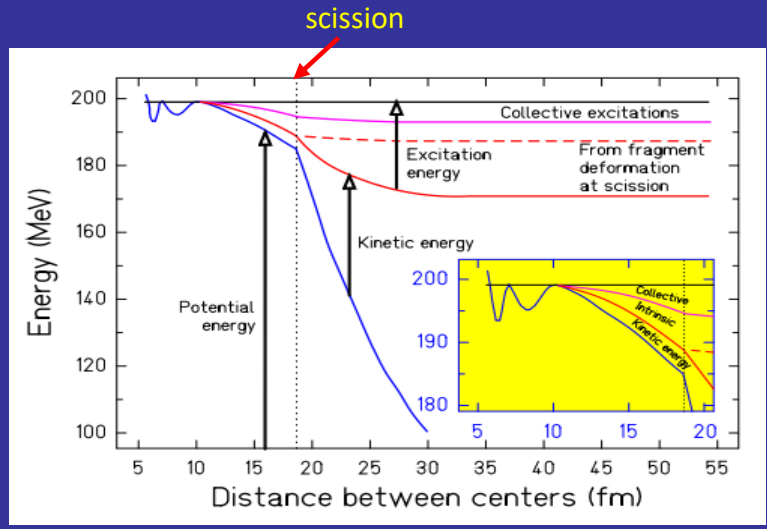

Schmidt&Jurado:Phys.Rev.C83:061601,2011

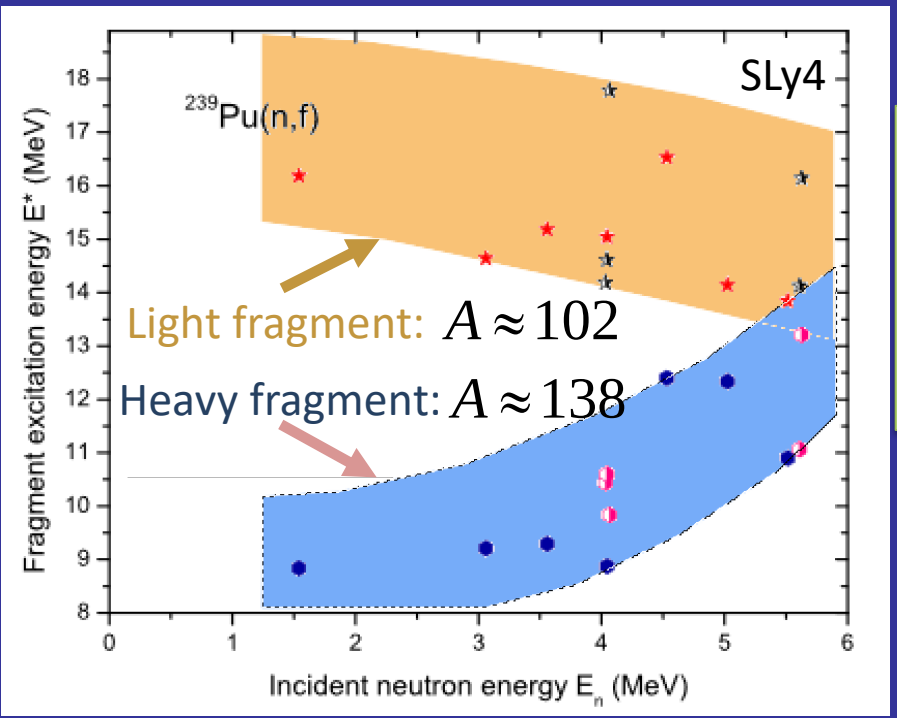

In TDDFT such a decomposition can be performed as well.
The intrinsic energy in TDDFT will be partitioned dynamically (no sufficient time for equilibration).

Short (selective) history:

- ✓In 1999 DeMarco and Jin created a degenerate atomic Fermi gas.
- ✓In 2005 Zwierlein/Ketterle group observed quantum vortices which survived when passing from BEC to unitarity – evidence for superfluidity!

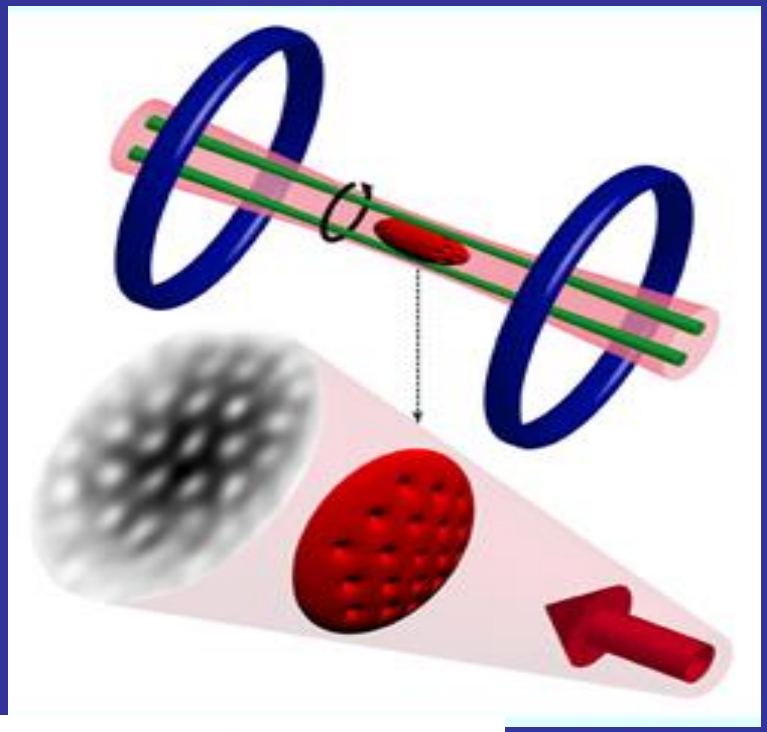

system of fermionic ^6Li atoms

Feshbach resonance: B=834G

BEC side: a>0

BCS side a<0

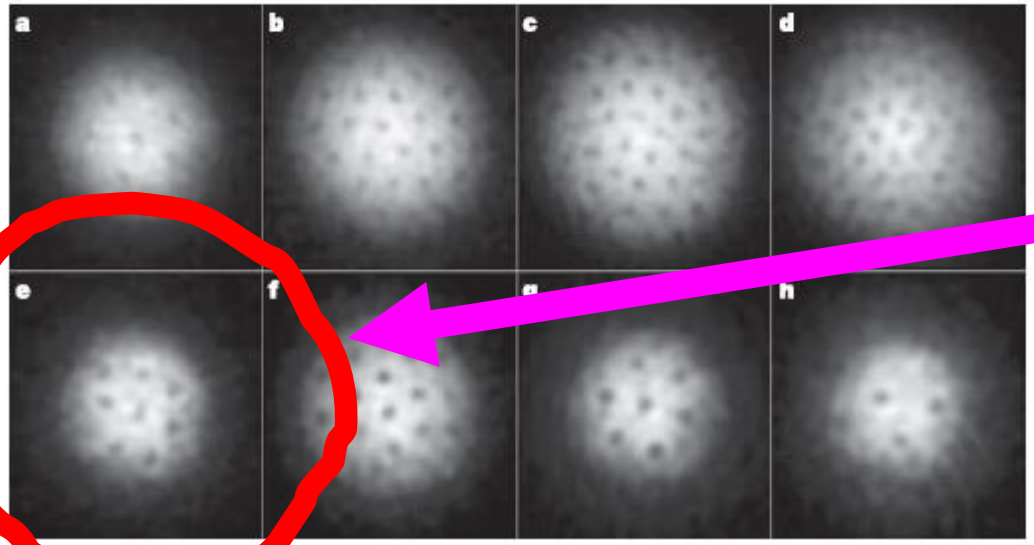

UNITARY REGIME

Figure 2 | Vortices in a strongly ... fermionic atoms on the BEC- and the BCS-side of the Feshbach resonance. At the given field, the cloud of lithium atoms was stirred for 300 ms (**a**) or 500 ms (**b**–**h**) followed by an equilibration time of 500 ms. After 2 ms of ballistic expansion, the magnetic field was ramped to 735 G for imaging (s... magnetic fields were 740 G (**a**), 766 G (**b**), 792 G (**c**... 843 G (**f**), 853 G (**g**) and 863 G (**h**). The field of vie... 880 μm × 880 μm.

M.W. Zwierlein *et al.*, Nature, 435, 1047 (2005)

BCS – BEC crossover

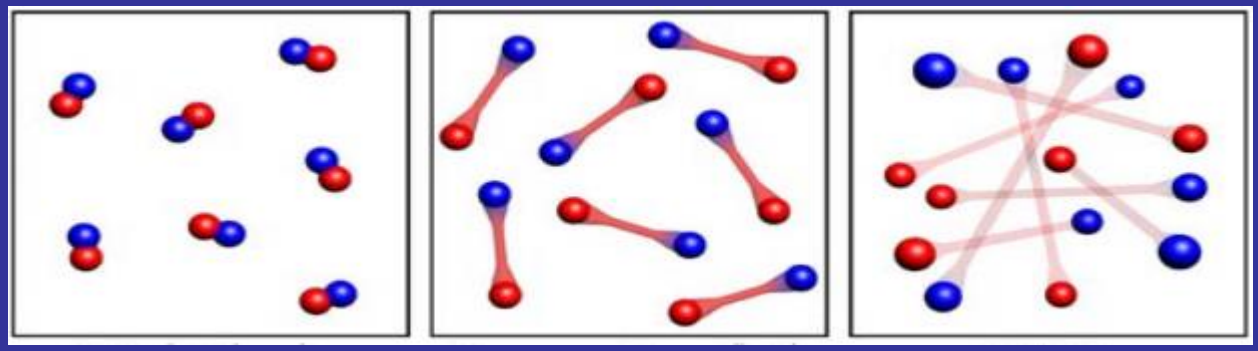

Interaction strength

Bose-Einstein condensate (BEC)
(bound fermion pairs = bosons)

Superconductor
(Cooper pairs)

No phase transition between BCS regimes and BEC regime!

Eagles (1969), Leggett (1980)

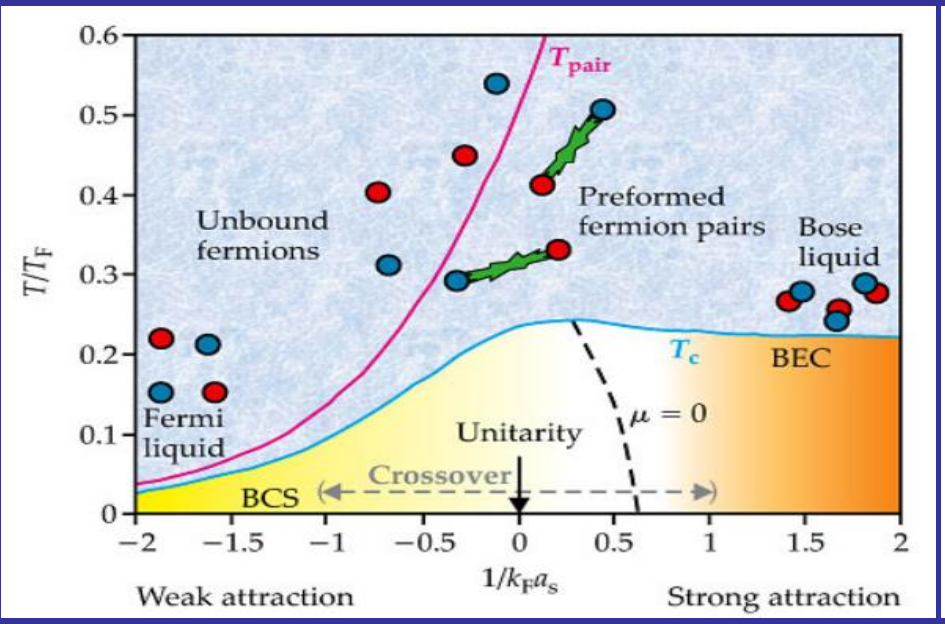

From Sa de Melo, Physics Today (2008)

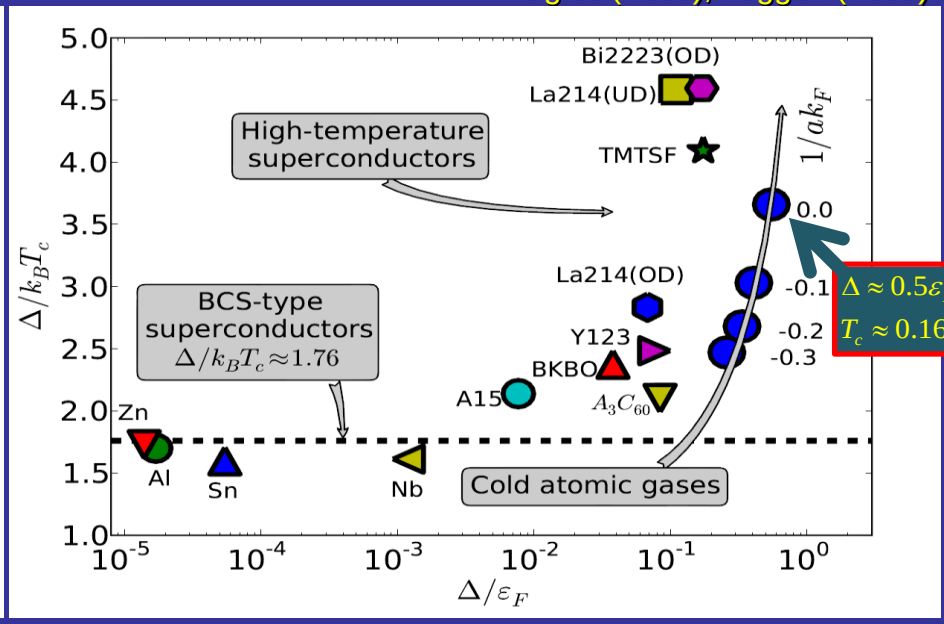

From Fischer et al., Rev. Mod. Phys. 79, 353 (2007)
P. Magierski, G. Wlazłowski, A. Bulgac, Phys. Rev. Lett. 107, 145304 (2011)

Surprising features of unitary gas hydrodynamics

In unitary Fermi gas there is no other length scale besides the average distance between particles.

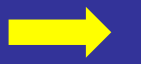

Isotropic gas expansion is an equilibrium process. Bulk viscosity vanishes!

Shear viscosity (η) :

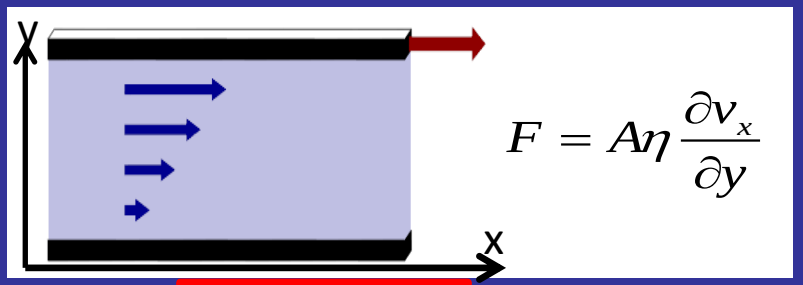

$$F = A\eta \frac{\partial v_x}{\partial y}$$

Conjecture: for every liquid the relation holds:
Kovtun, Son, Starinets, Phys.Rev.Lett. 94, 111601, (2005)

$$\frac{\eta}{S} \geq \frac{\hbar}{4\pi k_B}$$

Entropy density

Maxwell classical estimate: $\eta \sim$ mean free path

Perfect fluid $\frac{\eta}{S} = \frac{\hbar}{4\pi k_B}$ - strongly interacting quantum system = No well defined quasiparticles

Candidates : unitary Fermi gas, quark-gluon plasma

Theory prediction: $\frac{\eta}{S} = (0.15 - 0.2)\frac{\hbar}{k_B} > \frac{\hbar}{4\pi k_B}$

G.Wlazłowski, P.Magierski,J.E.Drut, Phys. Rev. Lett. 109, 020406 (2012)

Densities: $n_\sigma(\boldsymbol{r}) = \sum_{E_n<E_c} |v_{n,\sigma}(\boldsymbol{r})|^2, \qquad \tau_\sigma(\boldsymbol{r}) = \sum_{E_n<E_c} |\nabla v_{n,\sigma}(\boldsymbol{r})|^2,$

$$\nu(\boldsymbol{r}) = \sum_{E_n<E_c} u_{n,\uparrow}(\boldsymbol{r}) v^*_{n,\downarrow}(\boldsymbol{r}), \qquad \boldsymbol{j}_\sigma(\boldsymbol{r}) = \sum_{E_n<E_c} \mathrm{Im}[v^*_{n,\sigma}(\boldsymbol{r}) \nabla v_{n,\sigma}(\boldsymbol{r})],$$

Energy Density Functional for (spin-imbalanced) Unitary Fermi Gas:

$$\mathcal{H} = \alpha_\uparrow(p) \frac{\hbar^2 \tau_\uparrow}{2m_\uparrow} + \alpha_\downarrow(p) \frac{\hbar^2 \tau_\downarrow}{2m_\downarrow}$$

$$+ D(n_\uparrow, n_\downarrow)$$

$$+ g(n_\uparrow, n_\downarrow) \nu^\dagger \nu$$

$$+ [1-\alpha_\uparrow(p)] \frac{j^2_\uparrow}{2n_\uparrow} + [1-\alpha_\downarrow(p)] \frac{j^2_\downarrow}{2n_\downarrow}$$

In order to restore Galilean invariance of the functional

More details:
A. Bulgac, M.M. Forbes, P. Magierski,
The Unitary Fermi Gas: From Monte Carlo to Density Functionals,
Lecture Notes in Physics 836
ed. W. Zwerger, Springer (2011).

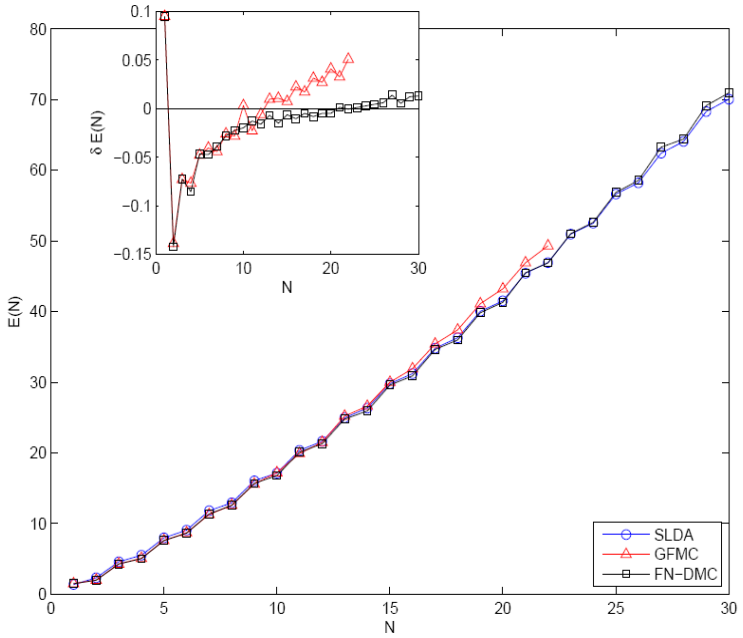

GFMC - Chang and Bertsch, Phys. Rev. A 76, 021603(R) (2007)
FN-DMC - von Stecher, Greene and Blume,
PRL 99, 233201 (2007), PRA 76, 053613 (2007)

Normal State				Superfluid State			
(N_a,N_b)	E_{FNDMC}	E_{ASLDA}	(error)	(N_a,N_b)	E_{FNDMC}	E_{ASLDA}	(error)
$(3,1)$	6.6 ± 0.01	6.687	1.3%	$(1,1)$	2.002 ± 0	2.302	15%
$(4,1)$	8.93 ± 0.01	8.962	0.36%	$(2,2)$	5.051 ± 0.009	5.405	7%
$(5,1)$	12.1 ± 0.1	12.22	0.97%	$(3,3)$	8.639 ± 0.03	8.939	3.5%
$(5,2)$	13.3 ± 0.1	13.54	1.8%	$(4,4)$	12.573 ± 0.03	12.63	0.48%
$(6,1)$	15.8 ± 0.1	15.65	0.93%	$(5,5)$	16.806 ± 0.04	16.19	3.7%
$(7,2)$	19.9 ± 0.1	20.11	1.1%	$(6,6)$	21.278 ± 0.05	21.13	0.69%
$(7,3)$	20.8 ± 0.1	21.23	2.1%	$(7,7)$	25.923 ± 0.05	25.31	2.4%
$(7,4)$	21.9 ± 0.1	22.42	2.4%	$(8,8)$	30.876 ± 0.06	30.49	1.2%
$(8,1)$	22.5 ± 0.1	22.53	0.14%	$(9,9)$	35.971 ± 0.07	34.87	3.1%
$(9,1)$	25.9 ± 0.1	25.97	0.27%	$(10,10)$	41.302 ± 0.08	40.54	1.8%
$(9,2)$	26.6 ± 0.1	26.73	0.5%	$(11,11)$	46.889 ± 0.09	45	4%
$(9,3)$	27.2 ± 0.1	27.55	1.3%	$(12,12)$	52.624 ± 0.2	51.23	2.7%
$(9,5)$	30 ± 0.1	30.77	2.6%	$(13,13)$	58.545 ± 0.18	56.25	3.9%
$(10,1)$	29.4 ± 0.1	29.41	0.034%	$(14,14)$	64.388 ± 0.31	62.52	2.9%
$(10,2)$	29.9 ± 0.1	30.05	0.52%	$(15,15)$	70.927 ± 0.3	68.72	3.1%
$(10,6)$	35 ± 0.1	35.93	2.7%	$(1,0)$	1.5 ± 0.0	1.5	0%
$(20,1)$	73.78 ± 0.01	73.83	0.061%	$(2,1)$	4.281 ± 0.004	4.417	3.2%
$(20,4)$	73.79 ± 0.01	74.01	0.3%	$(3,2)$	7.61 ± 0.01	7.602	0.1%
$(20,10)$	81.7 ± 0.1	82.57	1.1%	$(4,3)$	11.362 ± 0.02	11.31	0.49%
$(20,20)$	109.7 ± 0.1	113.8	3.7%	$(7,6)$	24.787 ± 0.09	24.04	3%
$(35,4)$	154 ± 0.1	154.1	0.078%	$(11,10)$	45.474 ± 0.15	43.98	3.3%
$(35,10)$	158.2 ± 0.1	158.6	0.27%	$(15,14)$	69.126 ± 0.31	62.55	9.5%
$(35,20)$	178.6 ± 0.1	180.4	1%				

Table 9.2 Comparison between the ASLDA density functional as described in this section and the FN-DMC calculations [136, 137] for a harmonically trapped unitary gas at zero temperature. The normal state energies are obtained by fixing $\Delta = 0$ in the functional: In the FN-DMC calculations, this is obtained by choosing a nodal ansatz without any pairing. In the case of small asymmetry, the resulting "normal states" may be a somewhat artificial construct as there is no clear way of preparing a physical system in this "normal state" when the ground state is superfluid.

Figure from: A. Bulgac, M.M. Forbes, P. Magierski, Lecture Notes in Physics, Vol. 836, Chap. 9, p.305-373 (2012)

Creation of vortices in Unitary Fermi Gas – TDDFT simulations

Stirring the atomic cloud with stirring velocity **lower** than the critical velocity

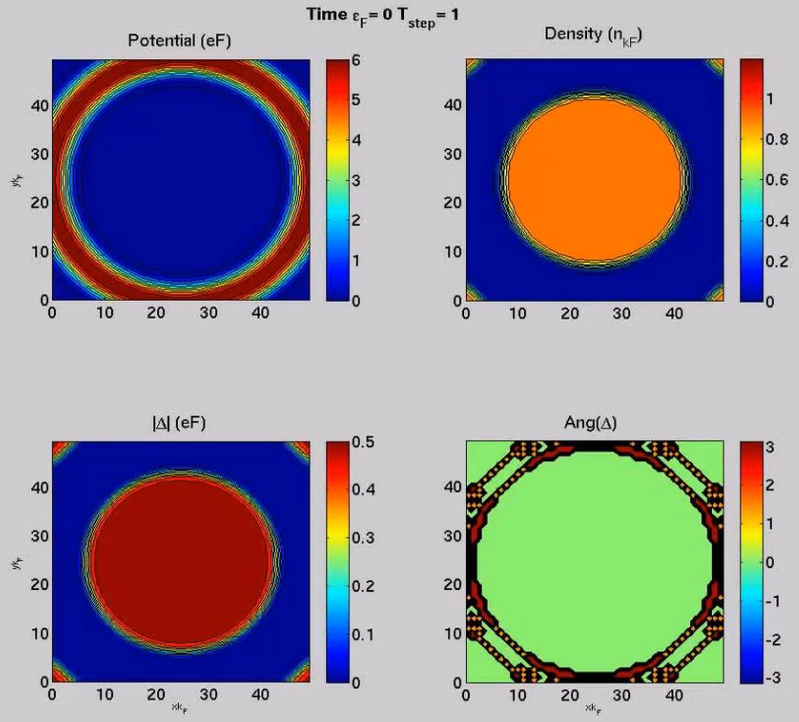

Stirring the atomic cloud with stirring velocity **exceeding** the critical velocity

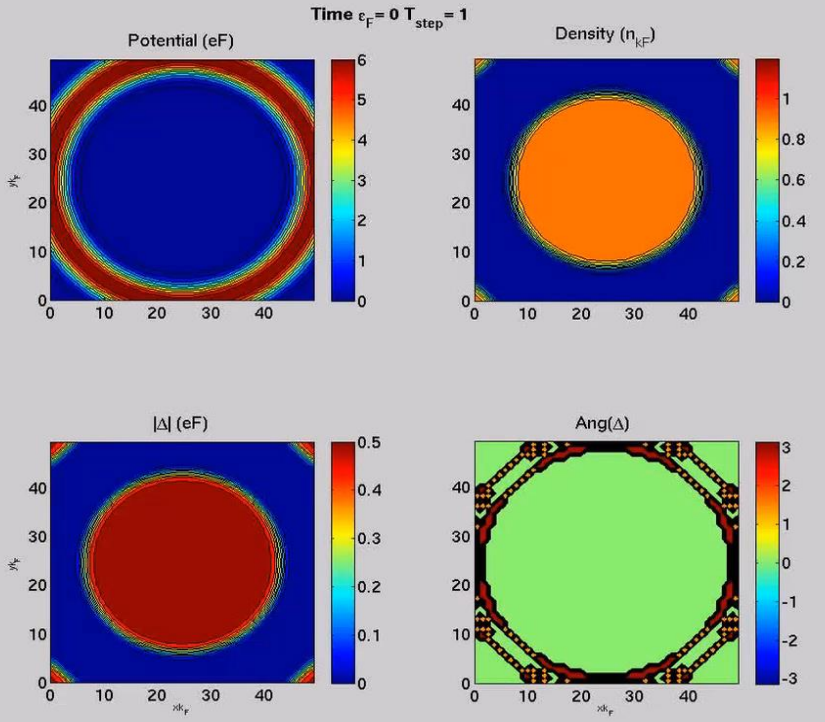

Bulgac, Luo, Magierski, Roche, Yu, *Science* 332, 1288 (2011)

Ultracold atomic gases: two regimes for realization of the Josephson junction

Weak coupling (weak link)

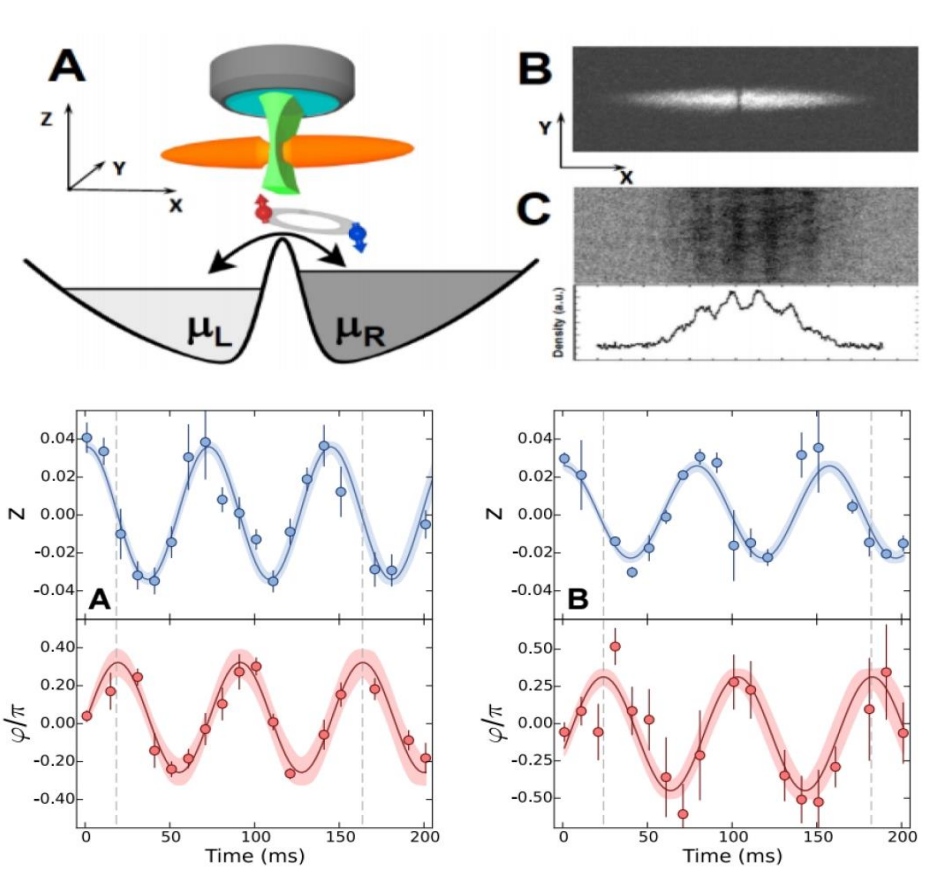

Observation of ***AC Josephson effect*** between two 6Li atomic clouds.

It need not to be accompanied by creation of a topological excitation.

G. Valtolina et al., Science 350, 1505 (2015).

Strong coupling

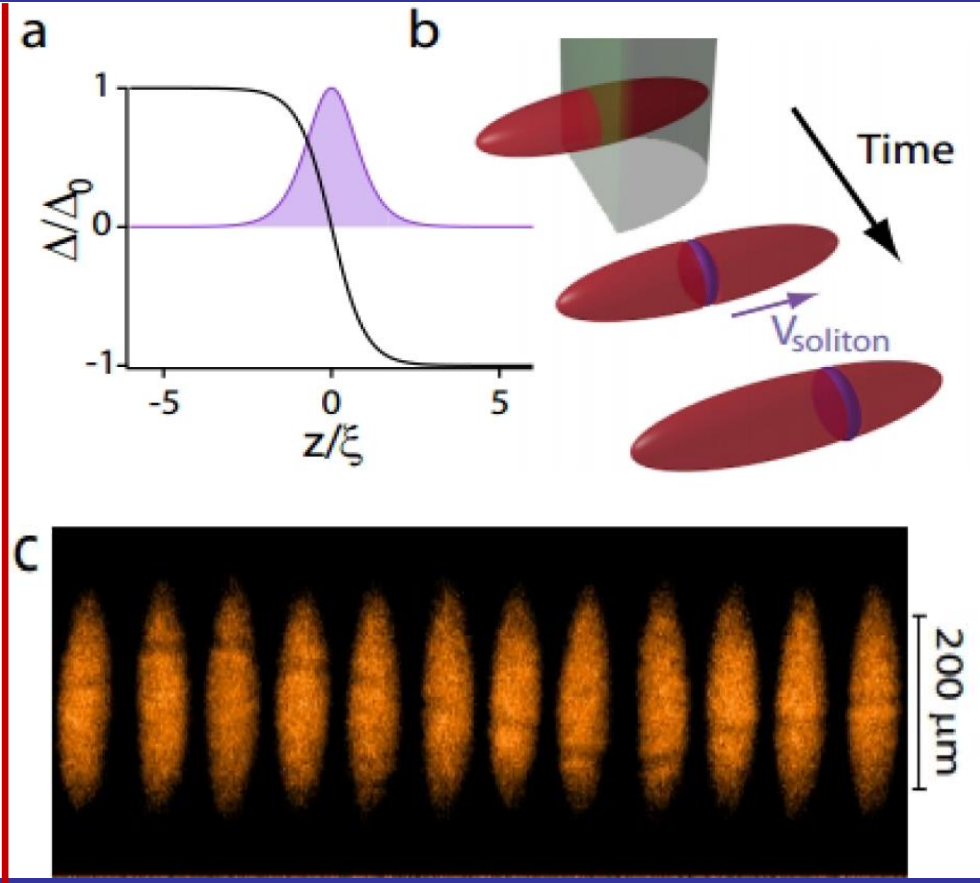

Creation of a „heavy soliton" after merging two superfluid atomic clouds.

T. Yefsah et al., Nature 499, 426 (2013).

Unstable pairing nodal structures: atomic cloud collisions

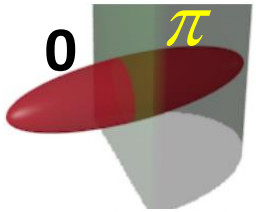

(a)

MIT experiment

Phys. Rev. Lett. 116, 045304 (2016)

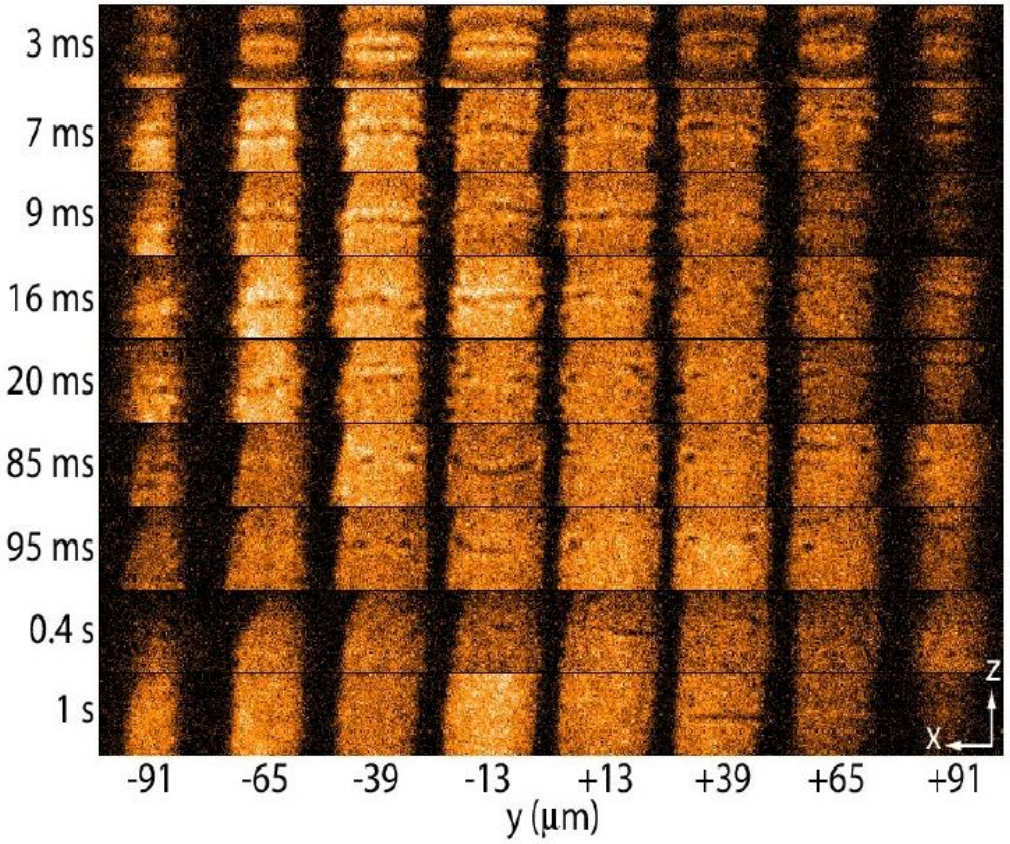

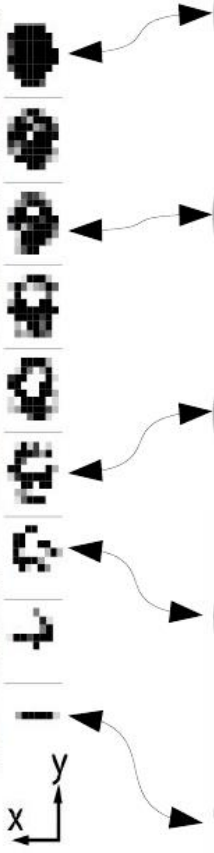

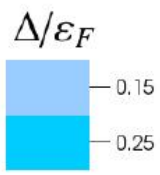

(b)

TDDFT results

Piz Daint

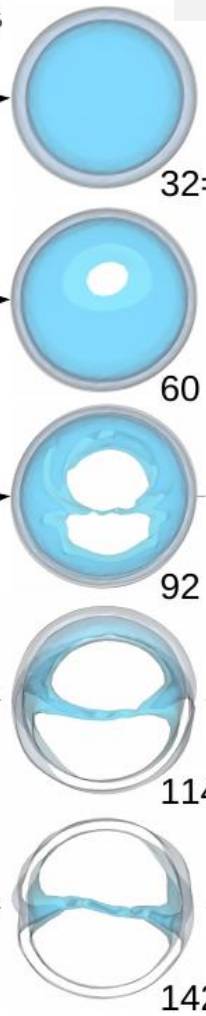

(c)

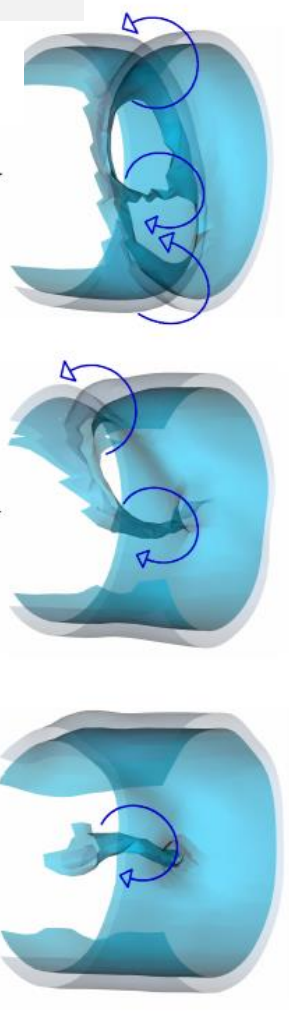

Decay of solitonic excitation (pairing nodal structure) generates a sequence of topological excitations involving: "Phi"-soliton and vortex line.

G. Wlazłowski, K. Sekizawa, M. Marchwiany, P. Magierski, Phys. Rev. Lett. **120**, 253002 (2018)

New effects predicted for spin-polarized systems:

Impact on the solitonic cascade:
final product of the cascade depends on the spin imbalance in the system

(can be verified experimentally with present setups)

P=20%: Dark soliton ⇒ Vortex ring ⇒ Vortex line

P=40%: Dark soliton ⇒ Vortex ring

P=50%: Dark soliton

⇐ **Cascade is suppressed by the polarization effects**

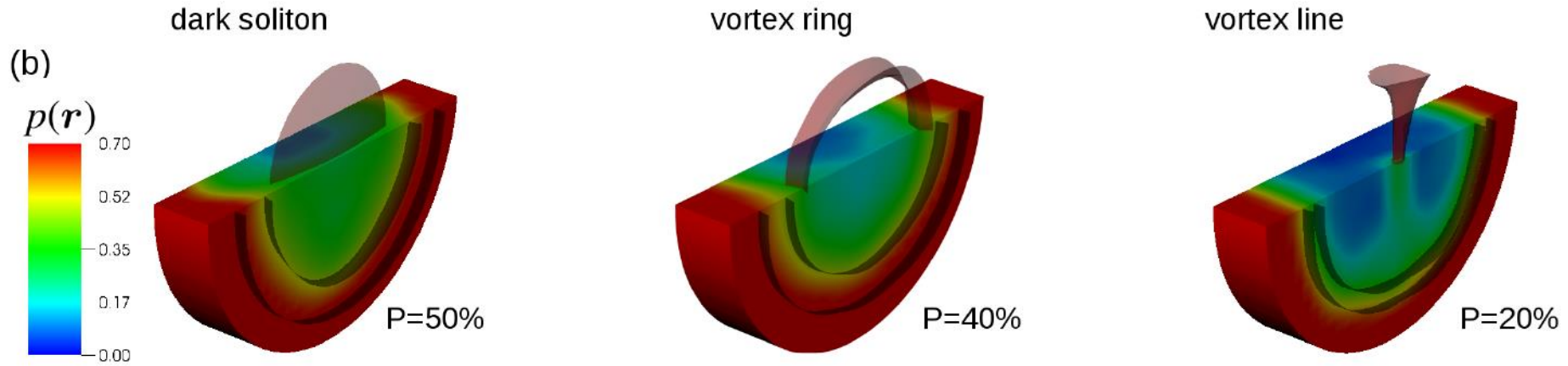

Stability of topological defect depends on its internal structure…

→ For sufficiently large spin-imbalance dark solitons become stable (no snake instability) (see also: Reichl & Mueller, PRA 95, 053637; Lombardi, et. al., PRA 96, 033609)

G. Wlazłowski, K. Sekizawa, M. Marchwiany, P. Magierski,
Phys. Rev. Lett. **120**, 253002 (2018)

Unstable pairing nodal structures: nuclear collisions

Collisions of superfluid nuclei having different phases of the pairing fields

The main questions are:

-how a possible solitonic structure can be manifested in nuclear system?

-what observable effect it may have on heavy ion reaction:
kinetic energy distribution of fragments, capture cross section, etc.?

Clearly, we cannot control phases of the pairing field in nuclear experiments and the possible signal need to be extracted after averaging over the phase difference.

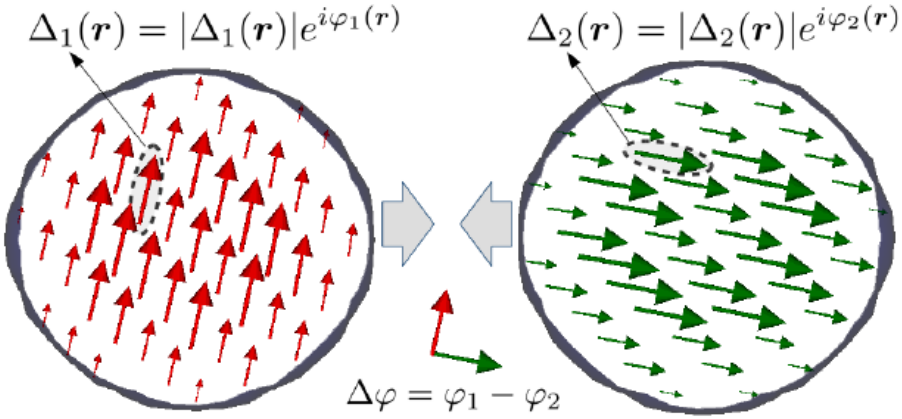

Estimates for the magnitude of the effect

At first one may think that the magnitude of the effect is determined by the nuclear pairing energy which is of the order of MeV's in atomic nuclei (according to the expression):

$$\frac{1}{2} g(\varepsilon_F)\left|\Delta\right|^2; \quad g(\varepsilon_F) \text{ - density of states}$$

On the other hand the energy stored in the junction can be estimated from Ginzburg-Landau (G-L) approach:

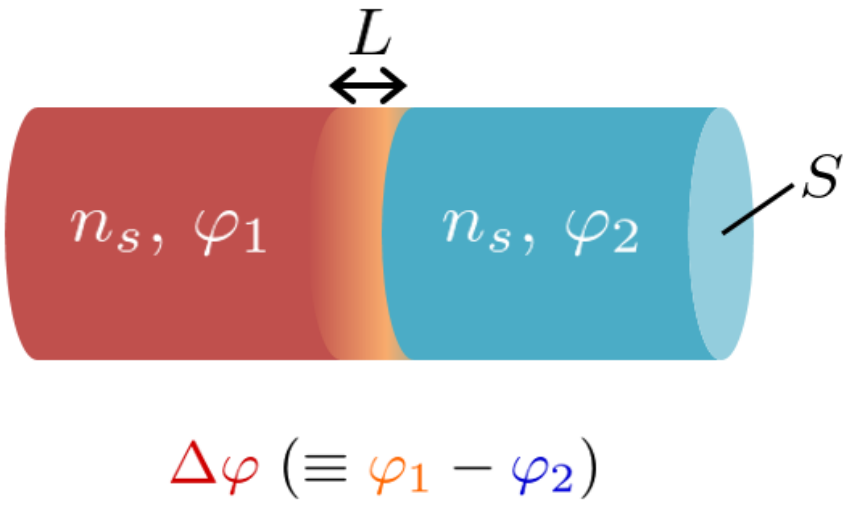

$$E_j = \frac{S}{L}\frac{\hbar^2}{2m} n_s \sin^2\frac{\Delta\varphi}{2}$$

For typical values characteristic for two medium nuclei: $E_j \approx 30 MeV$

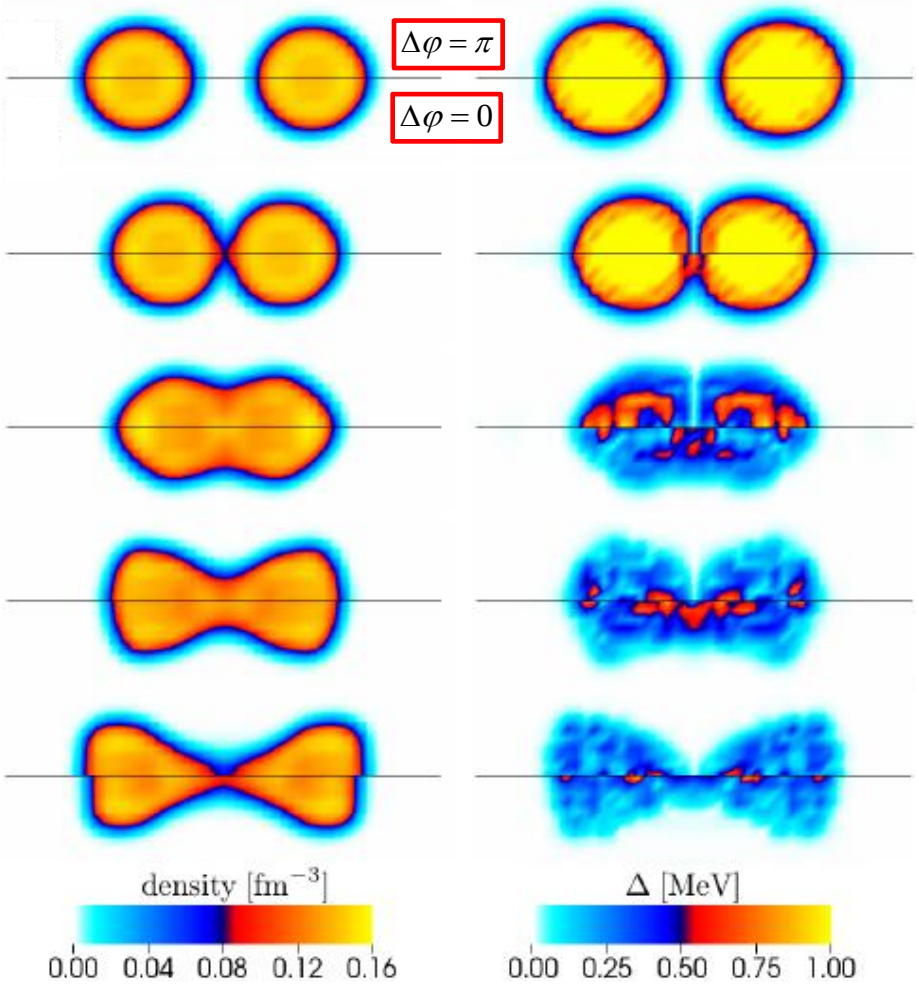

Total kinetic energy of the fragments (TKE)

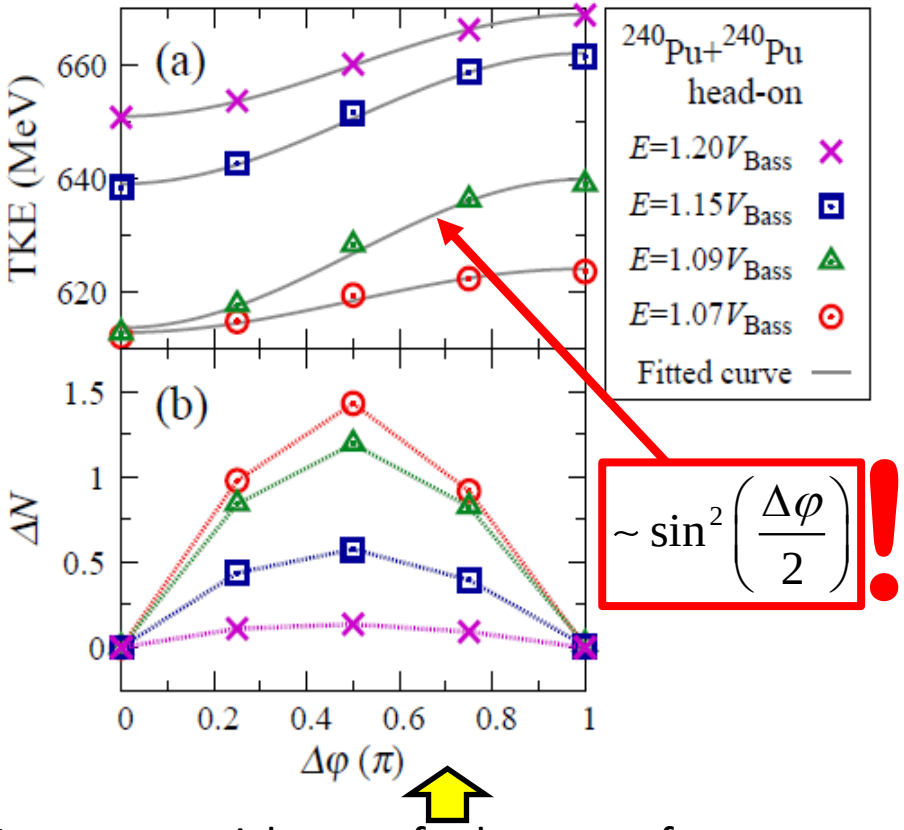

Average particle transfer between fragments.

Creation of the solitonic structure between colliding nuclei prevents energy transfer to internal degrees of freedom and consequently enhances the kinetic energy of outgoing fragments.
Surprisingly, the gauge angle dependence from the G-L approach is perfectly well reproduced in the kinetic energies of outgoing fragments!

$^{90}Zr + {}^{90}\mathrm{Zr}$ at energy $E \simeq V_{Bass}$

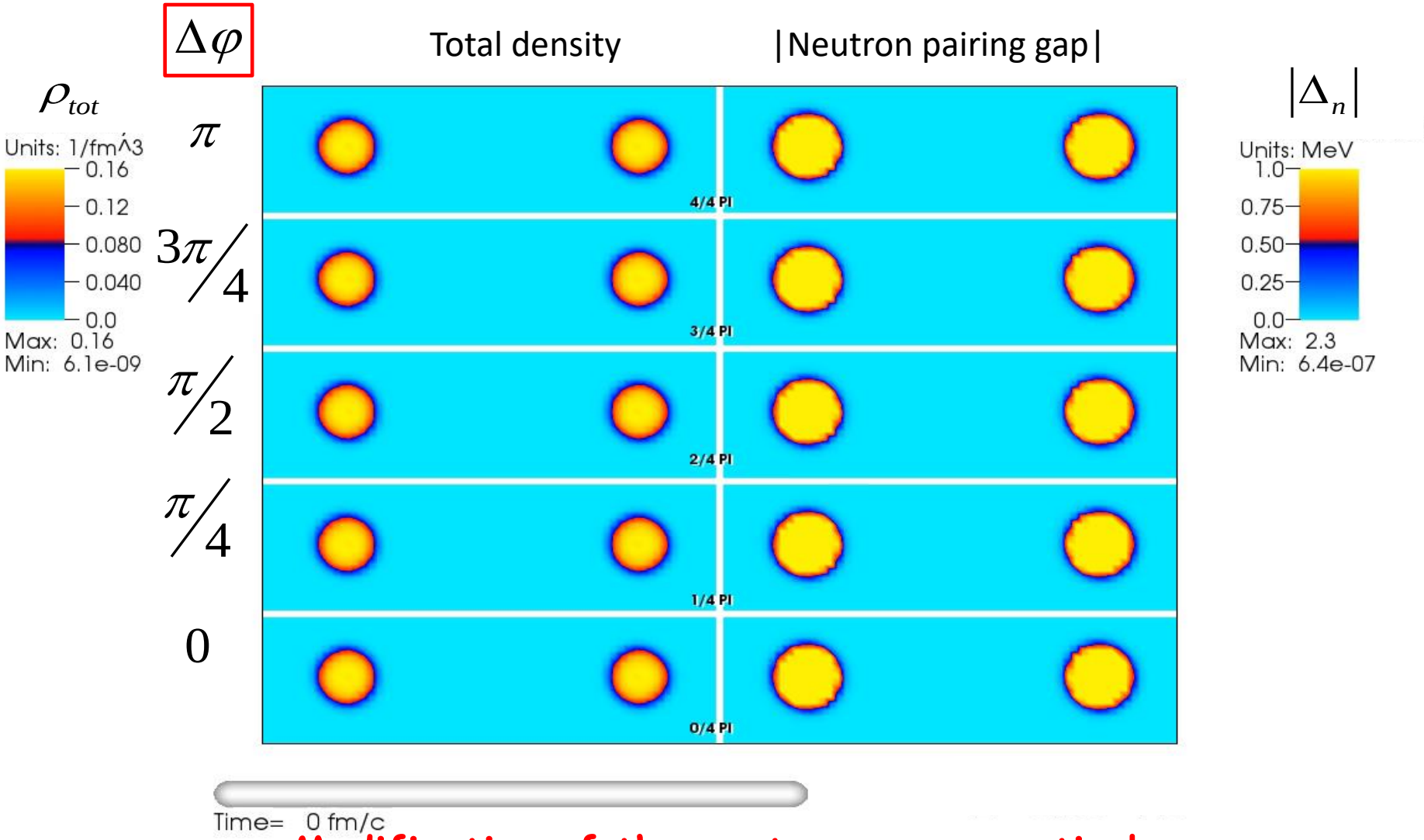

Modification of the capture cross section!

P. Magierski, K. Sekizawa, G. Wlazłowski, Phys. Rev. Lett. 119 042501 (2017)
See also for light nuclei: Y. Hashimoto, G. Scamps, Phys. Rev. C94, 014610 2016)

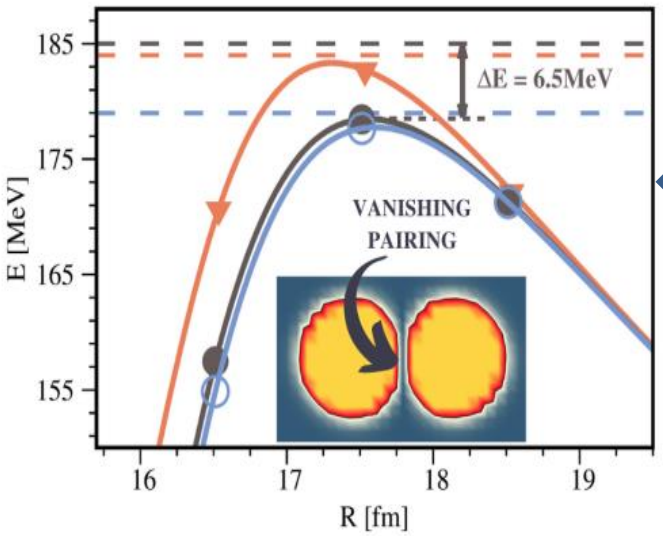

TABLE I: The minimum energies needed for capture in ^{90}Zr+^{90}Zr and ^{96}Zr+^{96}Zr for the case of $\Delta\phi = 0$ [$E_{\rm thresh}(0)$] and $\Delta\phi = \pi$ [$E_{\rm thresh}(\pi)$]. The energy difference between the two cases is shown in the last column. The average pairing gap $\overline{\Delta}_i$ is defined by Eq. (4).

	$\overline{\Delta}_q$ (MeV)	$E_{\rm thresh}(0)$ (MeV)	$E_{\rm thresh}(\pi)$ (MeV)	ΔE_s
^{90}Zr	$\overline{\Delta}_n = 0.00$ $\overline{\Delta}_p = 0.09$	184	184	0
^{96}Zr	$\overline{\Delta}_n = 1.98$ $\overline{\Delta}_p = 0.32$	179	185	6
	$\overline{\Delta}_n = 2.44$ $\overline{\Delta}_p = 0.33$	178	187	9
	$\overline{\Delta}_n = 2.94$ $\overline{\Delta}_p = 0.34$	178	187	9

Dynamic nature of the effect:

Solid lines: static barrier between two nuclei (with pairing included):
90Zr+90Zr - brown
96Zr+96Zr - black (0-phase diff.) and
blue (Pi-phase diff.)

Static barriers are practically insensitive to the phase difference of pairing fields.

Dashed lines: Actual threshold for capture obtained in dynamic calculations.
Hence ΔE measures the additional energy which has to be added to the system to merge nuclei.

Dependence of the additional energy on pairing gap in colliding nuclei

P. Magierski, A. Makowski, M. Barton, K. Sekizawa, G. Wlazłowski, Phys. Rev. C 105, 064602, (2022)

G. Scamps, Phys. Rev. C 97, 044611 (2018): ***barrier fluctuations extracted from experimental data provide evidence that the effect exists.***

Anatomy of the vortex core

Bosonic vortex structure:
weakly interacting Bose gas at T=0 → Gross-Pitaevskii eq. (GPE)

$$\left[-\frac{1}{2m}\nabla^2 + g|\psi(\vec{r})|^2 + V_{ext}(\vec{r})\right]\psi(\vec{r}) = \mu\psi(\vec{r})$$

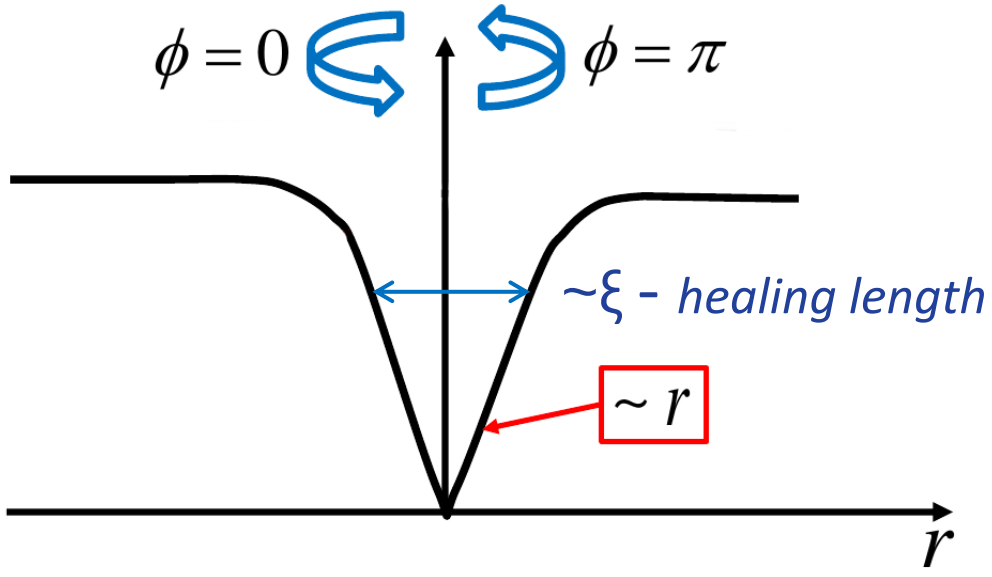

Order parameter:

$$\psi(\vec{r}) = \sqrt{n(\vec{r})}e^{i\phi}$$

$$v_S = \frac{\hbar}{m}\nabla\phi$$

$$\kappa = \oint d\vec{l}\cdot\vec{v}_S = \frac{\hbar}{m}$$

Fermionic vortex structure:

Weakly interacting Fermi gas → Bogoliubov de Gennes (BdG) eqs.

$$\begin{pmatrix} h_\uparrow & \Delta \\ \Delta^* & -h_\downarrow^* \end{pmatrix} \begin{pmatrix} u_{n,\uparrow} \\ v_{n,\downarrow} \end{pmatrix} = \varepsilon_n \begin{pmatrix} u_{n,\uparrow} \\ v_{n,\downarrow} \end{pmatrix}$$

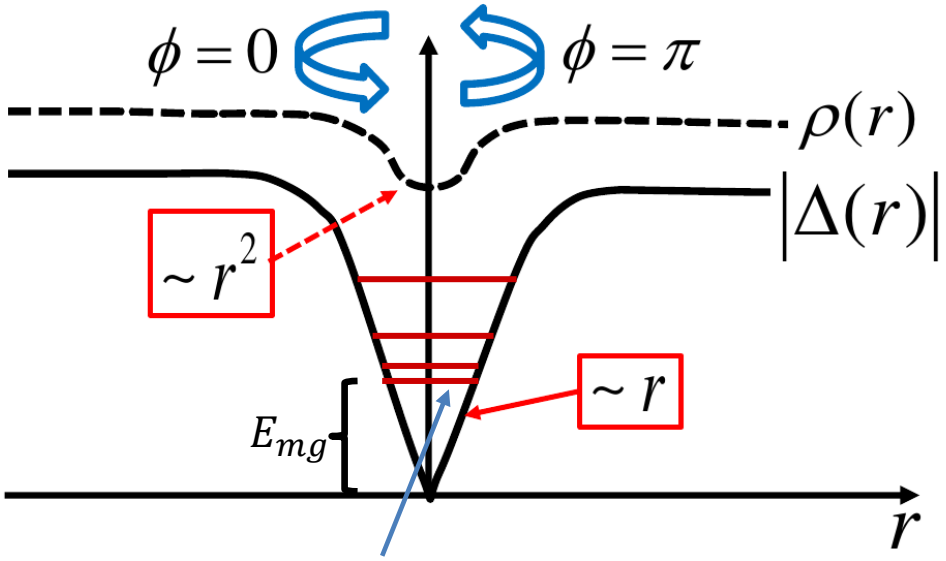

Form of the vortex-like solutions:

$$u_\eta(\mathbf{r}) = u_{nmk_z}(\rho) e^{im\varphi} e^{ik_z z}$$
$$v_\eta(\mathbf{r}) = v_{nmk_z}(\rho) e^{i(m+1)\varphi} e^{ik_z z}$$

CdGM (Andreev) states

C. Caroli, P. de Gennes, J. Matricon, Phys. Lett. 9, 307 (1964):

Minigap: $E_{mg} \sim \frac{|\Delta_\infty|^2}{\varepsilon_F}$ - energy scale for vortex core excitations.

Density of states: $g(\varepsilon) \sim \frac{\varepsilon_F}{|\Delta_\infty|^2}$; $\varepsilon \ll |\Delta_\infty|$

Vortex core structure in Andreev approximation:

$$\frac{E(0,L_z)}{\varepsilon_F}k_F r_V\sqrt{1-\left(\frac{L_z}{k_F r_V}\right)^2}+\arccos\left(\frac{-L_z}{k_F r_V}\right)-\arccos\left(\frac{E(0,L_z)}{|\Delta_\infty|}\right)=0$$

$$E(0,L_z)=E(0)L_z,\ E\ll|\Delta_\infty|$$

$$E(0,L_z)\approx\frac{|\Delta_\infty|^2}{\varepsilon_F\frac{r_V}{\xi}\left(\frac{r_V}{\xi}+1\right)}\frac{L_z}{\hbar},\qquad \xi=\frac{\varepsilon_F}{k_F|\Delta_\infty|}$$

Schematic section of the core

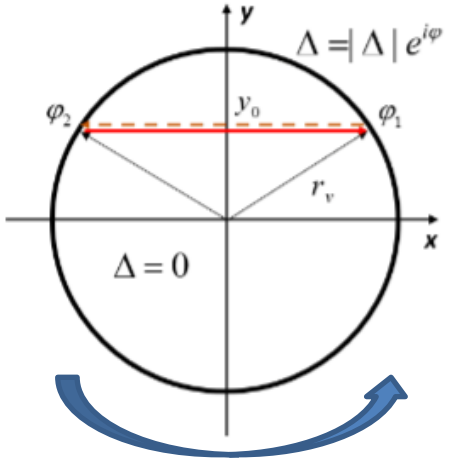

Spectrum of in-gap states

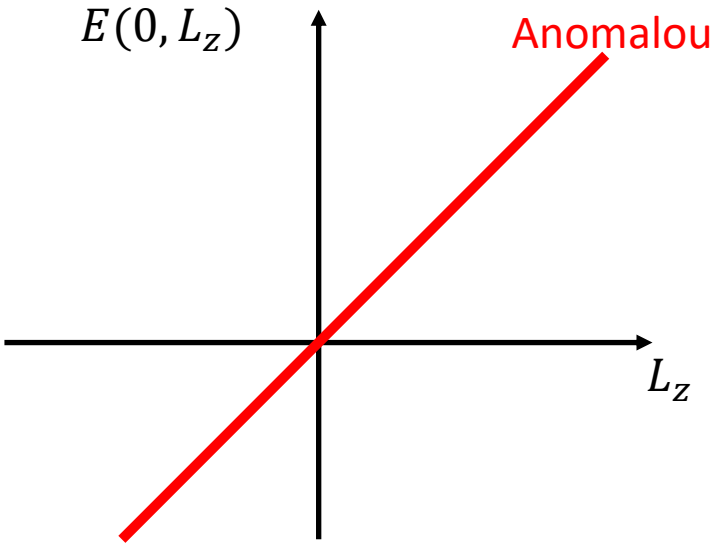

Anomalous branch (subgap states)

Works well in deep BCS limit: $\frac{1}{k_F a_s}\ll 0$

M. Stone, Phys. Rev. B 54, 13222 (1996)

P.M. G. Wlazłowski, A. Makowski, K. Kobuszewski, Phys. Rev. A 106, 033322 (2022)

Quasiparticle mobility along the vortex line

$$E(k_z) = \frac{E(0)}{\sqrt{1-\left(\frac{k_z}{k_F}\right)^2}} \; ; \; k_z < k_F$$

C. Caroli, P. de Gennes, J. Matricon, Phys. Lett. 9, 307 (1964):

In Andreev approximation:

$$\sqrt{\varepsilon_F + E}\,\sin\alpha = \sqrt{\varepsilon_F - E}\,\sin\beta$$

$$k_h = \sqrt{2(\varepsilon_F - E)}$$

$$k_p = \sqrt{2(\varepsilon_F + E)}$$

$$v_z = k_z \frac{\sqrt{k_p^2 - k_z^2} - \sqrt{k_h^2 - k_z^2}}{\sqrt{k_p^2 - k_z^2} + \sqrt{k_h^2 - k_z^2}}$$

Velocity component along the vortex line

It gives the same dispersion relations as above up to the second order.

$$M_{eff}^{-1}(L_z) \approx \frac{2}{3}\left(\frac{|\Delta_\infty|}{\varepsilon_F}\right)^2 \frac{L_z}{\hbar}$$

Effective mass of quasiparticle in the core carrying ang. mom. Lz

Schematic picture of Andreev reflection of particle-hole moving along the vortex line

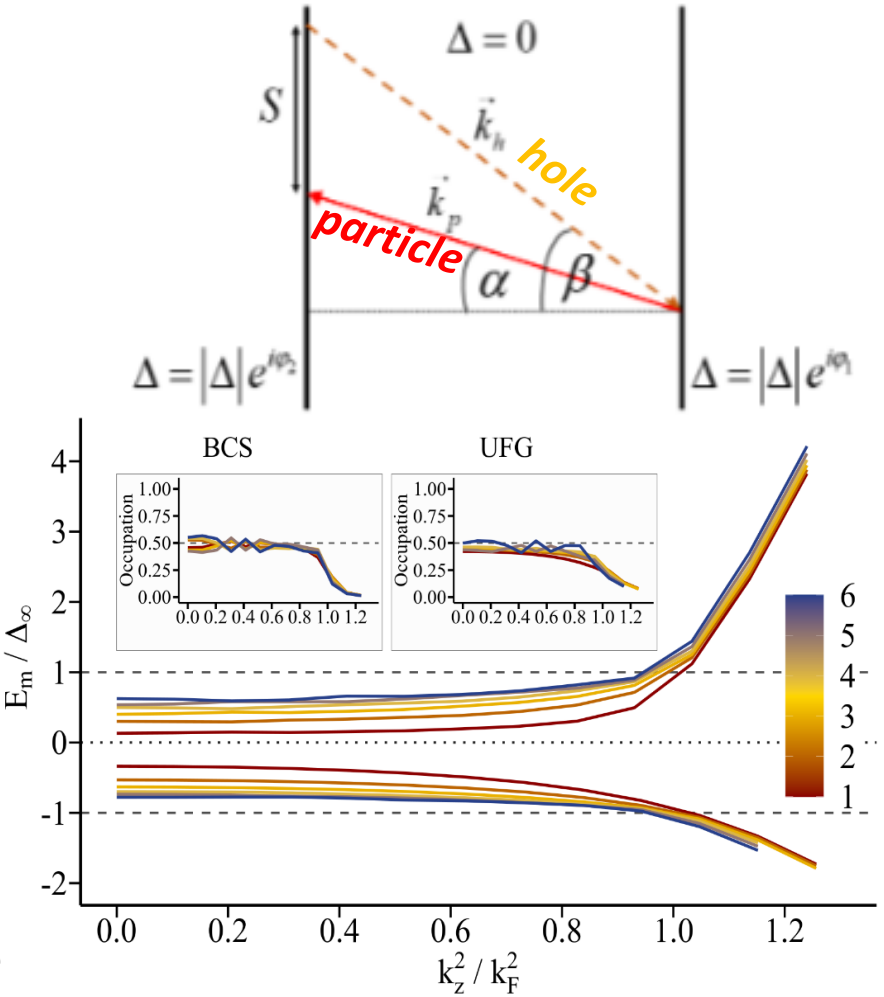

P.M. G. Wlazłowski, A. Makowski, K. Kobuszewski, Phys. Rev. A 106, 033322 (2022)

Note that large value of effective mass along the vortex line originate from the fact that the occupations of hole and particle states below the gap are approximately equal.

Changes of the core structure induced by spin polarization

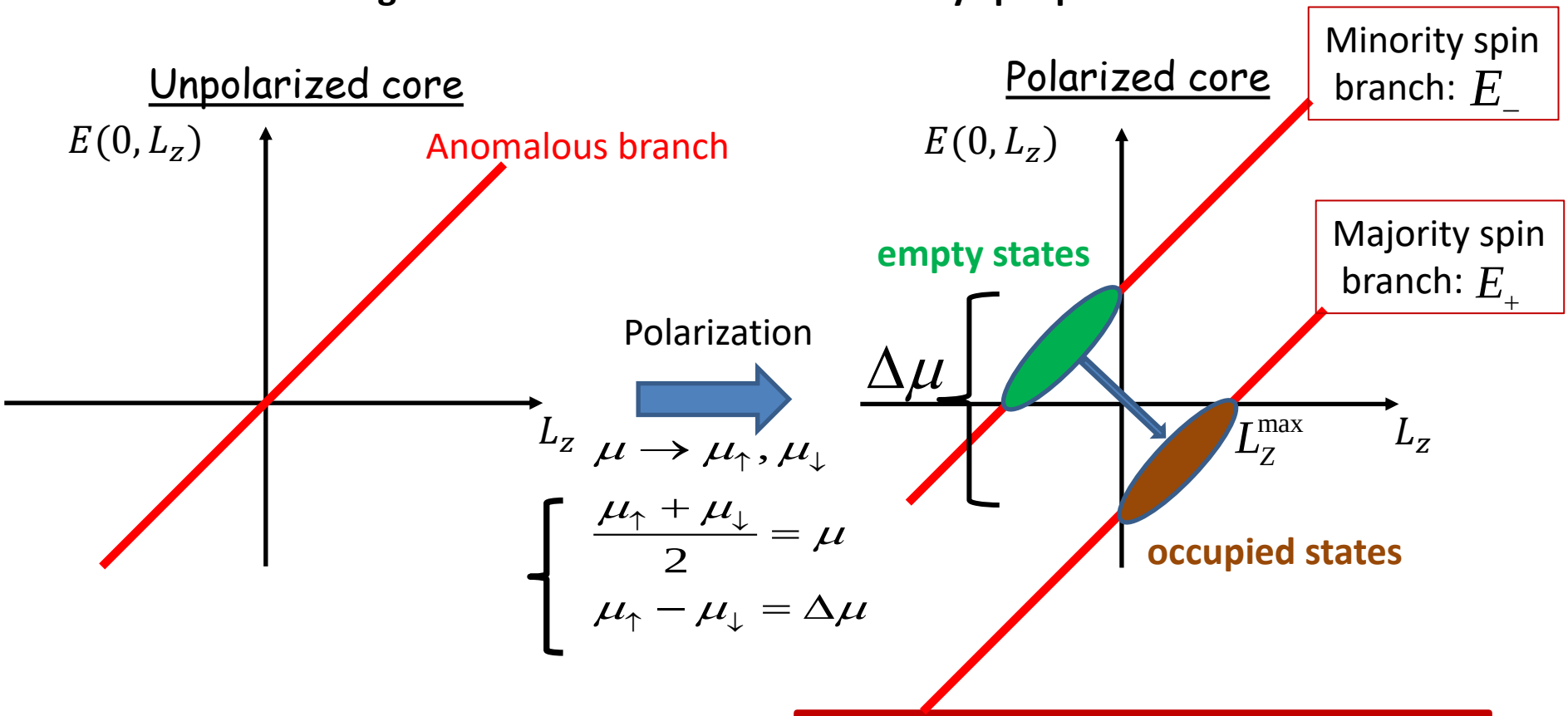

Branches are split proportionally to polarization

$$E_\pm(0, L_Z) \approx \frac{|\Delta_\infty|^2}{\varepsilon_F \frac{r_V}{\xi}\left(\frac{r_V}{\xi}+1\right)} \frac{L_Z}{\hbar} \mp \frac{\Delta\mu}{2}$$

Certain fraction of majority spin particles rotate in the opposite direction!

$$L_Z^{\max} \approx \frac{1}{2} \frac{\varepsilon_F}{|\Delta_\infty|^2} \frac{r_V}{\xi}\left(\frac{r_V}{\xi}+1\right) \hbar\Delta\mu$$

Two consequences of vortex core polarization:

1) Minigap vanishes.

2) Direction of the current in the core reverses.

1) Since the polarization correspond to relative shift of anomalous branches therefore the quasiparticle spectrum of spin-up and spin-down components is asymmetric for $k_z = 0$.

However the symmetry of the spectrum has to be restored in the limit of $k_z \to \infty$.
Since for a straight vortex one can decouple the degree of freedom along the vortex line:

$$H = \begin{pmatrix} h_{2D}(\mathbf{r}) + \frac{1}{2}k_z^2 - \mu_\uparrow & \Delta(\mathbf{r}) \\ \Delta^*(\mathbf{r}) & -h_{2D}^*(\mathbf{r}) - \frac{1}{2}k_z^2 + \mu_\downarrow \end{pmatrix}$$

therefore $E(k_z) \propto \pm k_z^2$ when $k_z \to \infty$

As a result there must exist a sequence of values: $k_z = \pm k_{z1}, \pm k_{z2}, \ldots$
for which:

$$E(\pm k_{zi}) = 0$$

Moreover the crossings occur between levels of particular projection of angular momentum on the vortex line.

Namely, the crossing occurs in such a way that the particle state: $v_\uparrow$ of ang. momentum ***m*** is converted into a hole $u_\uparrow$ of momentum ***–m+1***
Hence the configuration changes by $\Delta m = |2m-1|$

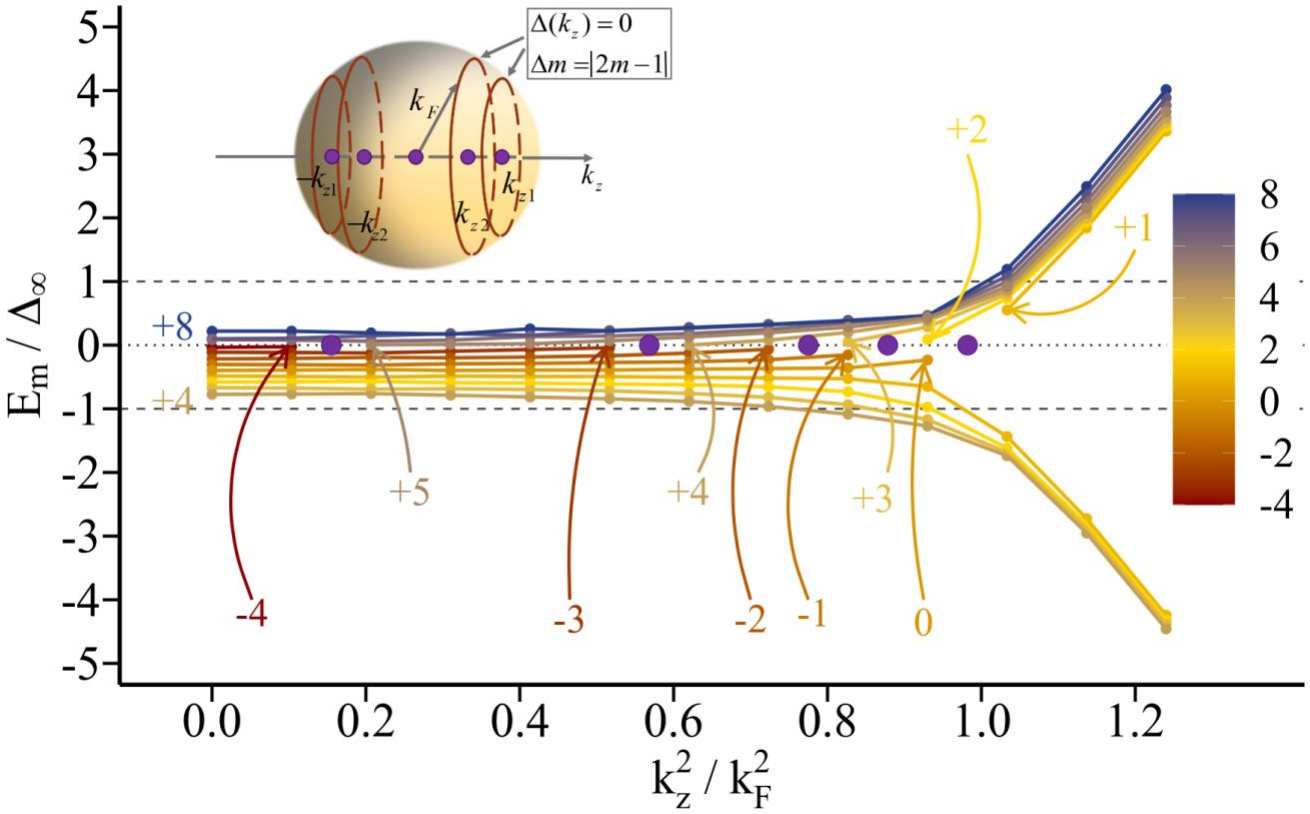

P.M. G. Wlazłowski, A. Makowski, K. Kobuszewski, Phys. Rev. A 106, 033322 (2022)

How can we measure the influence of core states in ultracold gases?

Dissipative processes involving vortex dynamics.

Silaev, Phys. Rev. Lett. 108, 045303 (2012)
Kopnin, Rep. Prog. Phys. 65, 1633 (2002)
Stone, Phys. Rev. B54, 13222 (1996)
Kopnin, Volovik, Phys. Rev. B57, 8526 (1998)
....

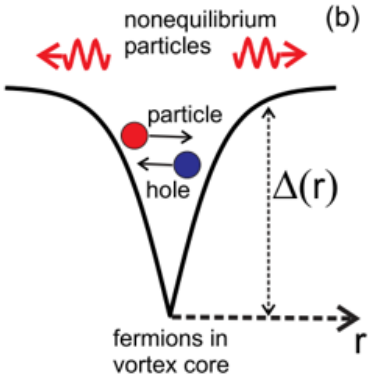

Classical treatment of states in the core (Boltzmann eq.).
More applicable in deep BCS limit unreachable in ultracold atoms.

Vortex-antivortex scattering in 2D

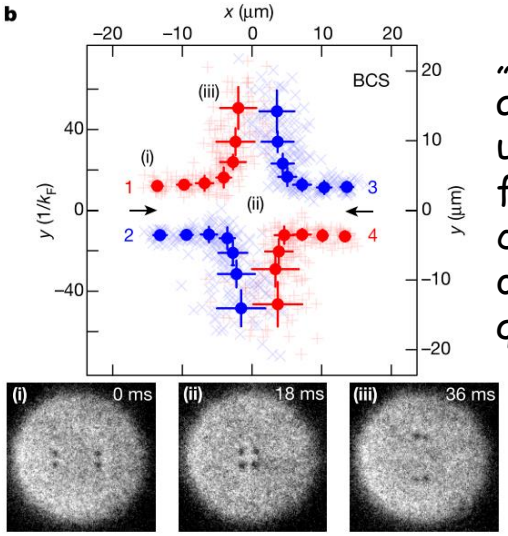

„Further, our few-vortex experiments extending across different superfluid regimes reveal non-universal dissipative dynamics, suggesting that fermionic quasiparticles localized inside the vortex core contribute significantly to dissipation, thereby opening the route to exploring new pathways for quantum turbulence decay, vortex by vortex."
W.J. Kwon et al. Nature **600**, 64 (2021)

Exciting quasiparticles in the vortex core

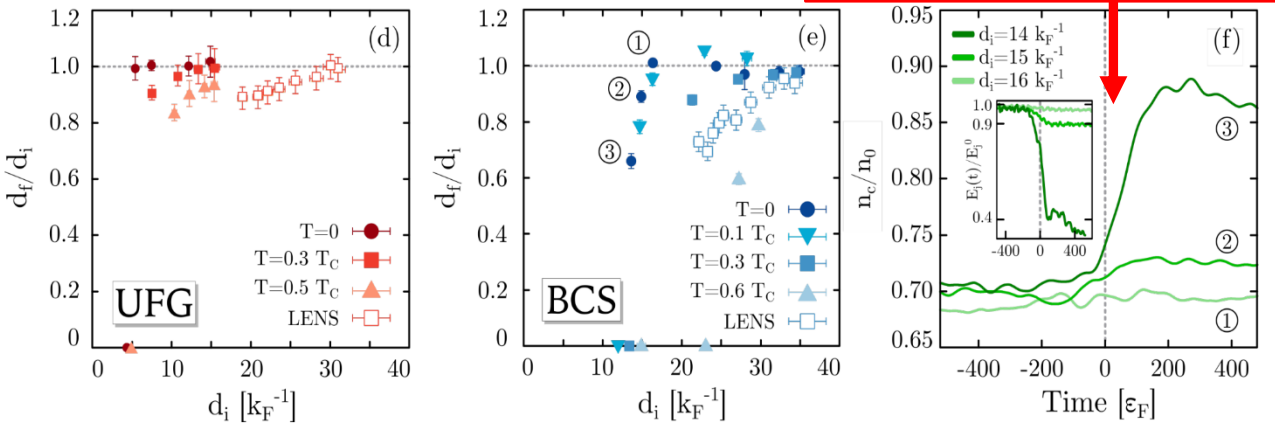

Indeed quasiparticles in the core are excited due to vortex acceleration but the effect is too weak to account for the total dissipation rate.

A. Barresi, A. Boulet, P.M., G. Wlazłowski, Phys. Rev. Lett. 130, 043001 (2023)

Modelling neutron star interior

Neutron star is a huge superfluid

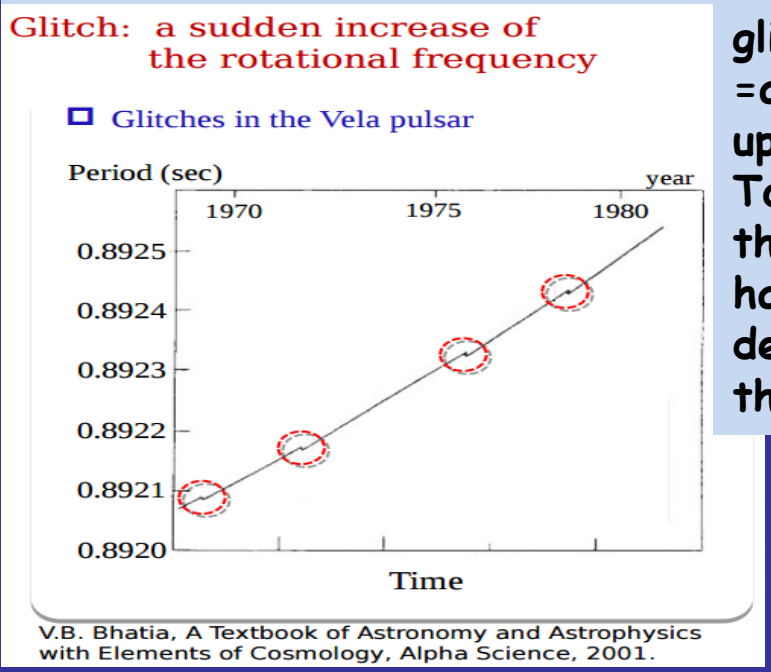

glitch phenomenon =a sudden speed up of rotation. To date more than 300 glitches have been detected in more than 100 pulsars

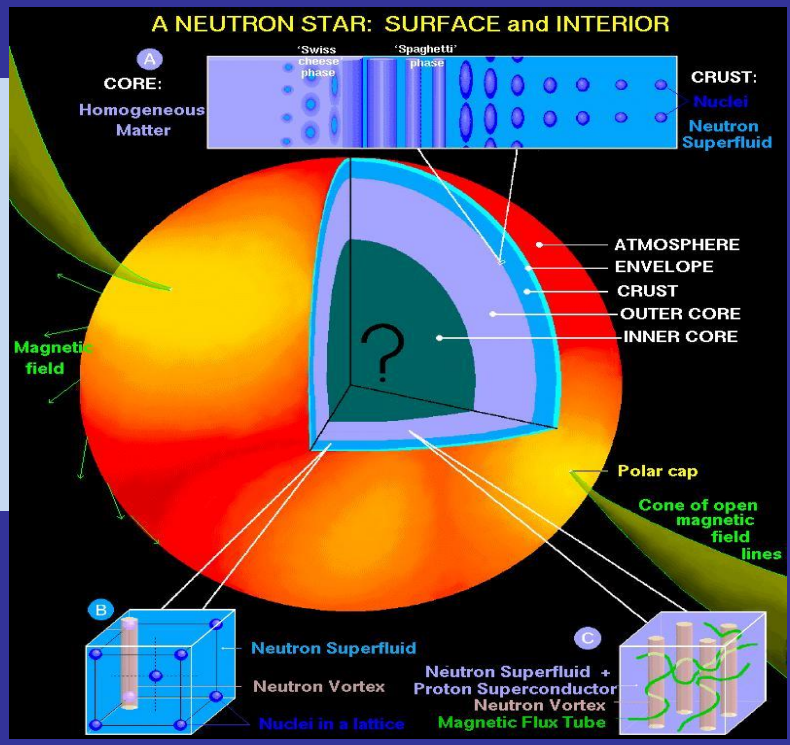

Glitch phenomenon is commonly believed to be related to rearrangement of vortices in the interior of neutron stars (Anderson,Itoh,Nature 256,25 (1975)) It would require however a correlated behavior of huge number of quantum vortices and the mechanism of such collective rearrangement is still a mystery.

Large scale dynamical model of neutron star interior (in particular neutron star crust), based on microscopic input from nuclear theory, is required.
In particular: vortex-impurity interaction, deformation modes of nuclear lattice, effective masses of nuclear impurities and couplings between lattice vibrations and neutron superfluid medium, need to be determined.

Example: vortices across the neutron star crust

Section through the vortex core

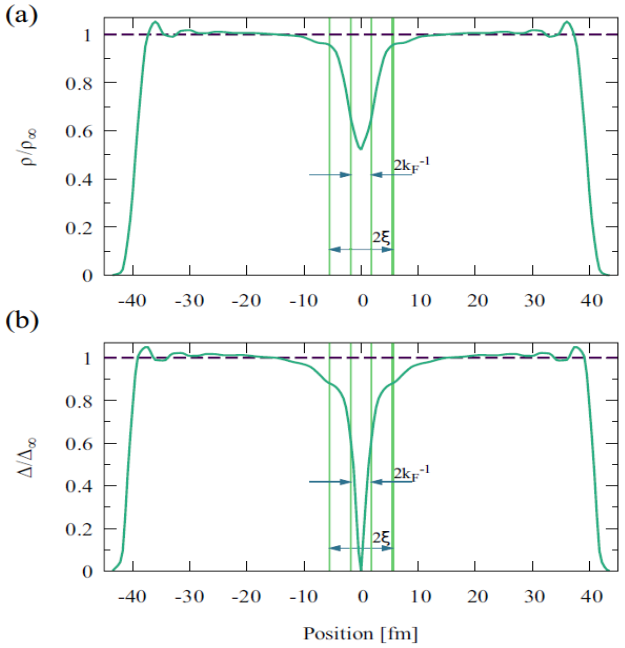

Normal density

Pairing field

Note two different length scales inside the core as explained by:
Sensarma, Randeria, Ho,
Phys. Rev. Lett. 96, 090403 (2006)

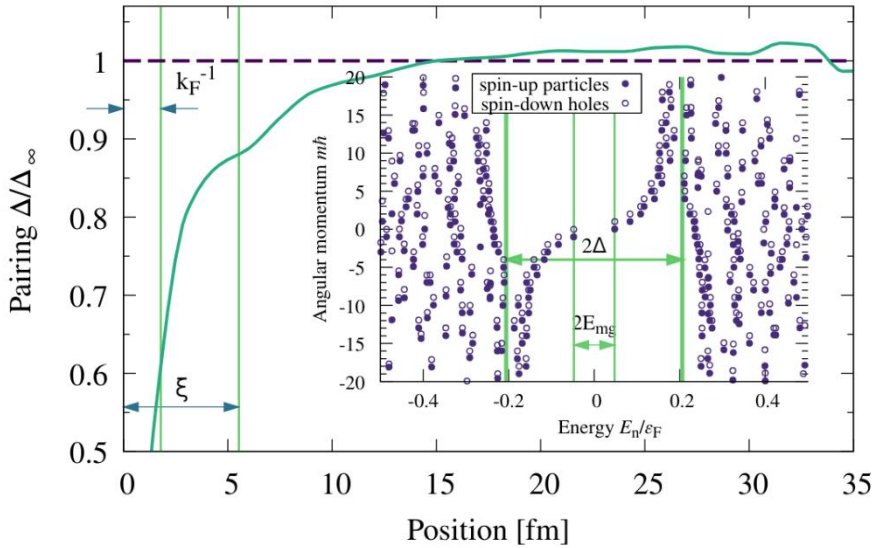

Specific heat contribution vs uniform matter

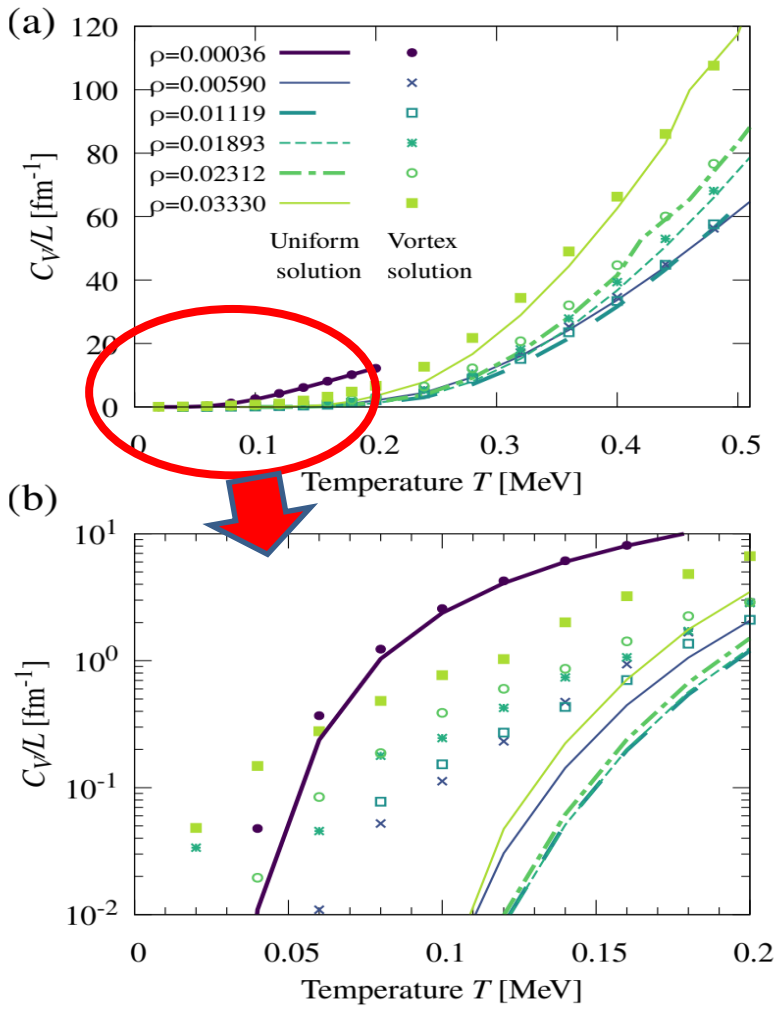

D. Pęcak, N. Chamel, P.M., G. Wlazłowski, Phys. Rev. C**104**, 055801 (2021)

Properties of a vortex across the neutron star crust

ρ_∞ (fm^{-3})	0.00036	0.0059	0.0112	0.0189	0.0231	0.0333
k_F^{-1} (fm)	4.52	1.79	1.45	1.21	1.14	1.01
ξ (fm)	8.44	5.53	5.97	7.00	7.78	10.28
$R_{\rm VFM}$ (fm)	15.0	10.5	10.5	12.0	13.5	16.5
Δ_∞ (MeV)	0.35	1.33	1.53	1.55	1.50	1.28
$T_{\rm crit}$ (MeV)	0.20	0.76	0.87	0.88	0.85	0.73
$\varepsilon_{\rm F}$ (MeV)	1.01	6.48	9.93	14.09	16.10	20.53
μ (MeV)	0.80	4.21	5.80	7.30	7.91	9.09
$E_{\rm mg}$ (MeV)	0.090	0.308	0.261	0.199	0.152	0.009
$B_{\rm crit}$ (10^{15} G)	7.76	26.5	22.5	17.2	13.1	0.82

Minigap values

Magnetic field needed to polarize the core

D. Pęcak, N. Chamel, P.M., G. Wlazłowski, Phys. Rev. C**104**, 055801 (2021)

Vortex – impurity interaction (pinning force)

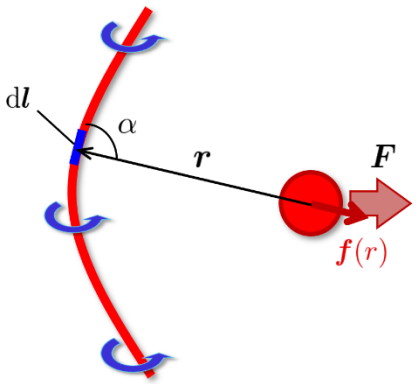

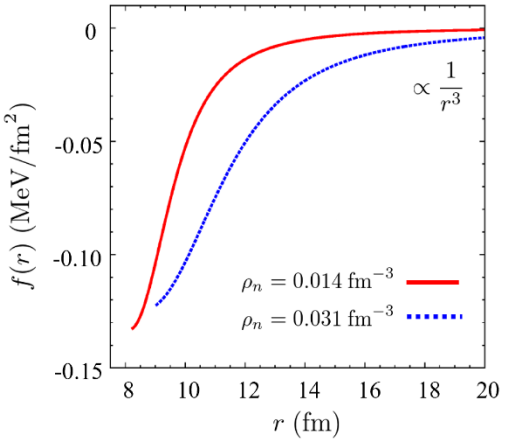

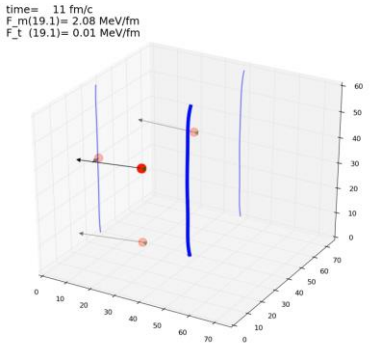

G. Wlazłowski, K. Sekizawa, P. Magierski, A. Bulgac, M.M. Forbes, Phys. Rev. Lett. 117, 232701(2016)

Is neutron star a turbulent system?

- What are differences and similarities of turbulence and its decay in Fermi and Bose superfluids?

A. Bulgac, A. Luo, P. Magierski, K.Roche, Y. Yu, Science 332, 1288 (2011).
M. Tylutki, G. Wlazłowski, Phys. Rev. A103, 051302 (2021).
K.Hossain, K.Kobuszewski, M.M.Forbes, P. Magierski, K.Sekizawa, G.Wlazłowski Phys. Rev. A 105, 013304 (2022).
G. Wlazłowski, M.M. Forbes, S.R. Sarkar, A. Marek, M. Szpindler, PNAS Nexus 3, 160 (2024).

Effective mass of a nucleus in superfluid neutron environment

Suppose we would like to evaluate an effective mass of a heavy particle immersed in a Fermi bath.
Can one come up with the effective (classical) equation of motion of the type:

$$M\frac{d^2q}{dt^2} - F_D\left(\frac{dq}{dt},\ldots\right) + \frac{dE}{dq} = 0 \quad ?$$

In general it is a complicated task as the first and the second term may not be unambiguously separated.

However for the superfluid system it can be done as for sufficiently slow motion (below the critical velocity) the second term may be neglected due to the presence of the pairing gap.

Dynamics of nuclear impurity in the neutron star crust: effective mass and energy dissipation

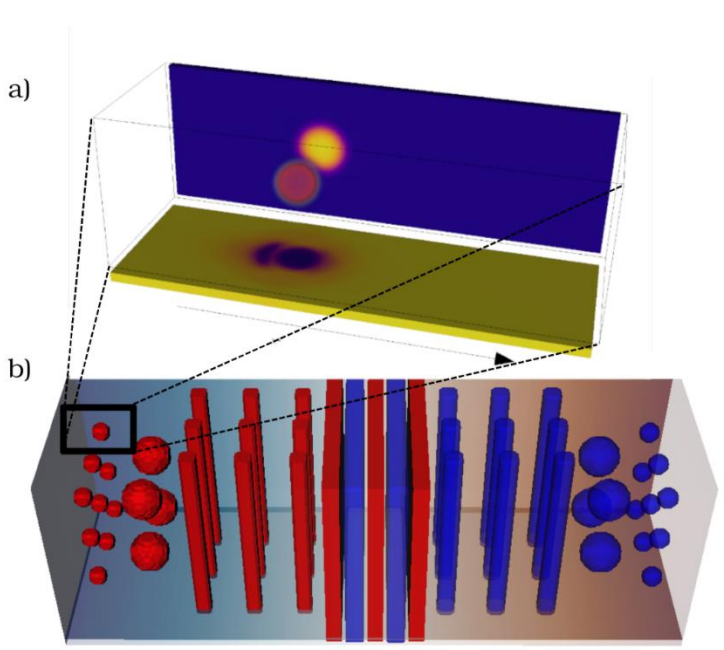

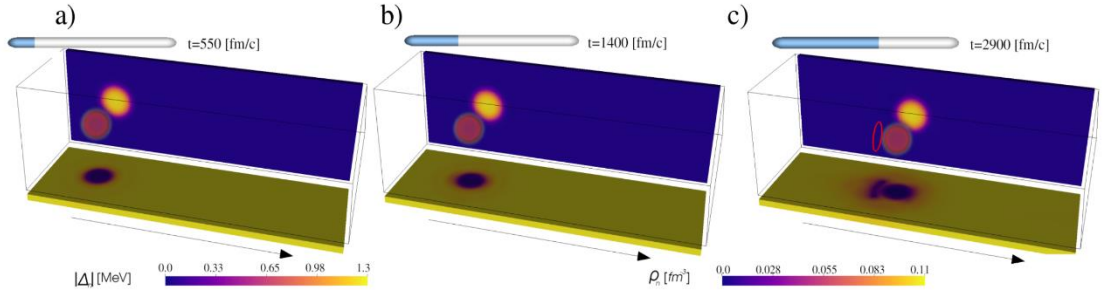

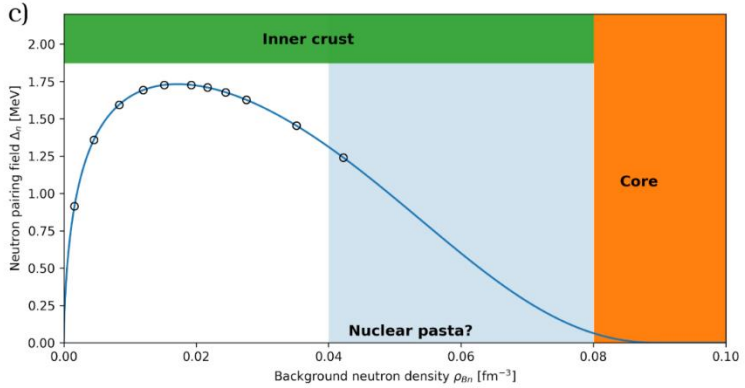

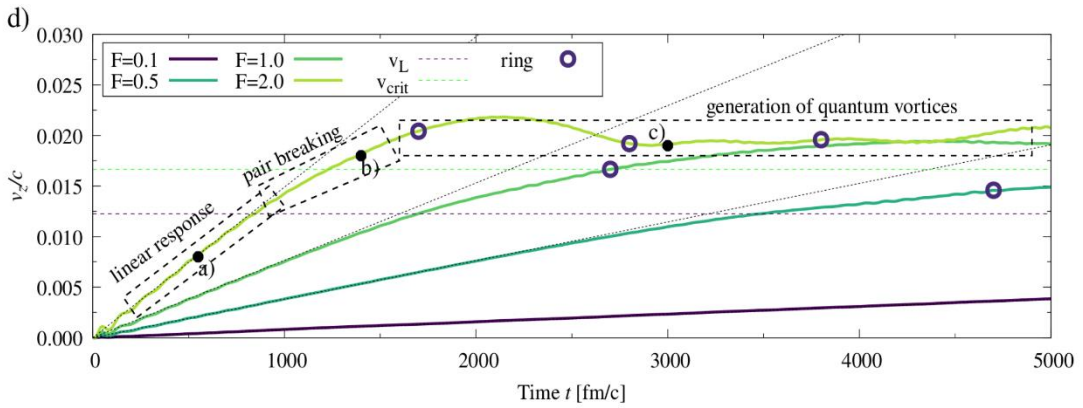

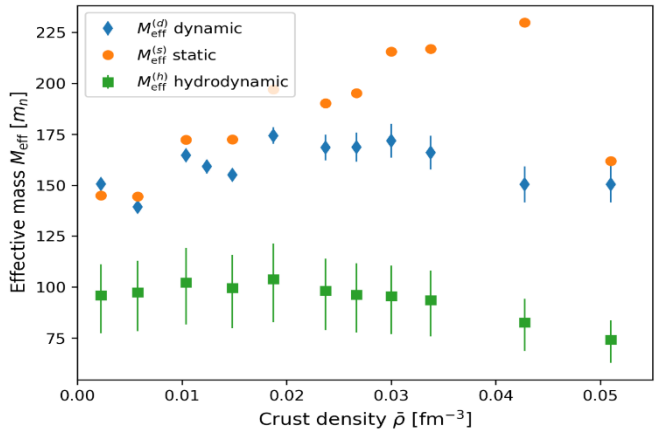

FIG. 4. The effective mass of the nucleus calculated with different approaches: dynamic $M^{(d)}_{\rm eff}$, static $M^{(s)}_{\rm eff}$, hydrodynamic $M^{(h)}_{\rm eff}$. The details, including how we determine the error bars are explained in the main text. The hydrodynamic approximation gives qualitative behavior, while static calculations match results in the low-density regime.

D. Pęcak, A.Zdanowicz, N. Chamel, P. Magierski, G. Wlazłowski, arXiv:2403.17499

Pairing in spin imbalanced superfluids

Clogston-Chandrasekhar condition sets the limit for the chemical potential difference at which superfluidity is lost: $\left|\mu_\downarrow - \mu_\uparrow\right| \propto \Delta$

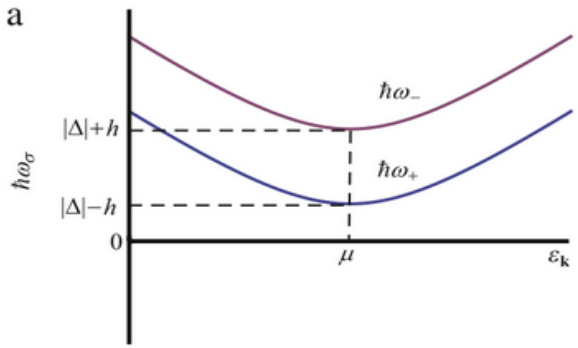

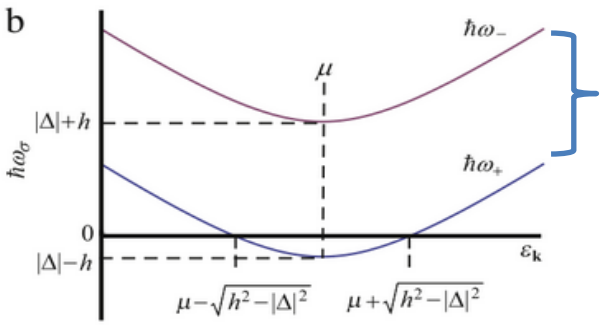

splitting of quasiparticle exc. energy branches for spin-up and spin-down fermions.

$h = \frac{1}{2}\left|\mu_\downarrow - \mu_\uparrow\right|$

Sarma (interior gap) phase

G. Sarma, J. Phys. Chem. Solids 24 (1963) 1029.
W.V. Liu, F. Wilczek, Phys. Rev. Lett. 90 (2003) 047002.

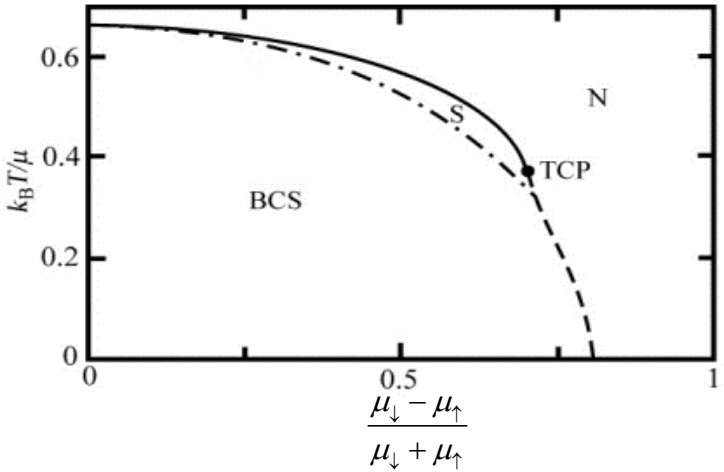

Unstable for balanced masses at T=0

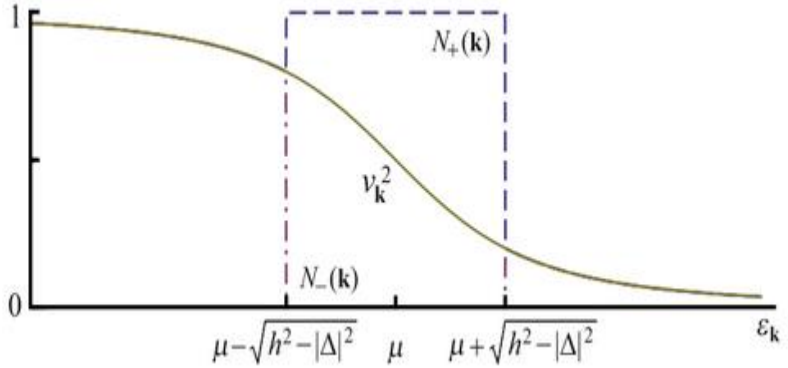

Phase separation in momentum space

K.B. Gubbels, H.T.C. Stoof / Physics Reports 525 (2013) 255–313

Inhomogeneous systems: Fulde-Ferrell-Larkin-Ovchinnikov (FFLO) phase

Larkin-Ovchinnikov (LO): $\Delta(r) \sim cos(\vec{q}\cdot\vec{r})$

Fulde-Ferrell (FF): $\Delta(r) \sim \exp(i\vec{q}\cdot\vec{r})$

A.I. Larkin and Y. N. Ovchinnikov, Sov. Phys. JETP 20, 762 (1965)
P. Fulde and R. A. Ferrell, Phys. Rev. 135, A550 (1964)

Spatial modulation of the pairing field cost energy proportional to q^2 but may be compensated by an increased pairing energy due to the mutual shift of Fermi spheres:

FF:

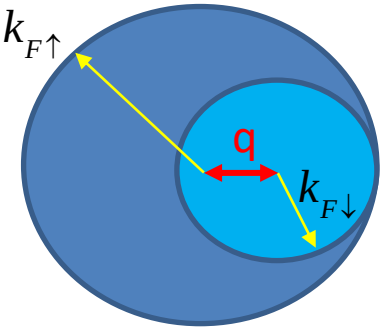

LO:

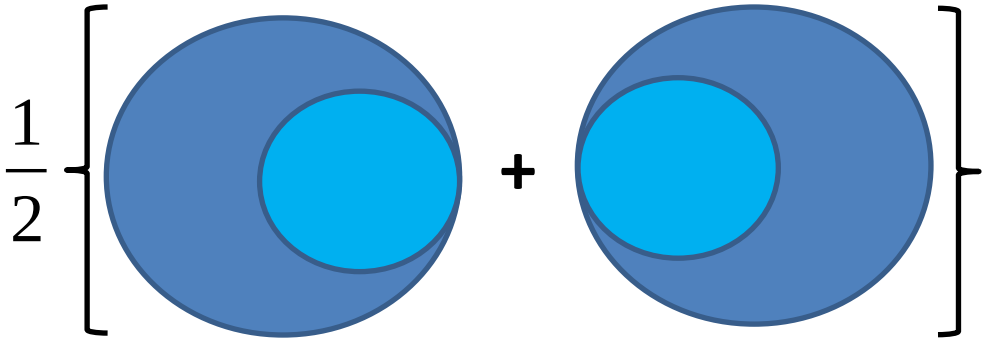

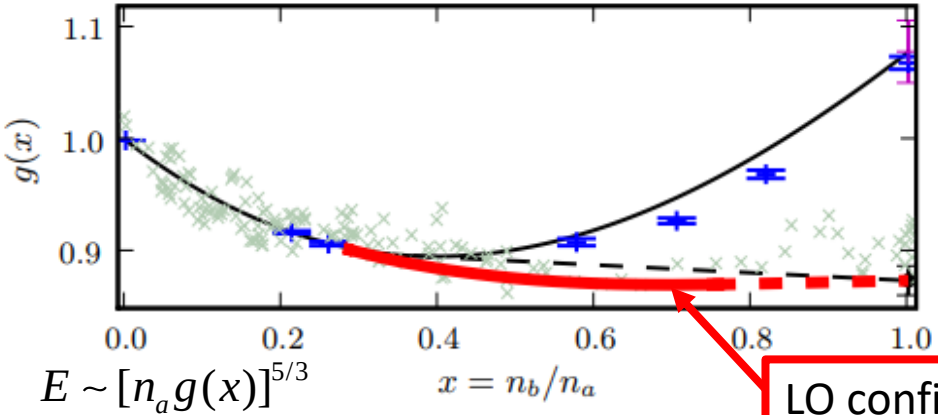

Bulgac & Forbes have shown, within DFT, that Larkin-Ovchinnikov (LO) phase may exist in the unitary Fermi gas (UFG) (realized experimentally in ultracold atomic clouds)

LO configuration – supersolid state

A. Bulgac, M.M.Forbes, Phys. Rev. Lett. 101,215301 (2008)
See also review of mean-field theories : Radzihovsky,Sheehy, Rep.Prog. Phys.73,076501(2010)

Andreev states and stability of pairing nodal points

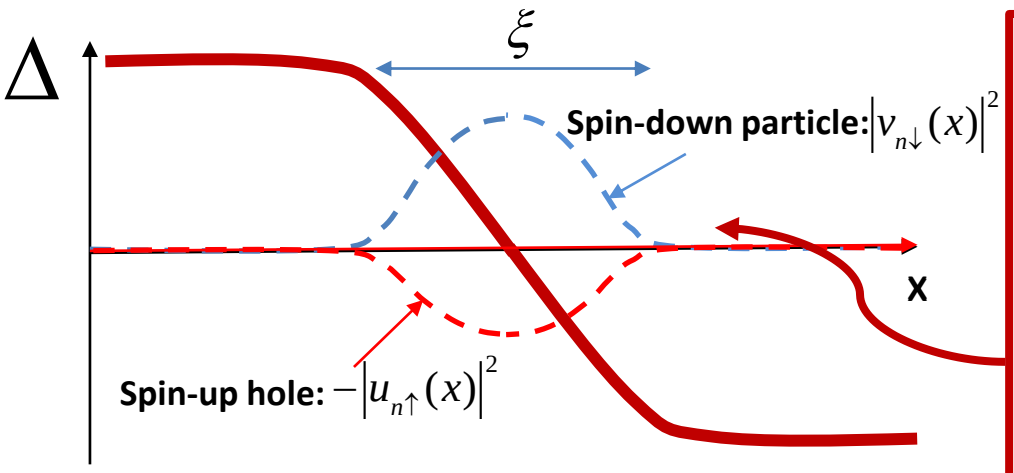

Due to quasiparticle scattering the localized Andreev states appear at the nodal point. These states induce local spin-polarization

BdG in the Andreev approx. ($\Delta \ll k_F^2$)

$$\begin{bmatrix} -2ik_F \dfrac{d}{dx} & \Delta(x) \\ \Delta^*(x) & 2ik_F \dfrac{d}{dx} \end{bmatrix} \begin{bmatrix} u_{n\uparrow}(x) \\ v_{n\downarrow}(x) \end{bmatrix} = E_n \begin{bmatrix} u_{n\uparrow}(x) \\ v_{n\downarrow}(x) \end{bmatrix}$$

Another perspective: superconductor-ferromagnet junction

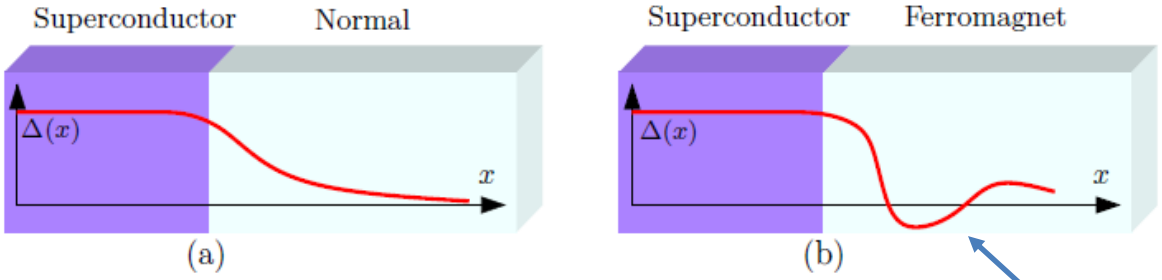

Due to the difference between Fermi momenta of spin-up and spin-down particles:

$$\left.\begin{aligned} k_{F\uparrow} &= k_F + \delta k_F \\ k_{F\downarrow} &= k_F - \delta k_F \end{aligned}\right\}$$

Induces spatial modulation of the order parameter of the period: $\dfrac{\pi}{\delta k_F}$

Creating Larkin-Ovchinnikov droplet (ferron) dynamically in unitary Fermi gas

Spin-selective potential applied locally leads to Cooper pair breaking

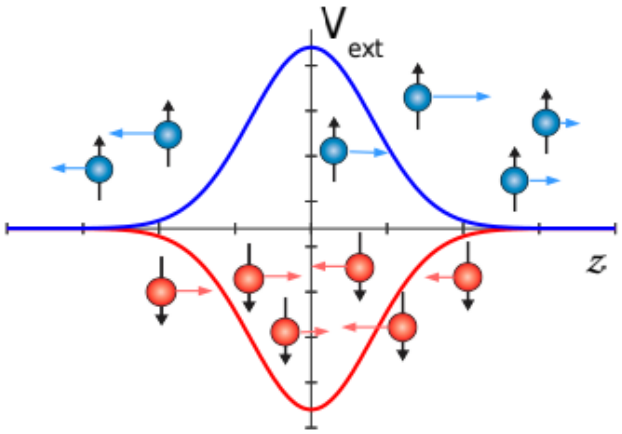

Pairing field nodal structure

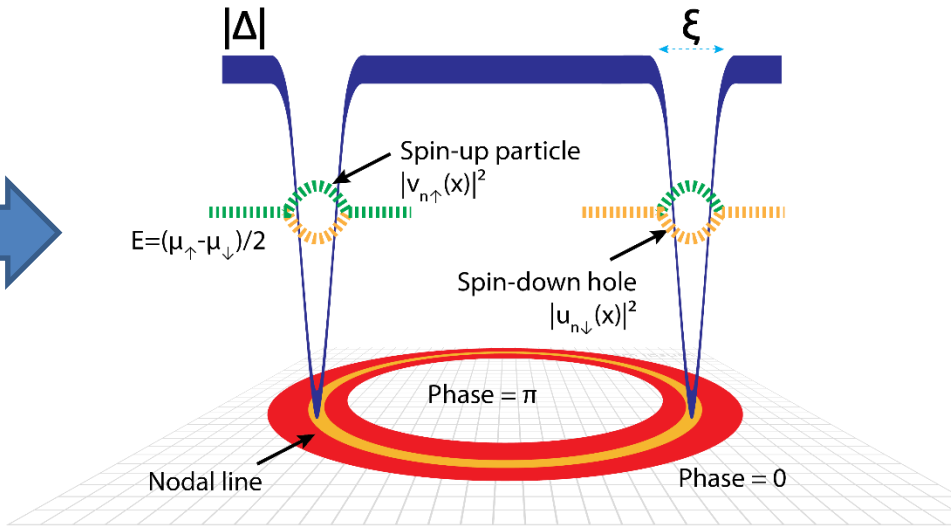

Generation of *ferron* in the unitary regime

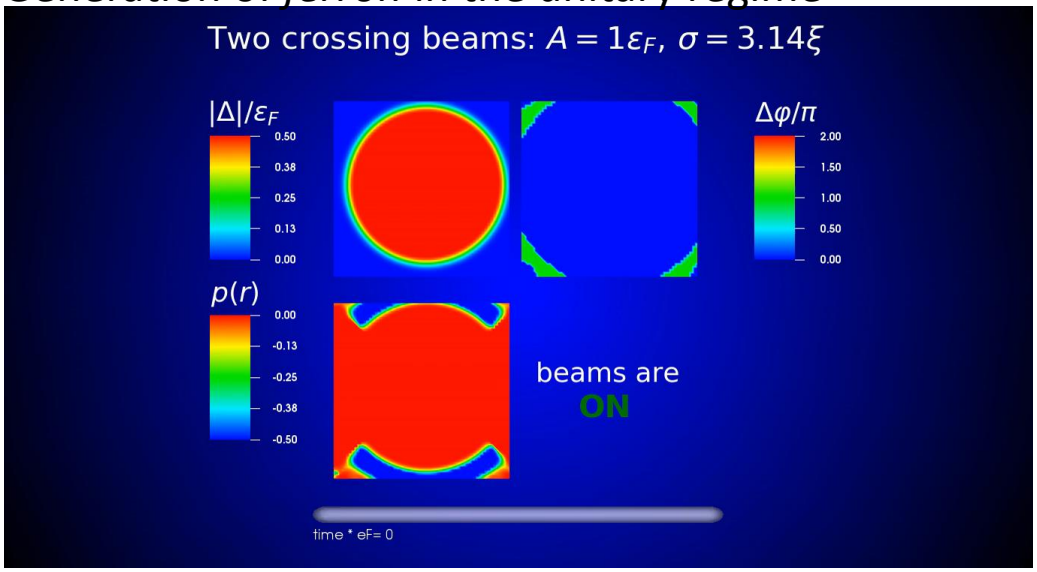

Ferron structure

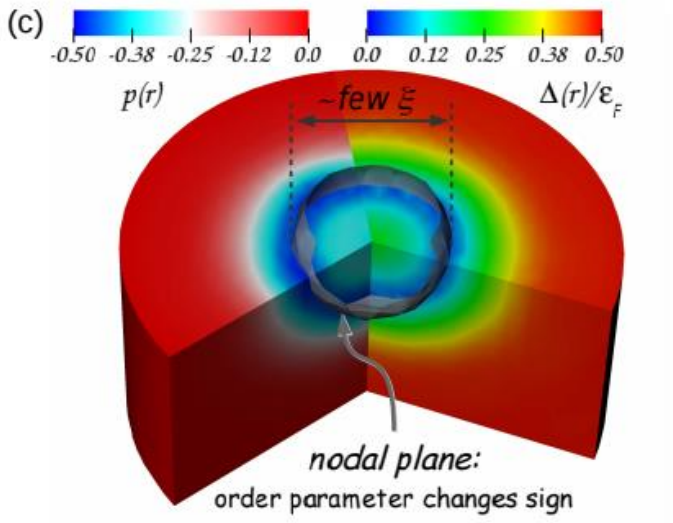

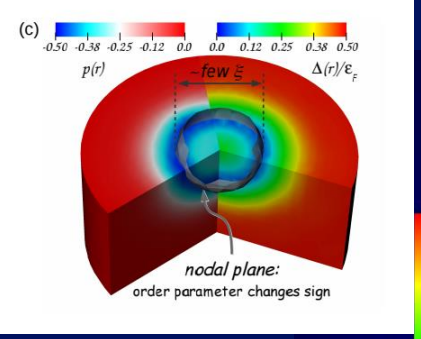

Forming a stable spherical nodal surface in Unitary Fermi Gas (UFG) - TDDFT calcs.

Polarization $p(r)$

Phase of Pairing $[\pi]$

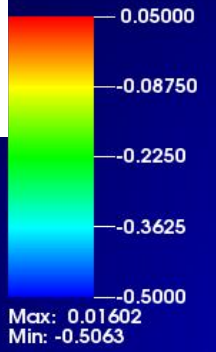

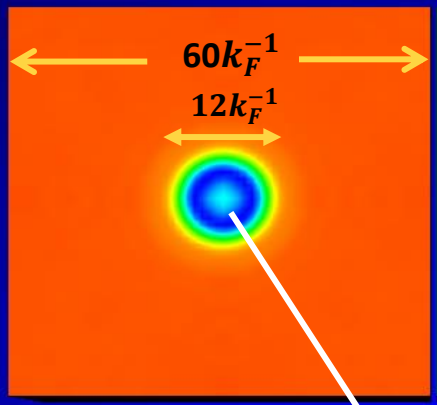

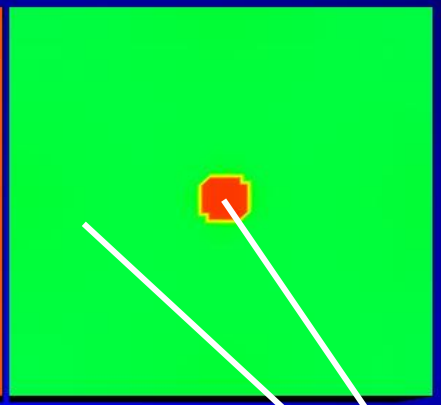

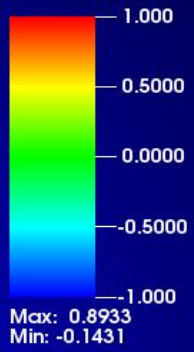

Pairing Gap $|\Delta/\varepsilon_F|$

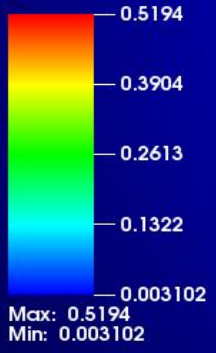

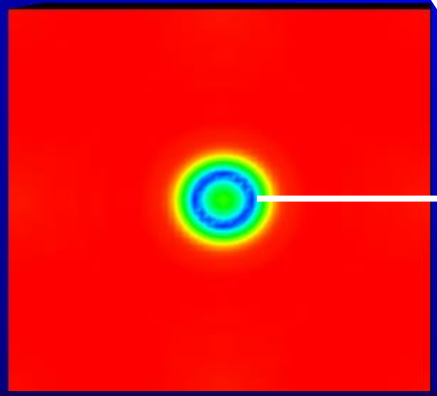

Phase difference is π

Maximum polarization occurs within a shell where the pairing field vanishes.

Contraction of the nodal sphere is prevented by the pairing potential barrier.
Expansion of the nodal sphere will cost the energy due to expansion of polarized shell.

As a result of the interplay between volume and surface energies keeps the impurity stable

P. Magierski, B.Tüzemen, G.Wlazłowski, Phys. Rev. A 100, 033613 (2019); Phys. Rev. A 104, 033304 (2021)

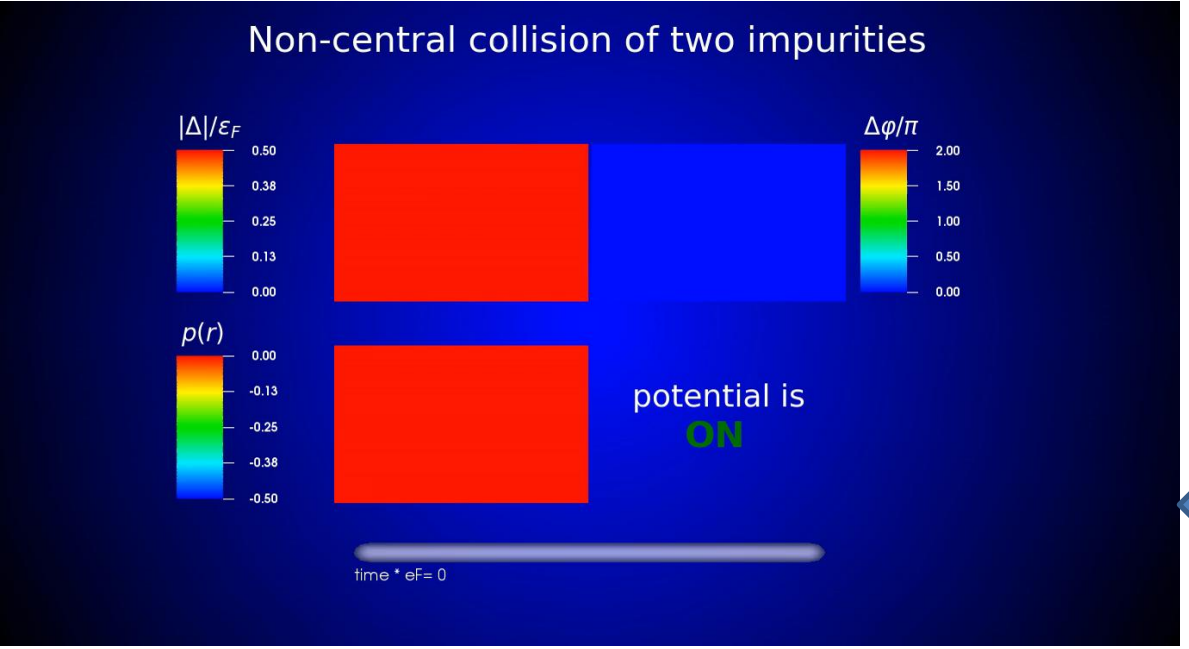

Moving impurity:

From Larkin-Ovchinnikov towards Fulde-Ferrell limit:

$$\Delta(r) : cos(\vec{q}\cdot\vec{r}) \Rightarrow \exp(i\vec{q}\cdot\vec{r})$$

Surprisingly, the nodal structure remains stable even during collisions

The velocities of impurites are about 30% of the velocity of sound.

Limiting velocity with respect to superfluid background

Note that the Fulde-Ferrell limit defines the **critical velocity** which is associated with the maximum spin current that can flow through the impurity ($\sim q = |k_{F\uparrow} - k_{F\downarrow}|$).

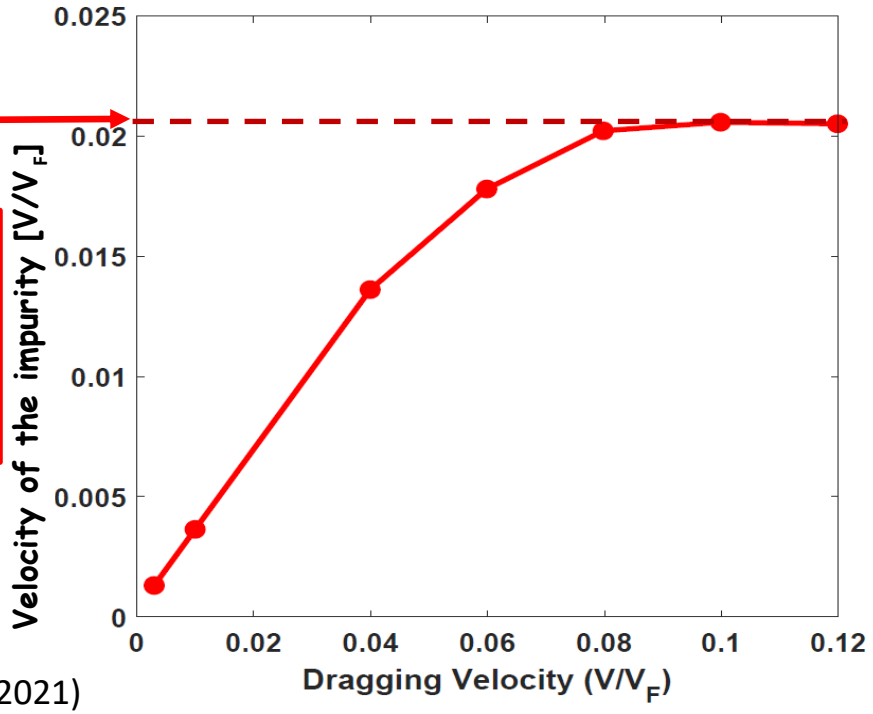

P.Magierski, B.Tüzemen, G.Wlazłowski, Phys. Rev. A 104, 033304 (2021)

What is going to happen if we introduce spin imbalance?

In general it will generate distortions of Fermi spheres locally and triggering the appearance of **pairing field inhomogeneity** leading to various patterns involving:

- **Separate impurititес (ferrons),**
- **Liquid crystal-like structure,**
- **Supersolids.**

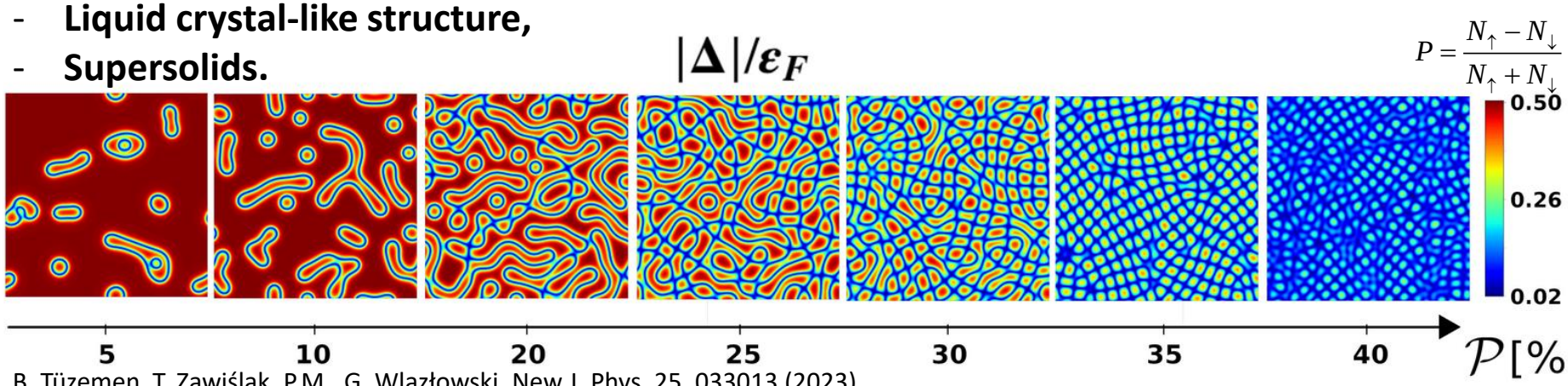

B. Tüzemen, T. Zawiślak, P.M., G. Wlazłowski, New J. Phys. 25, 033013 (2023).

Dynamics of a vortex dipole in spin imbalanced Fermi superfluid.
Strong enhancement of vortex dipole energy dissipation.

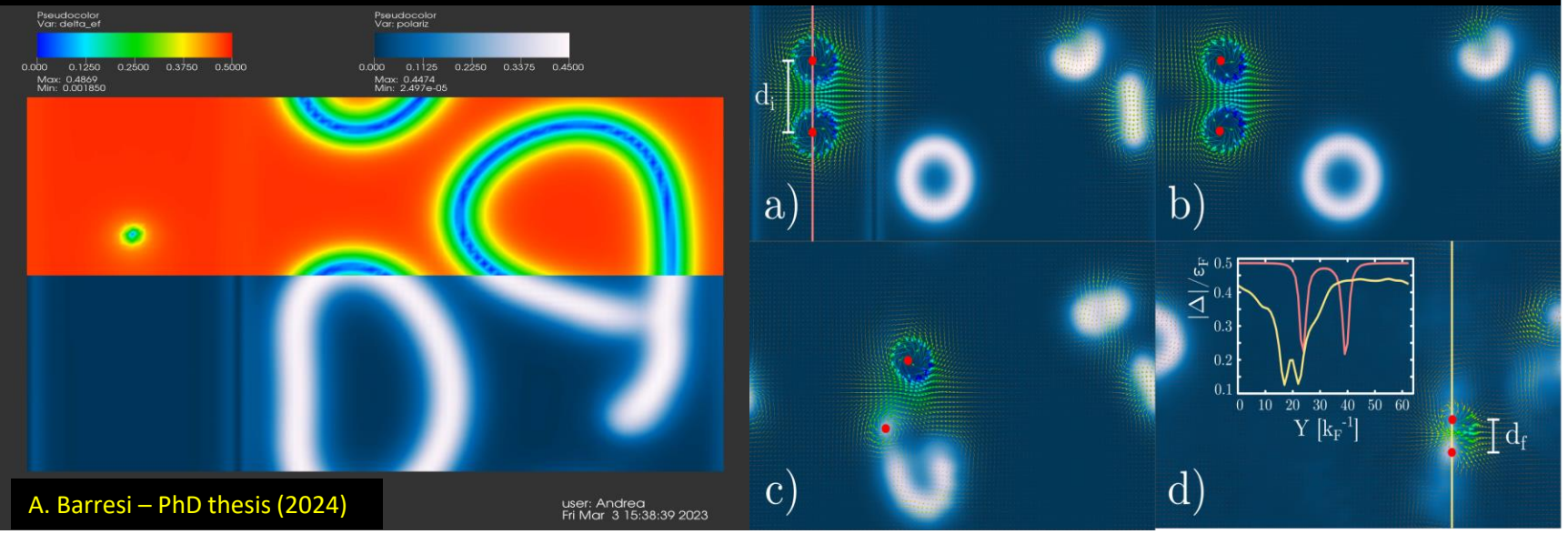

A. Barresi – PhD thesis (2024)

Open problems of TDDFT

1) There are easy and difficult observables in DFT.
   In general: easy observables are one-body observables. They are easily extracted and reliable.

2) But there are also important observables which are difficult to extract.
   For example:
   - S matrix
   - momentum distributions
   - transitional densities (defined in linear response regime)
   - various conditional probabilities
   - mass distributions

   Stochastic extensions of TDDFT are under investigation:

   D. Lacroix, A. Ayik, Ph. Chomaz, Prog.Part.Nucl.Phys.52(2004)497
   S.Ayik, Phys.Lett. B658 (2008) 174
   A. Bulgac, S.Jin, I. Stetcu, arxiv:1806.00694

3) Dissipation: transition between one-body dissipation regime and two-body dissipation regime.